

Title	NEW COMPOSITE CATALYSTS FOR RING OPENING POLYMERIZATION OF EPOXIDES AND PROPIOLACTONES
Author(s)	Hayase, Shuji
Citation	大阪大学, 1983, 博士論文
Version Type	VoR
URL	<a href="https://hdl.handle.net/11094/27754">https://hdl.handle.net/11094/27754</a>
rights	
Note	

*Osaka University Knowledge Archive : OUKA*

<https://ir.library.osaka-u.ac.jp/>

Osaka University

NEW COMPOSITE CATALYSTS FOR RING OPENING POLYMERIZATION  
OF EPOXIDES AND PROPIOLACTONES

BY

SHUZI HAYASE

NOVEMBER 1982

## CONTENTS

		Page
Chapter 1	General Introduction .....	1
Chapter 2	New Polymerization Catalyst .....	17
2-1	Introduction .....	17
2-2	Profile of polymerization .....	17
Chapter 3	Dependence of Catalytic Activity on Silanol Structure .....	23
3-1	Introduction .....	23
3-2	Stability of silanol compounds in self-condensation .....	23
3-3	Polymerization behavior with Al(acac) <sub>3</sub> /Ph <sub>3</sub> SiOH catalyst .....	25
3-4	Kinetics of polymerization with Al(acac) <sub>3</sub> /Ph <sub>3</sub> SiOH catalyst .....	28
3-5	Interaction of silanol with Al(acac) <sub>3</sub> .....	33
3-6	Conclusion .....	33
Chapter 4	Dependence of Catalyst Activity on the Structure of Chelating Ligand on Aluminum .....	37
4-1	Introduction .....	37
4-2	Polymerization with a tris- (β-diketonato)aluminum/triphenyl- silanol system .....	39

4-3	Polymerization with tris- ( $\beta$ -ketoesterato)aluminum/triphenyl- silanol system .....	41
4-4	Polymerization with a tris- (ortho-carbonylphenolato)aluminum/ triphenylsilanol system .....	43
4-5	Polymerization with N,O-chelates of aluminum compound/triphenylsilanol catalyst system .....	46
4-6	Spin lattice relaxation time for the $^1\text{H}$ -NMR signal assigned to SiOH group .....	48
4-7	Reaction scheme .....	48
4-8	Conclusion .....	56
Chapter 5	Catalyst Supported on Zeolite and Porous Silica .....	59
5-1	Introduction .....	59
5-2	Aluminum complex/silica gel catalyst system .....	59
5-3	Zeolite/silanol catalyst system .....	61
5-4	$\text{Al}(\text{acac})_3$ /silanol compound catalyst supported by porous silica .....	65
5-5	Molecular weight distribution of the polymer .....	74

	Page	
Chapter 6	Microstructure of Poly(cyclohexene oxide) .....	77
6-1	Introduction .....	77
6-2	Structure of poly(cyclohexene oxide) .....	77
Chapter 7	Effect of Intramolecular Hydrogen Bond of Silanol in the Catalyst Activity ....	85
7-1	Introduction .....	85
7-2	Aluminum complex/ $\text{HO}(\text{Ph}_2\text{SiO})_n\text{H}$ catalyst system .....	85
7-3	$\text{Al}(\text{SA})_3$ /Trimer+Dimer or Monomer catalyst system .....	91
7-4	Aluminum complex/1,4-bis(hydroxy-dimethylsilyl)benzene system .....	93
7-5	Aluminum complex/diphenyl(4-vinyl-phenyl)silanol catalyst system .....	98
7-6	Aluminum complex/SH6018 catalyst system .....	100
Chapter 8	Polymerization under UV-Radiation .....	103
8-1	Introduction .....	103
8-2	Polymerization profiles .....	103
Chapter 9	Thermal Properties of Epoxy Resin Cured by Aluminum Complex/Silanol Catalyst ...	109
9-1	Introduction .....	109

	Page
9-2	Difference in electrical properties between epoxy resin cured with BF <sub>3</sub> complex catalyst and that cured with Al(SA) <sub>3</sub> /DP catalyst ..... 109
9-3	Dependence of the electrical properties on the structure of catalyst ..... 122
Chapter 10	Latent catalyst ..... 127
10-1	Introduction ..... 127
10-2	Aluminum complex/hydrolyzable silicone compound system ..... 127
10-3	Aluminum complex/thermally generated silicone compound system ..... 131
10-4	Photogenerated catalyst (I) ..... 133
10-5	Photogenerated catalyst (II) ..... 148
10-6	Electrical properties of epoxy resin cured with latent catalysts .... 164
Chapter 11	Selective Synthesis of Structurally Isomeric Poly-β-ester and Poly-δ-ester from β-(2-acyloxyethyl)-β-propiolactone with Al-H <sub>2</sub> O and Zn-H <sub>2</sub> O catalysts ..... 167
11-1	Introduction ..... 167
11-2	Polymerization of β-(2-acetoxyethyl)- β-propiolactone (1) ..... 168

11-3 Polymerization of $\beta$ -(2-isopropyl- carboxyethyl)- $\beta$ -propiolactone (2) and $\beta$ -(2-(1-chloroethyl)-carboxy- ethyl)- $\beta$ -propiolactone (3) .....	195
Chapter 12 Experimental .....	213
Acknowledgments .....	235
List of Publication .....	237

## Chapter 1 General Introduction

### Part I A new catalyst for polymerization of epoxides

#### -- aluminum complex/silanol catalyst --

##### 1) Background

Epoxy resins have been utilized as insulating materials, coating materials, adhesives and laminating materials in many fields. They are preferred for their electrical and mechanical properties in consideration of the coat.<sup>1</sup> In electrical industries, a number of different epoxy resins have been used as the materials for insulation of coils in generators and motors, molding compounds for semiconductor encapsulation, and the laminates for circuit plates. Excellent insulating properties, high reliability and low cost have been required for these materials.

There is a recent trend for many electrical appliances to be of midget type, because of the savings in energy and the ease in processing. The motor and the generator is the example. The heat generated by electric current causes the rise of temperature of the insulating materials. The midget type enhances the temperature rise. Insulating properties for epoxy resin cured with commonly used catalyst are not sufficient for motor-use at temperature above 160°C. Therefore the insulation



properties and heat resistant properties must be improved, especially in the temperature range from 150°C to 220°C.

For semiconductor encapsulation use, ionic impurities in the molding compound, namely,  $H^+$ ,  $Na^+$ ,  $K^+$ ,  $Cl^-$ ,  $F^-$ ,  $R-NH_3^+$ ,  $BF_4^-$ ,  $AsF_6^-$  and so on, must be minimized to prevent corrosion of fine wiring from moisture and the impurities. Since the impurities deteriorate insulation of the molding compound, absence of impurities is preferred.

Epoxy resin monomers have more than two epoxy groups for curing. The monomer forms three dimensional networks in the presence of catalyst. The catalyst used is then buried in the matrix of the network. Therefore, the following properties will be influenced by the catalyst residue.

- 1) Insulation properties
- 2) Collosion properties on metal
- 3) Color change by aging at higher temperature
- 4) Heat resistant properties

The heat resistant properties mean weight loss of the cured resin when it was aged at high temperature. The catalyst for ring opening polymerization also degrades the polymer chain at that temperature. As shown above, the properties of cured epoxy resins can be improved by use of an appropriate catalyst or by modification of the catalyst.

The followings are curing catalysts which have been

commonly used for homopolymerization of epoxy resin monomers.<sup>2</sup>

- 1) tertiary amines (including heterocyclic bases such as imidazole and guanidine)
- 2)  $\text{BF}_3$ ·amine complexes (e.g.  $\text{BF}_3$ ·monoethylamine and  $\text{BF}_3$ ·piperidine)
- 3) ammonium salts ( $\text{C}_6\text{H}_5\text{NH}_3^+\cdot\text{AsF}_6^-$  and  $\text{C}_6\text{H}_5\text{NH}_3^+\cdot\text{PF}_6^-$ )

The dissipation factor of the epoxy resin cured with these catalysts increases rapidly at the temperature above  $150^\circ\text{C}$ .<sup>2</sup>

## 2) Requirements for new catalysts

The following points are important for the development of new catalysts.

- 1) Stability in air and toward moisture
- 2) Free from ionic species, e.g. halide anion, metal cation,  $\text{H}^+$ .
- 3) High catalytic activity for epoxide polymerization

Ethylene oxide is the simplest of epoxy resin monomers. Ethylene oxide has been polymerized by use of the following cationic and anionic catalyst.

- 1) Cationic catalyst<sup>3</sup>:  $\text{AlCl}_3$ ,  $\text{SbCl}_5$ ,  $\text{BF}_3$ ,  $\text{BCl}_3$ ,  
 $\text{BeCl}_2$ ,  $\text{FeCl}_3$ ,  $\text{FeBr}_3$ ,  $\text{SnCl}_4$ ,  
 $\text{TiCl}_4$ ,  $\text{ZrCl}_4$ ,  $\text{ZnCl}_2$ ,  $\text{PF}_5$ .

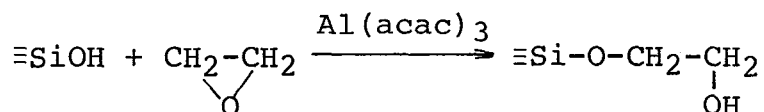
2) Anionic catalyst :  $\text{CH}_3\text{ONa}^4$ ,  $\text{CaO}$ ,  $\text{SrO}^5$ , alkali earth metal compounds<sup>6</sup>, organometallic catalysts<sup>7</sup>.

These catalysts are not stable in air and are buried in the cured resin matrix as ionic impurities.

Water, alcohols and phenols have been examined as co-catalyst of cationic polymerization in the presence of  $\text{BF}_3$  or  $\text{SnCl}_4$ .<sup>8</sup> As alcohols and phenols are non- or weakly ionic materials, they are suitable for the present catalyst. However when they were used in the presence of halogen-free-metal compound, namely, acetyl-acetonato complex and so on, their activities were insufficient.

### 3) Finding a new catalyst

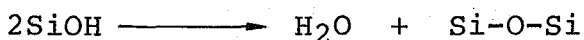
Silanol is a hydroxy compound whose acidity is larger than alcohol and smaller than phenol.<sup>9</sup> It is known that silanols react with epoxides, forming Si-O-C bonds, in the presence of a catalytic amount of an aluminum complex.<sup>10</sup>



These compounds are used as epoxy-silicone resin. It was considered that if silanol reacted with epoxide and produced ring-opened compounds, ring-opening polymerization might be caused in the presence of a catalytic amount of

a composite catalyst-aluminum complex and silanol.

The addition of silanol to epoxide is also considered to be a termination step of polymerization. In order to prevent the silanol from the addition of silanol to epoxide, silanols with phenyl groups which would make the vicinity of the SiOH moiety bulky, were considered. The introduction of phenyl group would also strengthen the acidity of silanol and increase the degree of polymerization and retard the termination. When silanols with phenyl groups were used, the composite catalyst system (aluminum complex/silanol) showed the catalyst activity. The silanol at the active site, namely, ionic species, would disappear gradually at the curing temperature as shown in the following transformation to give a siloxane and water.



Therefore the cured epoxy resin will have excellent electrical properties. The epoxy resins cured with this catalyst had excellent insulating properties, especially in the temperature region from 150°C to 220°C, as mentioned later.

#### 4) Activation of the catalyst

To improve the catalyst, reaction mechanism of the catalytic polymerization was investigated. The catalyst

activity was examined by use of cyclohexene oxide as a model compound of epoxy resin.

Substituent groups on SiOH would affect the polymerization largely, as mentioned in 3). Therefore, dependence of the catalytic activity on the structure of the silanol was investigated. The results are shown in chapter 3.

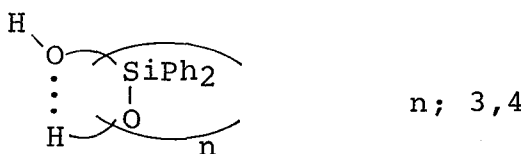
Phenol or thiol, whose acidity is stronger than that of silanol, did not have the catalytic activity. The results implied that the interaction between silanol and an aluminum complex was important in order to activate the catalyst. Therefore the dependence of the catalytic activity on the structure of aluminum complex and relation between the interaction strength and the catalytic activity were investigated (see Chapter 4).

From consideration of the substitution effects, two interaction mechanisms are possible. The active site was considered to be similar to Brönsted acid site of a silica-alumina catalyst.<sup>11</sup> The polymerization will be initiated by proton released by the interaction between the aluminum complex and silanol. The formation of an atactic polymer was also a consequence of a cationic mechanism.

Active site of the aluminum complex/silanol catalyst is SiO-H. If the properties of SiOH, for example, acidity or stability against self-condensation, were varied, the catalytic activity might be affected. Porous silica and

zeolite were known to interact with hydroxy compounds. Therefore the activity of the aluminum complex/silanol catalyst supported on the porous silica or zeolite was investigated. The porous silica and zeolite resisted deactivation more than the  $\text{Al}(\text{acac})_3$  only, and had higher activity. The mechanism of the activation was examined by use of  $^1\text{H}$ -NMR spectroscopy (see Chapter 5).

The results from kinetics of the polymerization showed reaction order on concentration of silanol to be about 1.9. The results implied that aggregation of silanols was important. Therefore effects of intramolecular hydrogen bond of silanol on catalyst activity were examined. In the preexperiment using diphenylsilanediol oligomer ( $\text{HO}(\text{Ph}_2\text{SiO})_n\text{H}$ ;  $n: 2,3,4$ ) as model of silanol polymers, the trimer and the tetramer gave active catalyst than the dimer in presence of the tris(acetylacetonato)-aluminum, because they form an intramolecular hydrogen bond.



Catalyst activation caused by use of a silanol polymer was also observed in case of tris(acetylacetonato)-aluminum/silanol polymer. The experimental results using silanol oligomer explained well the behavior of the polymerization with aluminum complex/silanol polymer. Bulky

groups neighboring the SiOH part and rigidity of silanol polymer chain are important for catalyst activation.

It was found that the interaction between aluminum complex and silanol was important for catalyst activation. The interaction was considered to be induced by UV-radiation, because it is known that acid dissociation was promoted and the hydrogen bonding, for example, one between cytosine and guanine, strengthens under UV-radiation.<sup>12</sup> The catalyst activity of the tris(acetylacetonato)aluminum/triphenylsilanol system increased about 3 - 4 times under UV-radiation (see Chapter 8).

#### 5) Electrical properties of epoxy resin cured with aluminum complex/silanol catalyst

The electrical properties of epoxy resins (bisphenol A type, epikote 828, shell) cured with the present catalyst were compared with that cured with ordinary catalysts, namely, imidazole and  $\text{BF}_3 \cdot \text{complex}$ .<sup>2</sup> The value of electrical dissipation factor, volume resistivity and breakdown-voltage of the epoxy resin cured were excellent, compared with that cured by  $\text{BF}_3 \cdot \text{complex}$ .<sup>2</sup> The reason of such excellent electrical properties was examined by use of thermal depolarization charge (see Chapter 9). The results showed that the absence of any appreciable ionic species was important for the excellent electrical properties. As the polymerization was considered to be caused

cationically, disappearance mechanism of the cation was examined (see Chapter 9). Dependence of the electrical properties on the structure of the catalyst was also examined.

## 6) Latent catalyst

### 6-1) Activation by heat

A "clean" and active catalyst for epoxide polymerization was obtained as described above. For practical use, epoxy resins are provided as a composition containing catalyst. The epoxy resin composition must be stable before use and must be cured rapidly. Therefore, molecular design is necessary for the active catalyst which is generated by a trigger. Heat or UV-radiation is usually used as the trigger. This type of catalyst is called a latent catalyst. Compounds containing Si-OR groups were used as latent catalysts components. The SiOR group will be hydrolyzed by a small amount of water in epoxy resin at higher temperature, and silanol produced by hydrolysis will start the polymerization. The catalyst activity of aluminum complex/SiOR and the curing process were examined.

In the aluminum complex/alkoxysilane catalyst, the alkoxysilane was gradually hydrolyzed even at room temperature and the epoxy resin was gradually crosslinked. In order to prevent the reaction at room temperature, water in the epoxy resin was eliminated with zeolite 4A.



However the adsorbed water will be released at the temperature above 100°C. The composition was more stable in the presence of zeolite and the gelation of the composition was faster above 100°C.

The silicone compound which thermally liberates silanol in the absence of H<sub>2</sub>O was found (see Chapter 10). The epoxide composition containing the catalyst was more stable at room temperature and active at higher temperature. The insulation properties for the epoxy resin cured with these catalysts were also excellent.

#### 6-2) Activation by UV-radiation

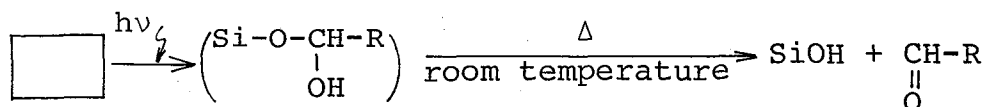
The catalyst-curing epoxy resin with irradiation have recently attracted interest due to the processability and to the energy saving. The photo-generated catalyst will be most important as latent catalyst, because reaction starts at low temperature. Long pot life is necessary in the absence of UV-radiation.

Diazonium salts and some onium salts are known to be effective for the UV curing of the epoxy resins.<sup>13</sup> However diazonium salts had disadvantages; evolution of N<sub>2</sub> gas, and presence of ionic species which disturb insulation.

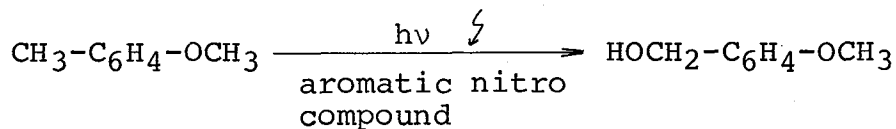
The UV-curable epoxy resins with good electrical properties may be obtained by the present photocatalyst. Such photoactive catalyst is composed by silylketones.

For example,  $\text{Ph}_3\text{SiCOPh}$  ( $n-\pi^*$  absorption at 424 nm ( $\epsilon = 292$ ) and  $\pi-\pi^*$  absorption (257 nm (16200))) photodecomposes to  $\text{Ph}_3\text{SiOH}$  in the presence of  $\text{H}_2\text{O}$  or alcohols.<sup>14</sup> A new catalyst system (aluminum complex/ $\text{Ph}_3\text{SiCOPh}$ /alcohol) was thus investigated.

Other silicone compounds which isomerize to silanol directly under UV radiation were also investigated. However high activity has not been obtained. A compound with hemiacetal structure,  $\text{SiOCH(OH)}$ , formed by photolysis was considered to be suitable for the present purpose. If the hemiacetal is formed under UV-radiation, the silicon compound will decompose rapidly even at room temperature, forming silanol, as follows.

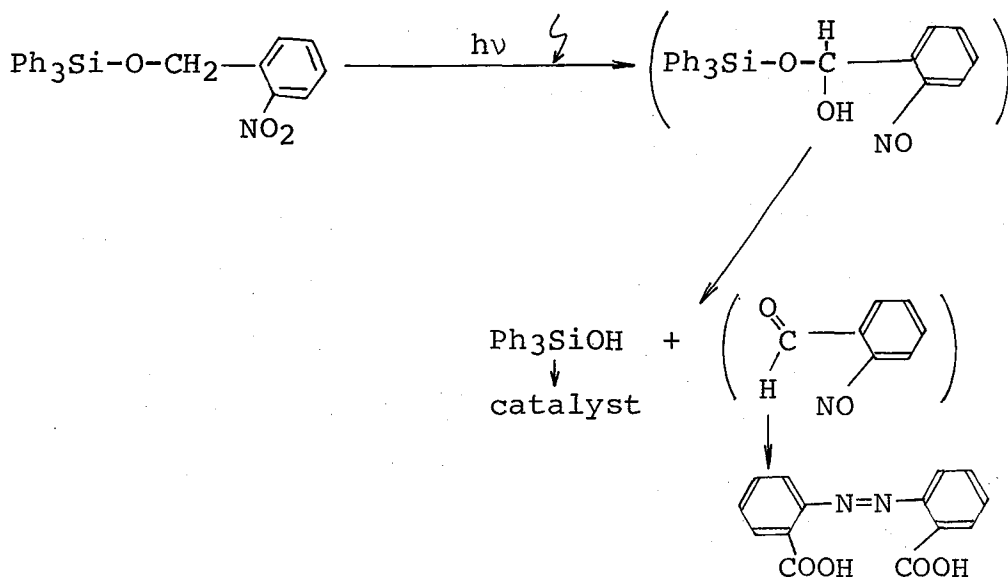


The hemiacetal may be produced by photooxidation of  $\text{Si-O-CH}_2\text{-Ph}$  with aromatic nitro compound since it is known that p-methoxytoluene is photooxidized to p-methoxybenzylalcohol.<sup>15</sup>



The photopolymerization catalyst, aluminum complex/triphenylsilylbenzyl ether/aromatic nitro compound system, polymerized cyclohexene oxide under UV radiation.

Expecting neighboring effects, ortho-nitrobenzylsilyl ether was examined. The decomposition rate of the silyl ether was fast and high catalyst activity was obtained. The dependence of the catalyst activity on the wavelength of UV and quantum yield were examined.



Epoxy resins with above photopolymerization catalyst could be cured within 20 sec. and the cured epoxy resin had excellent electrical and high heat resistance properties.

Part II Selective synthesis of structurally isomeric poly- $\beta$ -ester and poly- $\delta$ -ester from  $\beta$ -(2-acyloxy-ethyl)- $\beta$ -propiolactone with  $\text{AlEt}_3\text{-H}_2\text{O}$  and  $\text{ZnEt}_2\text{-H}_2\text{O}$  catalyst

The polymerization of  $\beta$ -substituted- $\beta$ -propiolactones

have been studied in view of stereoregular polymerization in a systematic manner.<sup>16</sup> It has been found that an organoaluminum catalyst  $(\text{EtAlO})_n$ , which is a modification of  $\text{AlEt}_3\text{-H}_2\text{O}$  catalyst, tends to give stereoregular polymers while a related organozinc catalyst  $(\text{Et}(\text{ZnO})_2\text{ZnEt})$ , which is  $\text{ZnEt}_2\text{-H}_2\text{O}$  catalyst, has little capability for stereoregulation. It is of interest to examine stereoregulation when ester group was introduced to the side chain of the lactone, because ester group of lactone ring might compete with that of side chain in coordination.

Thus, it was found that structurally isomeric polymers were formed by the ring opening polymerization of  $\beta$ -(2-acetoxyethyl)- $\beta$ -propiolactone with  $(\text{EtAlO})_n$  and  $\text{Et}(\text{ZnO})_2\text{ZnEt}$  catalyst. That is, the Al-catalyst catalyzed normal polymerization leading to the poly- $\beta$ -ester, and the Zn catalyst formed isomerized poly- $\delta$ -ester as main product. The polymer structure was determined by NMR,  $T_1$ -value, thermal decomposition product and  $T_g$ . The dependence of the isomerization ratio on the structure of terminal substituent groups in the side-chain, and the reaction mechanism were examined.

## References

1. H. Kakiuchi, "Epokishi Jushi" p.3, (1977), Shoko-do, printed in Japan; K. Hashimoto, "Epokishi Jushi" p.37 (1969), Nikkan Kogyo Shinbunsha, printed in Japan; P. B. Kekky, J. Appl. Polymer Sci., 6, 425 (1962); W. Erich, M. Bodnar, *ibid.*, 3, 296 (1960); Shell Chemical Corp., Technical Literature; H. Lee, K. Neville, "Handbook of Epoxy Resins", McGraw-Hill, (1967); R. L. De Hoff, Corrosion, 17, 83 (1961); M. B. Neiman, J. Polymer Sci., 56, 383 (1962); H. Hirsch, F. Koved, Mod. Plastics, 42, 133 (1964); W. Colletti, L. Rebori, Insulation, 11, 27 (1965); E. Klopfenstein, H. Lee, Insulation, 4, 13 (1958).
2. P. Noak, M. Saure, Kunststoffe, 54, 557 (1964); F. X. Ventrice, Mod. Plastics, 45, 201 (1967); H. L. Vincent, P. E. Oppliger and C. L. Frye, ACS Preprints "Organic coating and plastics chemistry", 28, 504 (1968); J. Clark, D. D. Perrin, Quart. Rev. 18, 295 (1964); H. K. Hall, J. Am. Chem. Soc., 79, 5441 (1957); W. A. Henderson, C. A. Streuli, J. Am. Chem. Soc., 82, 5791 (1960); E. S. Narracott, Brit. Plastics, 26, 120 (1966); J. J. Harris, S. C. Temin, J. Appl. Polymer Sci., 10, 523 (1966); A. S. Sherr, A. A. Krupnik, J. Appl. Polymer Sci., 9, 2707 (1965).
3. A. S. Eastham, Fortschr. Hochpolymer-Forsch., 2, 18 (1960)

4. S. Perry, H. Hibbert, *Can. J. Res.*, 8, 102 (1933)
5. H. Staudinger, H. Lehmann, *Ann.*, 505, 41 (1933)
6. A. E. Gurgiolo, *U. S. Pat.*, 2,934,505;  
W. L. Bresslar, A. E. Gurgiolo, *U. S. Pat.*,  
2,917,470
7. R. O. Colclough, G. Gee, W. C. E. Higginson,  
J. B. Jackson, M. Litt, *J. Polymer Sci.*, 34, 171  
(1959); N. Nakaniwa, K. Ozaki, J. Furukawa, *Macromol.*  
*Chem.*, 138, 197 (1970)
8. K. E. Russell and L. G. M. C. Vail, *Can. J. Chem.*,  
57, 2355 (1979); R. F. Bauer, R. T. LaFlair and  
K. E. Russell, *Can. J. Chem.*, 48, 1251 (1970)
9. R. M. Salinger and R. West, *J. Organometal. Chem.*  
11, 631 (1968)
10. H. M. Bank, *U. S. Pat.* 3971747
11. H. A. Benesi, *J. Phys. Chem.*, 61, 970 (1957);  
R. H. Hansford, *Ind. Eng. Chem.*, 39, 849 (1947);  
C. L. Thomas, *Ind. Eng. Chem.*, 41, 2564 (1949);  
M. W. Tamele, *Discussions Faraday Soc.*, 8, 270 (1960);  
P. B. Venuto, L. A. Hamilton and P. S. Landis, *J.*  
*Catalysis*, 5, 484 (1966); G. T. Kerr, *ibid.*, 15,  
200 (1969); W. K. Hall, *Chem. Eng. Progr. Symp.*  
*Ser.*, 63, 68 (1967)
12. P. Suppan, *Principles of Photochemistry*, The Chemical  
Society Monographs, No.22, The Chemistry Society  
Publications (1972), T. Matuura, "Yuki Hikari Kagaku",

Chemistry Monograph No.20, p.179, Kagaku Dojin,  
Kyoto (1976)

13. J. V. Crivello, J. H. W. Lam, J. E. Moore and  
S. H. Schroster, *J. Radiat. Curing*, 5, 2 (1978);  
J. V. Crivello, J. H. W. Lam, *Macromolecules*, 10,  
1307 (1977); J. V. Crivello, J. H. W. Lam,  
*J. Polymer Sci., Polym. Chem. Ed.*, 17, 2877 (1979);  
*ibid.*, 17, 1047 (1979); *ibid.*, 1021 (1980); *ibid.*,  
17, 977 (1979); *ibid.*, 16, 2441 (1978)
14. A. G. Brook, *J. Am. Chem. Soc.*, 82, 5102 (1960);  
*ibid.*, 91, 355 (1969)
15. J. Libman, *J. Chem. Soc., Chem. Comm.*, 868 (1977);  
R. Hurley, A. C. Test, *J. Am. Chem. Soc.*, 88, 4330  
(1966); J. A. Barltop, N. J. Bunce, *J. Chem. Soc.*,  
(C), 1467 (1968)
16. K. Teranishi, T. Araki and H. Tani, *Macromolecules*,  
5, 660 (1972); H. Tani, S. Yamashita and K. Teranishi,  
*Polym. J.*, 3, 417 (1972); K. Teranishi, M. Iida,  
T. Araki, S. Yamashita and H. Tani, *Macromolecules*,  
7, 421 (1974); M. Iida, T. Araki, K. Teranishi and  
H. Tani, *Macromolecules*, 10, 275 (1977); M. Iida,  
S. Hayase and T. Araki, *Macromolecules*, 11, 490  
(1978)

## Chapter 2 New Polymerization Catalyst

### 2-1 Introduction

From the concept of new catalyst described in Chapter 1, a new composite polymerization catalysts were found. In this Chapter, profiles of the catalyst are described.

### 2-2 Profiles of the composite catalysts

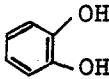
The new catalytic systems are composed of an aluminum complex and a silanol compound. As shown in Table 1. conversion in polymerization of cyclohexene oxide with  $\text{Al}(\text{acac})_3/\text{Ph}_2\text{Si}(\text{OH})_2$  catalyst is compared with that with other catalyst systems: metal complex/ $\text{Ph}_2\text{Si}(\text{OH})_2$  or  $\text{Al}(\text{acac})_3$ /hydroxy compound.

The metal complex or  $\text{Ph}_2\text{Si}(\text{OH})_2$  alone was not active in the polymerization. However, the addition of  $\text{Ph}_2\text{Si}(\text{OH})_2$  to the metal complex catalytically polymerized cyclohexene oxide.  $\text{Al}(\text{acac})_3$  and  $\text{Al}(\text{O-iPr})_3$  had high activity when they were combined with  $\text{Ph}_2\text{Si}(\text{OH})_2$ . The resulting poly(cyclohexene oxide) (soft temp. (50°C)) had about 4400 molecular weight by gel permeation chromatography. A polymer prepared with conventional cationic catalysts ( $\text{OEt}_3\text{BF}_4$  and  $\text{BF}_3 \cdot \text{OEt}_2$ ) was tacky and the molecular weight was only 900.

Composite systems of  $\text{Al}(\text{acac})_3$  with mono- and difunctional alcohols, phenols and monofunctional thiol were



Table 1 Polymerization of Cyclohexene Oxide by Various Catalyst Systems<sup>a</sup>

Metal compound	-OH compound	Polymerization time (h)	Polymer yield(%)	MW
—	Ph <sub>2</sub> Si(OH) <sub>2</sub>	40	0	—
Al(acac) <sub>3</sub>	—	46	0	—
Al(OiPr) <sub>3</sub>	—	46	0	—
BF <sub>3</sub> OEt <sub>2</sub> <sup>b</sup>	—	46	70	900
TiO(acac) <sub>2</sub>	Ph <sub>2</sub> Si(OH) <sub>2</sub>	46	12	3200
Cr(acac) <sub>3</sub>	Ph <sub>2</sub> Si(OH) <sub>2</sub>	46	7	4000
Zr(acac) <sub>4</sub>	Ph <sub>2</sub> Si(OH) <sub>2</sub>	46	4	1700
Zn(acac) <sub>2</sub>	Ph <sub>2</sub> Si(OH) <sub>2</sub>	46	3	—
Co(acac) <sub>3</sub>	Ph <sub>2</sub> Si(OH) <sub>2</sub>	50	3	3300
Cu(acac) <sub>2</sub>	Ph <sub>2</sub> Si(OH) <sub>2</sub>	46	2	3300
Fe(acac) <sub>3</sub>	Ph <sub>2</sub> Si(OH) <sub>2</sub>	50	2	2800
Mn(acac) <sub>2</sub>	Ph <sub>2</sub> Si(OH) <sub>2</sub>	46	1	3000
VO(acac) <sub>2</sub>	Ph <sub>2</sub> Si(OH) <sub>2</sub>	46	1	3000
Ni(acac) <sub>2</sub>	Ph <sub>2</sub> Si(OH) <sub>2</sub>	46	0.5	4000
Al(OiPr) <sub>3</sub>	Ph <sub>2</sub> Si(OH) <sub>2</sub> <sup>c</sup>	47	16	4400
Al(acac) <sub>3</sub>	Ph <sub>2</sub> Si(OH) <sub>2</sub>	40	30	4400
OEt <sub>3</sub> BF <sub>4</sub> <sup>d</sup>	—	40	9	—
Al(acac) <sub>3</sub>	PhSH	40	0	—
Al(acac) <sub>3</sub>	Ph <sub>3</sub> CSH	40	0	—
Al(acac) <sub>3</sub>	PhOH	40	0	—
Al(acac) <sub>3</sub>	Ph <sub>3</sub> COH	40	0	—
Al(acac) <sub>3</sub>	EtOH	40	0	—
Al(acac) <sub>3</sub>	HOCH <sub>2</sub> CH <sub>2</sub> OH	40	0	—
Al(acac) <sub>3</sub>	Ph <sub>3</sub> SiOH <sup>e</sup>	20	52	—
Al(acac) <sub>3</sub>		20	0	—
Al(acac) <sub>3</sub>	Ph <sub>3</sub> GeOH	5	0	—
Al(acac) <sub>3</sub>	Ph <sub>3</sub> SnOH	5	0	—

<sup>a</sup>Polymerization temperature, 40°C; catalyst concentration, metal compound, 0.05 mol%; OH compound, 0.15 OH equivalent %.

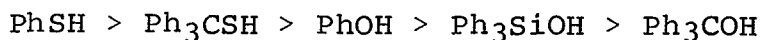
<sup>b</sup>0.01 mol%.

<sup>c</sup>0.05 OH equivalent %.

<sup>d</sup>0.2 mol%.

<sup>e</sup>0.05 OH equivalent %.

inactive for the polymerization of cyclohexene oxide. Salinger and West<sup>1</sup> reported the acidity of various silanols, alcohols, phenols, and thiols by potentiometry and gave the following sequence:



The acidity of  $\text{Ph}_2\text{Si}(\text{OH})_2$  appears to be between the values for  $\text{Ph}_3\text{SiOH}$  and  $\text{Ph}_3\text{COH}$ . Among  $\text{Al}(\text{acac})_3$ /hydroxy compound systems only the  $\text{Al}(\text{acac})_3$ /silanol system, such as  $\text{Al}(\text{acac})_3/\text{Ph}_2\text{Si}(\text{OH})_2$  and  $\text{Al}(\text{acac})_3/\text{Ph}_3\text{SiOH}$ , was active in the polymerization of cyclohexene oxide (Table 1) and the catalyst activity of the  $\text{Al}(\text{acac})_3$ /OH-containing systems did not relate directly to the acidity of hydroxy compounds.

West et al.<sup>2</sup> related the acidity of silanol to  $p\pi-d\pi$ -orbital interaction between the vacant p-orbital of Si and the p-orbital of oxygen. Therefore, the hydroxides of Ge and Sn, which have electron configurations similar to those of Si(IV group), could also be cocatalysts. Among the systems,  $\text{Ph}_3\text{SiOH}/\text{Al}(\text{acac})_3$ ,  $\text{Ph}_3\text{GeOH}/\text{Al}(\text{acac})_3$ , and  $\text{Ph}_3\text{SnOH}/\text{Al}(\text{acac})_3$ , however, only  $\text{Ph}_3\text{SiOH}/\text{Al}(\text{acac})_3$  catalyst showed catalytic activity. West et al.<sup>2</sup> also reported that the  $p\pi-d\pi$  interaction between metal and oxygen decreased in the sequence  $\text{Si-O} > \text{Ge-O} > \text{Sn-O}$ . The difference in catalytic activity is to be attributed to the strength of the interaction.

Figure 1 shows the time-conversion curves when  $\text{Al}(\text{acac})_3/\text{Ph}_2\text{Si}(\text{OH})_2$  and  $\text{Al}(\text{acac})_3/\text{SH6018}$  were used as catalysts. Polymerization with  $\text{Al}(\text{acac})_3/\text{Ph}_2\text{Si}(\text{OH})_2$  catalyst was initially fast but stopped at low conversion. On the other hand, polymerization with  $\text{Al}(\text{acac})_3/\text{SH6018}$  catalyst continued for a longer time. The difference in catalytic activity between  $\text{Ph}_2\text{Si}(\text{OH})_2$  and SH6018 may be due to the polymer effects described in Chapter 7.

Figure 1 also shows a time-conversion curve in which additional SH6018 was added to the polymerization system at the point at which the polymerization rate became slow. In this case polymer conversion increased at the point of SH6018 addition. Addition of  $\text{Al}(\text{acac})_3$ , however, did not increase polymer conversion. From the above the decrease in polymer conversion probably occurs because the silanol is consumed. Thus silanol probably plays an important role in the polymerization of cyclohexene oxide.

Table 2 shows the influence of  $\text{Ph}_2\text{Si}(\text{OH})_2/\text{Al}(\text{acac})_3$  ratio on polymer conversion, where the  $\text{Al}(\text{acac})_3$  is constant at 0.05 mol%. Polymer conversion increased in proportion to the  $\text{Ph}_2\text{Si}(\text{OH})_2/\text{Al}(\text{acac})_3$  ratio. The molecular weight of polymers was constant at 4400. On the other hand, the influence of  $\text{Al}(\text{acac})_3/\text{Ph}_2\text{Si}(\text{OH})_2$  ratio on polymer conversion, where  $\text{Ph}_2\text{Si}(\text{OH})_2$  is constant at 0.15 OH equivalent %, is also shown in Table 2. Polymer yield was decreased with an increase in the  $\text{Al}(\text{acac})_3/\text{Ph}_2\text{Si}(\text{OH})_2$

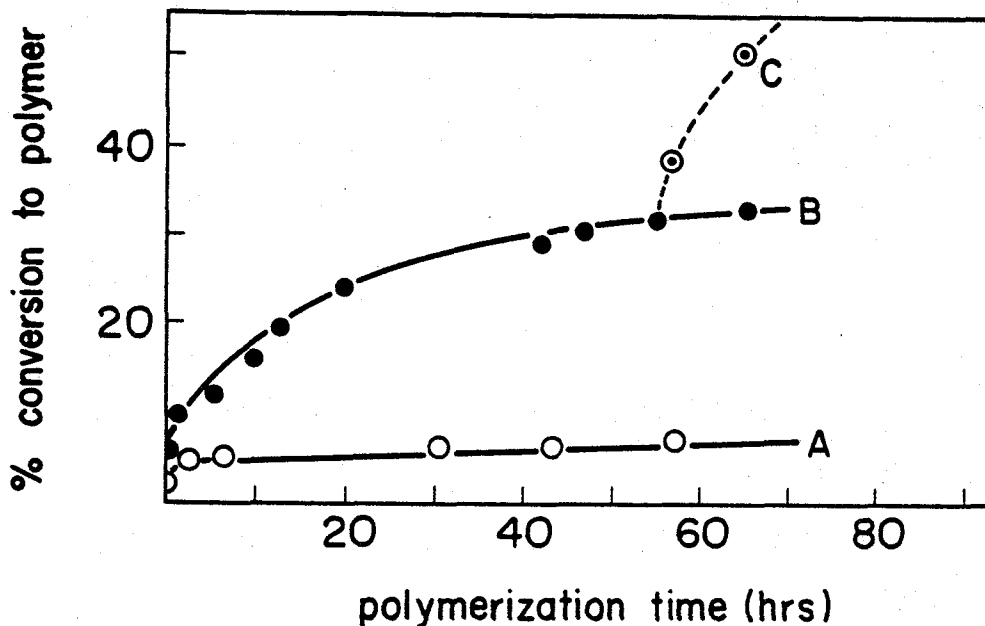


Figure 1 Polymerization of cyclohexene oxide: polymerization temperature, 40°C; Al(acac)<sub>3</sub>, 0.05 mol%; Ph<sub>2</sub>Si(OH)<sub>2</sub>, 0.05 OH equivalent %; SH6018, 0.05 OH equivalent %. (A) Al(acac)<sub>3</sub>/Ph<sub>2</sub>Si(OH)<sub>2</sub>; (B) Al(acac)<sub>3</sub>/SH6018; (C) addition of more SH6018 to (B) at 55 h (0.05 OH equivalent %).

Table 2 Polymerization of Cyclohexene Oxide<sup>a)</sup>

Al(acac) <sub>3</sub> mol %	Ph <sub>2</sub> Si(OH) <sub>2</sub> mol %	Polymerization time (h)	conversion (%)	M.W.
0.05	0.05	1	5	4400
0.05	0.10	1	9	4400
0.05	0.15	1	12	4400
0.05	0.20	1	17	4400
1.5	0.075	86	27	-
3.0	0.075	86	24	-
8.7	0.075	86	20	-

a) polymerization temperature 40°C.

ratio. This polymerization behavior is explained by a decrease in SiOH in the polymerization system which is consumed by the side reactions discussed in Chapter 3.

#### References

1. R. M. Salinger and R. West, J. Organometal. Chem. 11, 631 (1968)
2. R. West and R. H. Baney, J. Am. Chem. Soc., 81, 6145 (1959)

## Chapter 3 Dependence of Catalytic Activity on Silanol Structure

### 3-1 Introduction

Profile of polymerization of cyclohexene oxide with  $\text{Al}(\text{acac})_3$ /Silanol catalyst showed that silanol plays an important role for the polymerization. In this Chapter, the structure of silanol was varied, and the dependence of the catalyst activity on the structure of silanol was described.

### 3-2 Stability of silanol compounds in self-condensation

Silanols are unstable and in some cases condense to oligo or polysiloxanes. The stability of the silanols used as cocatalysts was examined in THF in the presence of  $\text{Al}(\text{acac})_3$ , shown in Figure 1. Disubstituted Si compounds like  $\text{Ph}_2\text{Si}(\text{OH})_2$  and  $\text{MePhSi}(\text{OH})_2$  were thermally unstable, but trisubstituted compounds like  $\text{Et}_3\text{SiOH}$ ,  $\text{Ph}_3\text{SiOH}$ ,  $\text{MePh}_2\text{SiOH}$ , and  $\text{Me}_2\text{PhSiOH}$  were relatively stable. These compounds did not condense under polymerization conditions. Therefore polymerization behavior was examined by using trisubstituted compounds as cocatalysts to eliminate any effect due to self-condensation.

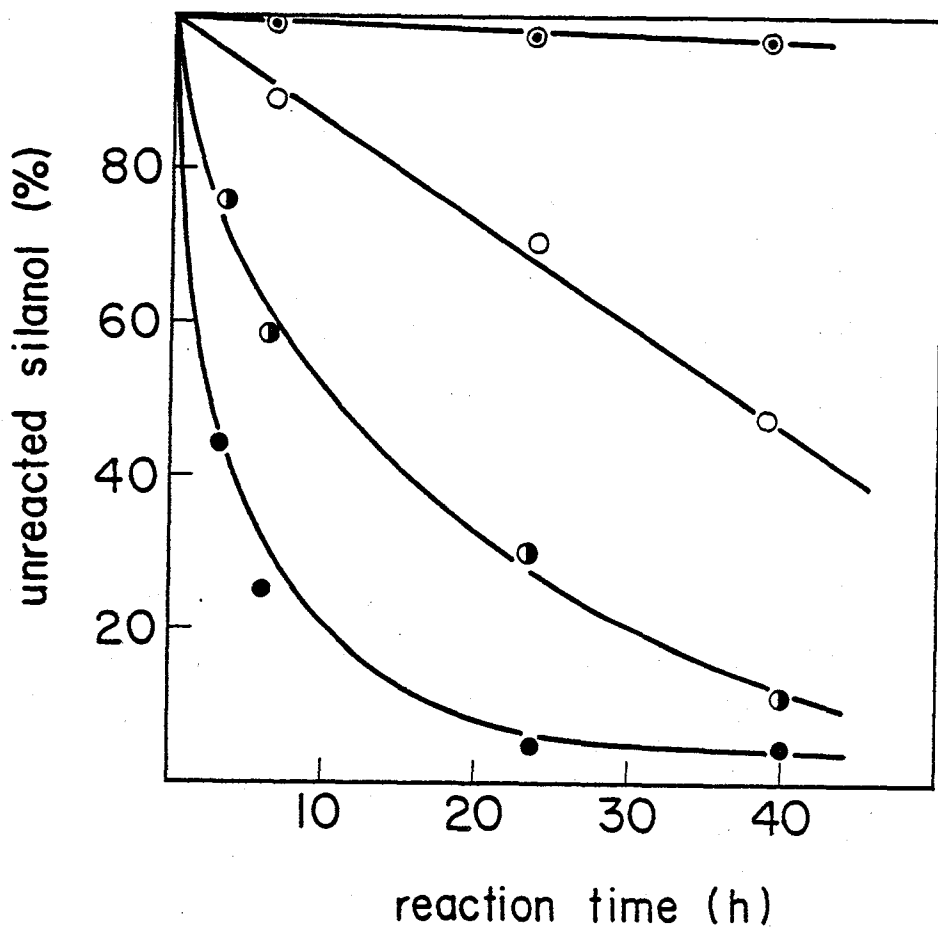


Figure 1 Stability of various silanols: (—●—)  $\text{MePhSi(OH)}_2\text{-Al(acac)}_3$ ; (—●—)  $\text{EtPhSi(OH)}_2\text{-Al(acac)}_3$ ; (—○—)  $\text{Ph}_2\text{Si(OH)}_2\text{-Al(acac)}_3$ ; (—⊙—)  $\text{R}_3\text{SiOH-Al(acac)}_3$ ;  $\text{R}_3\text{SiOH}$ ;  $\text{Ph}_3\text{SiOH}$ ,  $\text{Ph}_2(\text{CH}_2=\text{CH})\text{SiOH}$ ,  $\text{MePh}_2\text{SiOH}$ ,  $\text{Me}_2\text{PhSiOH}$ ,  $\text{Et}_3\text{SiOH}$ .

### 3-3 Polymerization behavior with Al(acac)<sub>3</sub>-R<sub>3</sub>SiOH

#### catalyst

Figure 2 shows the conversion-time curve of polymer with Al(acac)<sub>3</sub>-R<sub>3</sub>SiOH catalysts. The catalytic activity for silanols with electron-withdrawing substituents like Ph<sub>3</sub>SiOH or Ph<sub>2</sub>(CH<sub>2</sub>=CH)SiOH was higher than that for silanols with electron-donating substituents like MePh<sub>2</sub>SiOH or Me<sub>2</sub>PhSiOH. The relationship between the relative acidity of these cocatalysts and the relative catalytic activity is described in Figure 3. The abscissa shows the difference in <sup>1</sup>H-NMR chemical shift between the SiOH signal measured in d<sub>6</sub>-DMSO and that measured in CDCl<sub>3</sub> as the relative acidity. The ordinate shows the initial rate of polymerization, when the rate with Al(acac)<sub>3</sub>-Ph<sub>3</sub>SiOH catalyst is 1, as the catalytic activity. Apparently, the larger the relative acidity of silanol, the higher the relative catalytic activity.

In Figure 2 polymerization behavior with Al(acac)<sub>3</sub>/Ph<sub>3</sub>SiOH catalyst is different from the behavior with Al(acac)<sub>3</sub>/Ph<sub>2</sub>(CH<sub>2</sub>=CH)SiOH catalyst; that is, the former polymerization continued with time but the latter stopped at low conversion. Cyclohexene oxide was polymerized by 10 mol% of Al(acac)<sub>3</sub> and 10 mol% of silanol in d<sub>8</sub>-THF, and the polymerization behavior was examined by <sup>1</sup>H-NMR to determine the difference. The intensity of signal due to SiOH decreased with polymerization time, but the rate of



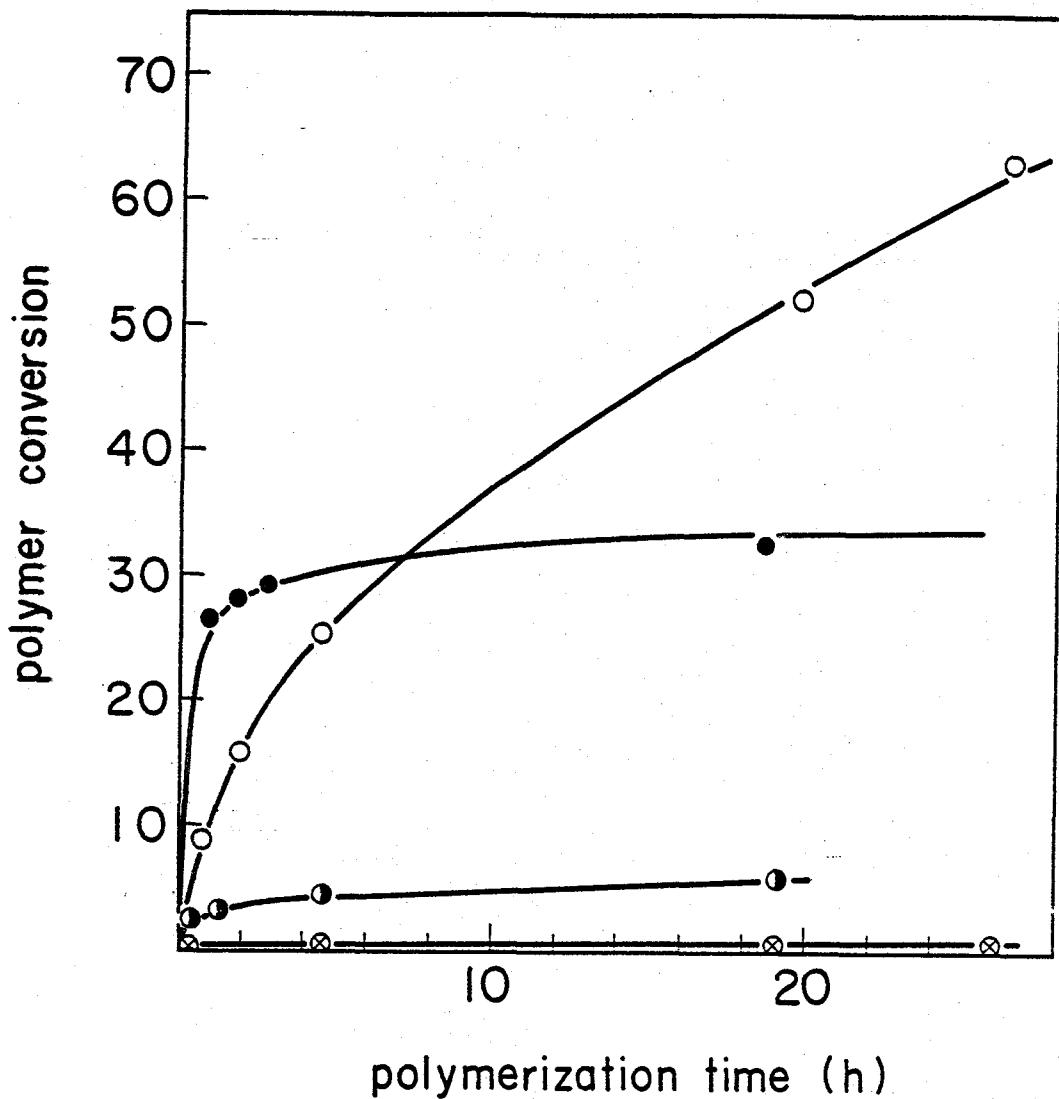


Figure 2 Polymerization of cyclohexene oxide: (—○—)  $\text{Ph}_3\text{SiOH-Al}(\text{acac})_3$ ; (—●—)  $\text{Ph}_2(\text{CH}_2=\text{CH})\text{SiOH-Al}(\text{acac})_3$ ; (—●—)  $\text{MePh}_2\text{SiOH-Al}(\text{acac})_3$ ; (—⊗—)  $\text{Me}_2\text{PhSiOH-Al}(\text{acac})_3$ .  $\text{Al}(\text{acac})_3$  0.05 mol%, silanol 0.05 mol%, 40°C,

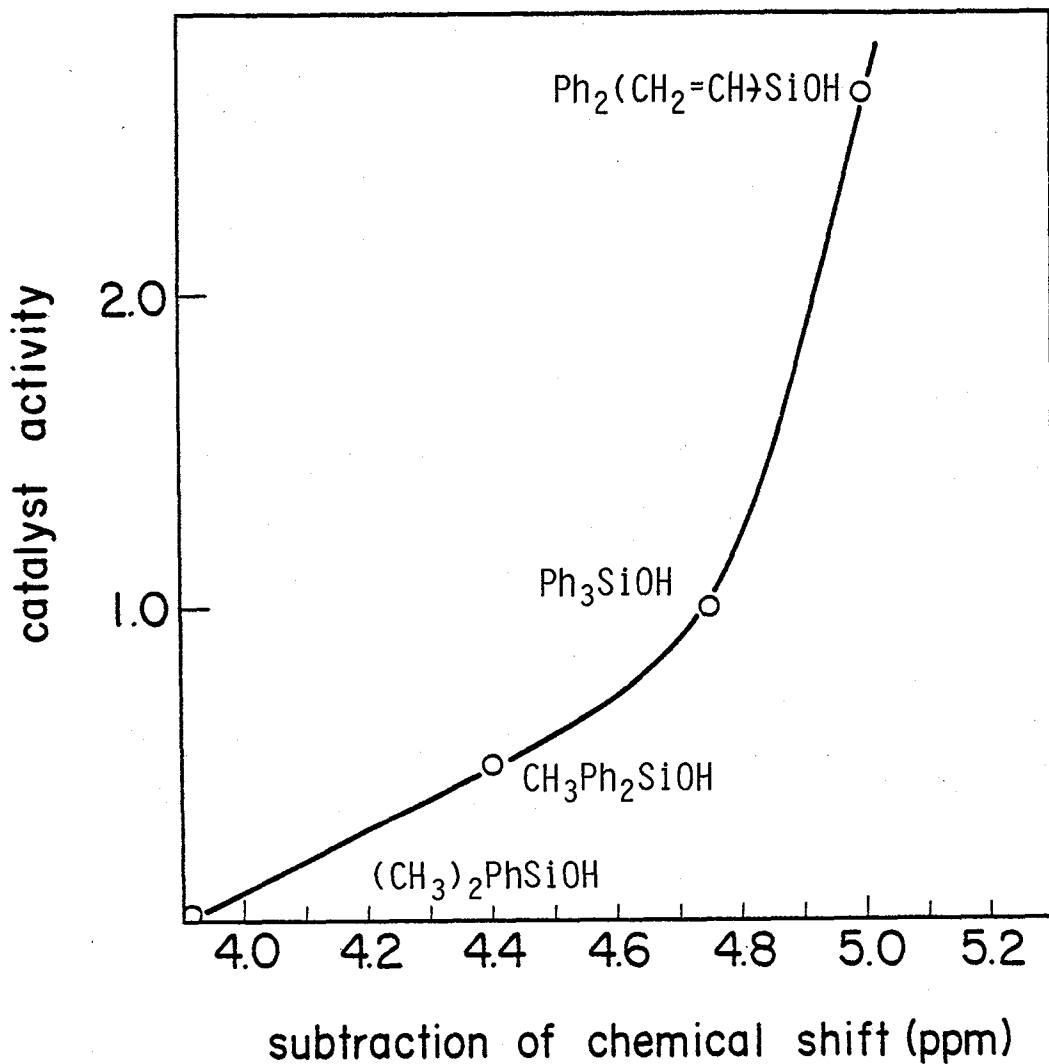


Figure 3 Relation between the relative catalytic activity and the relative acidity. Relative catalytic activity: the rate with  $\text{Al}(\text{acac})_3\text{-Ph}_3\text{SiOH}$  catalyst = 1. Polymerization conditions, see Figure 2.

decrease with  $\text{Ph}_3\text{SiOH}$  was smaller than the corresponding rate with  $\text{MePh}_2\text{SiOH}$  and  $\text{Ph}_2(\text{CH}_2=\text{CH})\text{SiOH}$ , as shown in Figure 4. It was believed that these decreases were not caused by self-condensation of silanols (Fig. 1) but by the addition of the silanol to the epoxide. In case of  $\text{Al}(\text{acac})_3/\text{Ph}_3\text{SiOH}$  catalyst the polymerization continues with time because steric hindrance makes it difficult to add  $\text{Ph}_3\text{SiOH}$  to epoxide. In case of  $\text{Al}(\text{acac})_3/\text{MePh}_2\text{SiOH}$  and  $\text{Al}(\text{acac})_3/\text{Ph}_2(\text{CH}_2=\text{CH})\text{SiOH}$  catalysts, however,  $\text{Ph}_2(\text{CH}_2=\text{CH})\text{SiOH}$  and  $\text{MePh}_2\text{SiOH}$  add to the epoxide more easily than  $\text{Ph}_3\text{SiOH}$  because of the reduced steric hindrance.

Figure 5 shows that the molecular weight of the polymer obtained by  $\text{Al}(\text{acac})_3\text{-Ph}_3\text{SiOH}$  catalyst is larger than that obtained by  $\text{Al}(\text{acac})_3\text{-MePh}_2\text{SiOH}$  catalyst. The termination step may be slower with the bulky silanol.

#### 3-4 Kinetics of polymerization with $\text{Al}(\text{acac})_3\text{-Ph}_3\text{SiOH}$ catalyst

The polymer conversion was plotted against the polymerization time to find a first order of concentration of cyclohexene oxide (Fig. 6).

The  $k$  (rate constant) was determined by the slope in Figure 6 and  $\log k$  was plotted against  $\log$  (silanol) (concentration of silanol), as shown in Figure 7. The reaction order  $n$  of the concentration of silanol was about

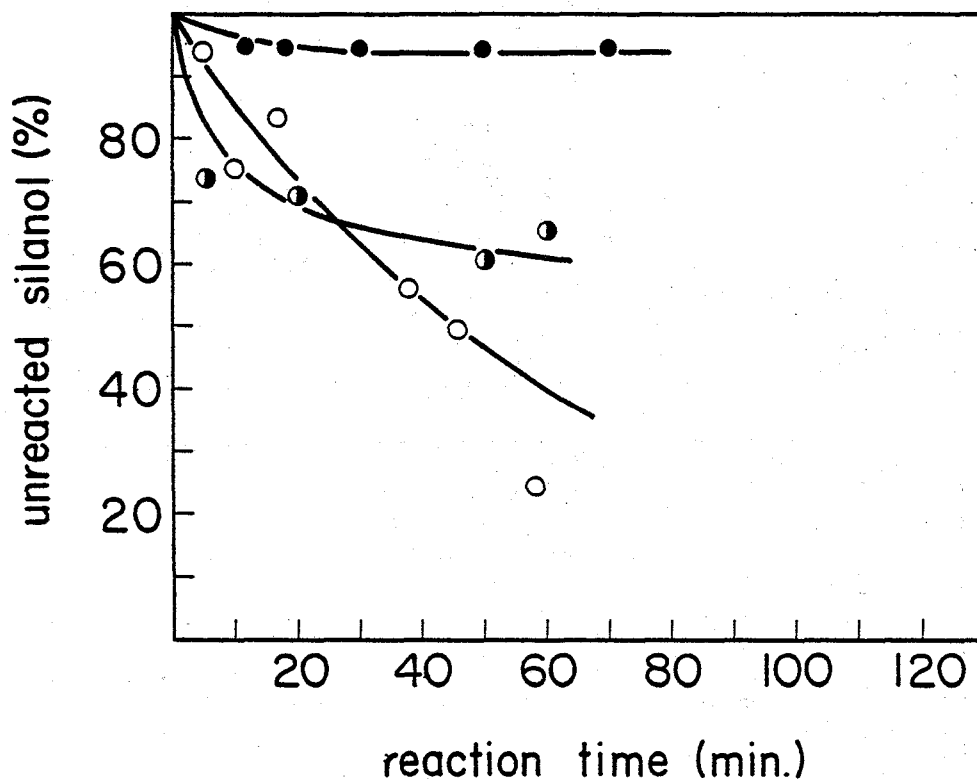


Figure 4 Decrease in silanol compounds in the polymerization system: (—●—) Ph<sub>3</sub>SiOH/Al(acac)<sub>3</sub>; (—●—) MePh<sub>2</sub>SiOH/Al(acac)<sub>3</sub>; (—○—) Ph<sub>2</sub>(CH<sub>2</sub>=CH)SiOH/Al(acac)<sub>3</sub>

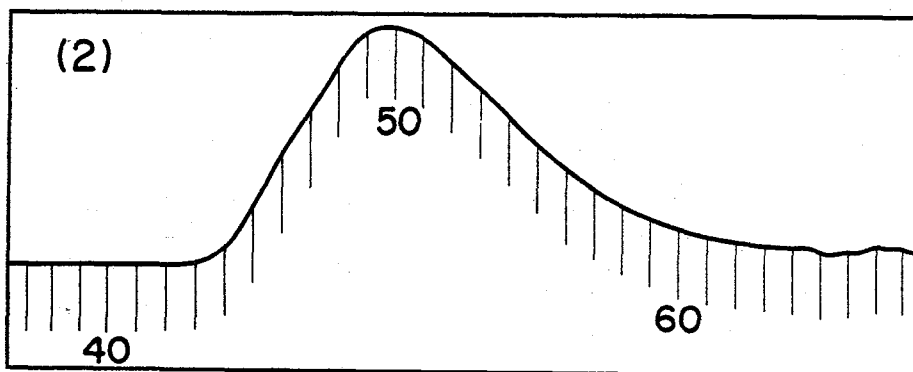
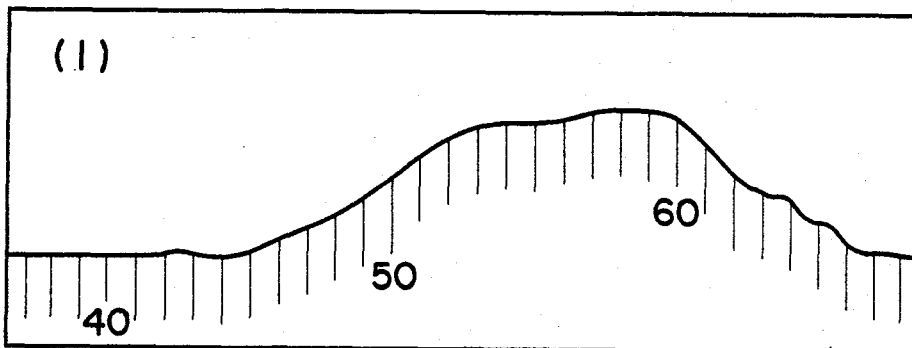


Figure 5 GPC curves of polycyclohexene oxide:

(1)  $\text{Ph}_2\text{MeSiOH}/\text{Al}(\text{acac})_3$ ; (2)  $\text{Ph}_3\text{SiOH}/\text{Al}(\text{acac})_3$

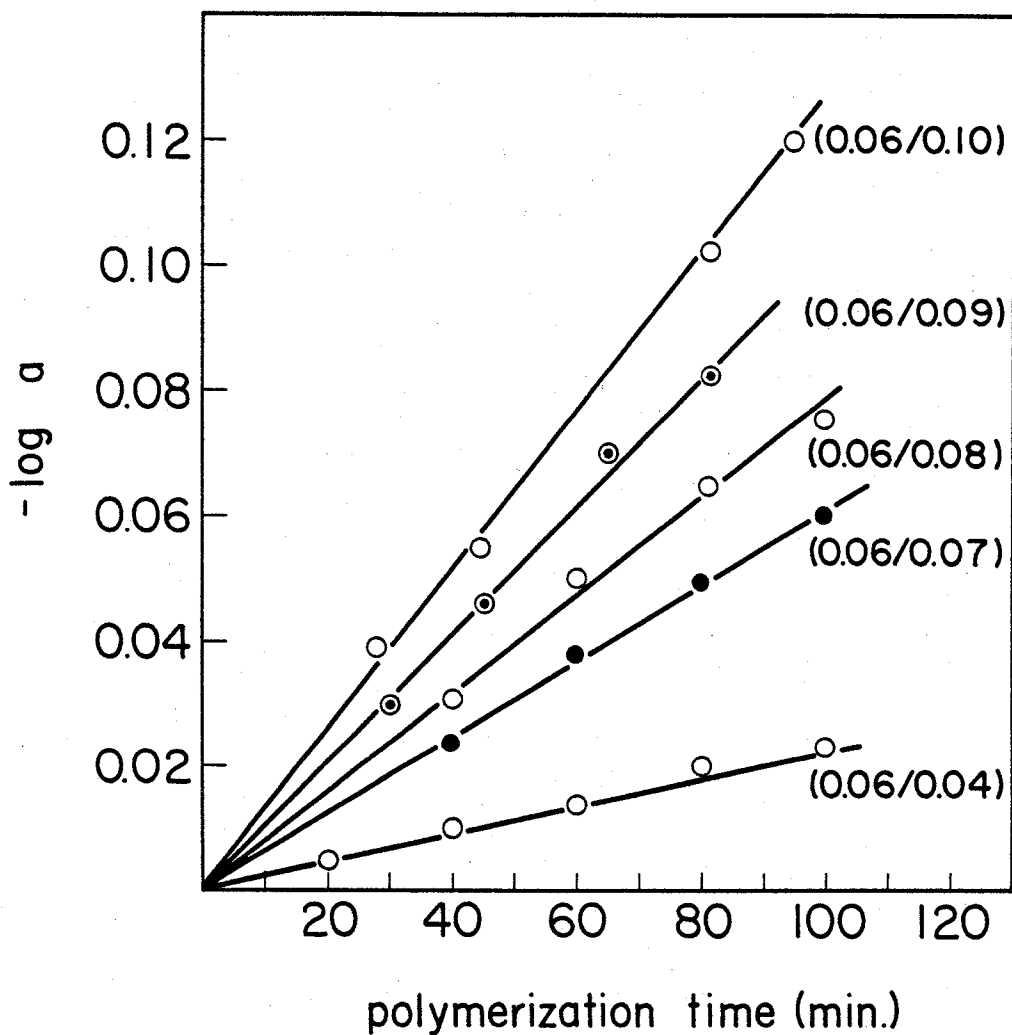


Figure 6 First-order plot of cyclohexene oxide polymerization. The values in parentheses show catalytic concentration ( $\text{Al}(\text{acac})_3/\text{Ph}_3\text{SiOH}$ ) (mol%/mol%): (a) polymer conversion.

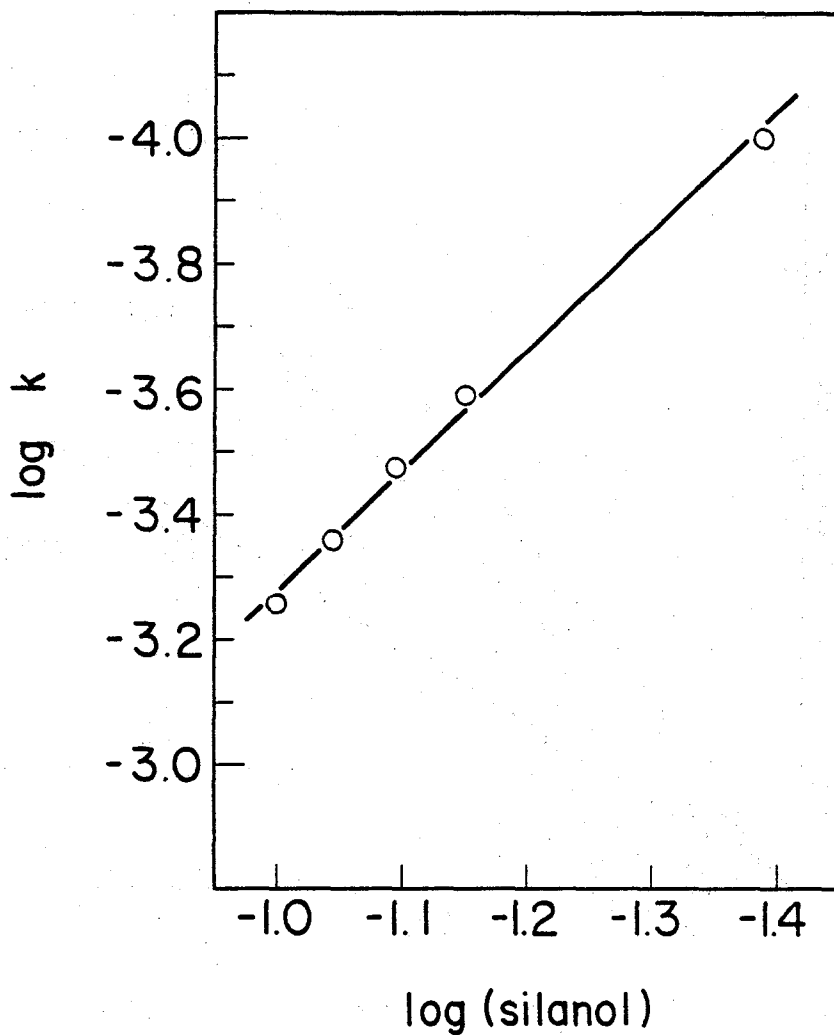


Figure 7 Relation between  $\log k$  and  $\log (\text{silanol})$ :  
 $k$ ; rate constant,  $(\text{silanol})$ ; concentration of  
silanol.

1.9 from the slope. Therefore it is believed that two silanol groups participate in the polymerization reaction.

### 3-5 Interaction of silanol with $\text{Al}(\text{acac})_3$

$\text{Al}(\text{acac})_3$  could not react with silanol and could not form another compound before polymerization, a condition supported by the fact that the signal of  $\text{Al}(\text{acac})_3$  did not change when the polymerization catalyzed by 10 mol% of  $\text{Al}(\text{acac})_3$  and  $\text{Ph}_3\text{SiOH}$  was followed by  $^1\text{H-NMR}$ . Therefore it is believed that the interaction between  $\text{Al}(\text{acac})_3$  and silanol is important for polymerization. When the  $^1\text{H-NMR}$  spectrum of the  $\text{Ph}_3\text{SiOH}$  alone was measured in  $\text{CDCl}_3$  the sharp signal of  $\text{SiOH}$  was observed. This signal shifted to a lower field and broadened when  $\text{Al}(\text{acac})_3$  was added. The shift was larger as the  $\text{Al}(\text{acac})_3/\text{Ph}_3\text{SiOH}$  ratio was increased, as shown in Table 1. Measured at the same concentration, the value of the shift decreased in the following sequence:  $\text{Al}(\text{acac})_3\text{-Ph}_3\text{SiOH} > \text{Al}(\text{acac})_3\text{-Ph}_2\text{MeSiOH} > \text{Al}(\text{acac})_3\text{-Ph}_3\text{GeOH}$ , which related to the catalytic activity.

### 3-6 Conclusion

The results showed that in order to obtain active catalyst, it was necessary to strengthen the acidity of the silanol, to prevent the silanol from self-condensa-



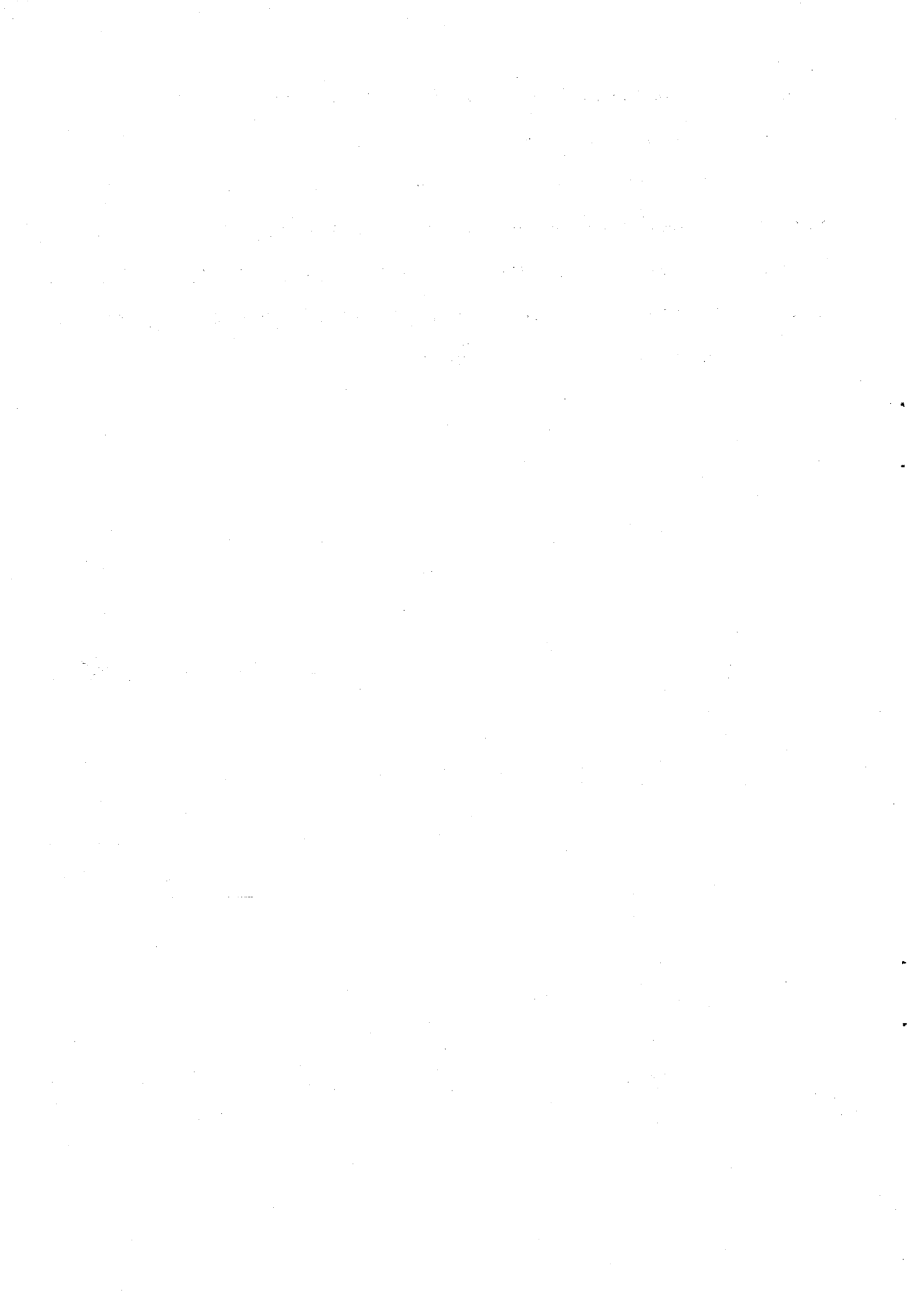
Table 1 Chemical Shift of OH Signal<sup>a)</sup>

OH compound	Presence of Al(acac) <sub>3</sub>		Absence of Al(acac) <sub>3</sub>		(A) - (B) or (C) - (B) (ppm)
	Al(acac) <sub>3</sub>		in CDCl <sub>3</sub> (B) (ppm)	in DMSO (A) (ppm)	
	OH compound (mol/mol)	in CDCl <sub>3</sub> (C) (ppm)			
Ph <sub>3</sub> SiOH	1/3b)	2.49	2.36	—	0.13
Ph <sub>3</sub> SiOH	2/3b)	2.55	2.36	—	0.19
Ph <sub>3</sub> SiOH	1b)	2.60	2.36	—	0.24
Ph <sub>3</sub> SiOH	4/3b)	2.63	2.36	—	0.27
MePh <sub>2</sub> SiOH	1/3b)	2.11	2.03	—	0.08
MePh <sub>2</sub> SiOH	2/3b)	2.16	2.03	—	0.13
MePh <sub>2</sub> SiOH	1b)	2.21	2.03	—	0.18
MePh <sub>2</sub> SiOH	4/3b)	2.24	2.03	—	0.21
Ph <sub>3</sub> GeOH	1b)	1.72	1.60	—	0.12
Ph <sub>3</sub> SiOH	—	—	2.36	7.12	4.73
Ph <sub>3</sub> GeOH	—	—	1.60	5.36	3.76
Ph <sub>3</sub> SnOH	—	—	1.71	3.00	1.29

a) Measuring condition, 35°C.

b) Concentration of silanols was constant at 0.17 mol/L in CDCl<sub>3</sub>.

tion and to prevent the silanol from the addition to epoxide, which terminated the polymerization. To realize such properties, it seems necessary to introduce an electron-withdrawing group and a bulky group in the neighbour of silanol moiety. Silanols such as diphenylsilanediol, triphenylsilanol and diphenylvinylsilanol were effective as an active catalyst component.



## Chapter 4 Dependence of Catalytic Activity in the Structure of Chelating Ligand on Aluminum

### 4-1 Introduction

The polymerization of cyclohexene oxide with various metal compound/diphenylsilanediol catalyst systems has been examined. Since the catalysts were deactivated after a certain period, the catalyst deactivation caused by self-condensation of diphenylsilanediol and the addition to epoxides had to be considered. Therefore, the catalyst activity was examined with a triphenylsilanol which does not self-condense and add to epoxides easily, as shown in Table 1. The catalyst activity varied with identity of metal chelates, as follows:  $\text{Al}(\text{acac})_3 > \text{SnCl}_2(\text{acac})_2 > \text{MoO}_2(\text{acac})_2 > \text{Zr}(\text{acac})_4 > \text{Cr}(\text{acac})_3 > \text{Fe}(\text{acac})_3 > \text{Rh}(\text{acac})_3$ . In order to examine the interaction between these compounds and the triphenylsilanol, the half-value width of the SiOH in the triphenylsilanol was measured with  $^1\text{H-NMR}$  in an equimolar solution of metal compound/triphenylsilanol in  $\text{CDCl}_3$ , as shown in Table 1. The polymer conversion correlated with the interaction strength. Table 1 also shows the relation between the polymer conversion and the interaction of  $\text{Al}(\text{acac})_3$ -phenol,  $\text{Al}(\text{acac})_3$ -thiophenol. The extent of the interaction between them was much smaller than that between the  $\text{Al}(\text{acac})_3$  and the triphenylsilanol with lower acidity than that of the thiophenol or

Table 1 Polymerization of CHO with a Metal  
Compound/ $\text{Ph}_3\text{SiOH}$  Catalyst<sup>a)</sup>

Metal compound	Polymer conversion (%)	Half value width of silanol (Hz)
$\text{Al}(\text{acac})_3$	100	24
$\text{SnCl}_2(\text{acac})_2$	25.0	14
$\text{MoO}_2(\text{acac})_2$	12.0	—
$\text{Zr}(\text{acac})_4$	8.5	10
$\text{Rh}(\text{acac})_3$	1.9	10
$\text{Fe}(\text{acac})_3$	2.4	—
$\text{Cr}(\text{acac})_3$	2.6	—
* $\text{Al}(\text{acac})_3\text{-PhOH}$	0	8
* $\text{Al}(\text{acac})_3\text{-PhSH}$	0	9

a) Polymerization conditions: 48 h at 40°C, metal compound 0.05 mol%,  $\text{Ph}_3\text{SiOH}$  0.05 mol%.

\*PhOH or PhSH was added instead of the  $\text{Ph}_3\text{SiOH}$ .

the phenol.<sup>1</sup> The polymer conversion was also low. Therefore, the interaction strength between them was not caused by the acidity of OH compounds only. The interaction was appreciable especially in the case of the combination between aluminum complex and silanol, and a high catalyst activity was found.

#### 4-2 Polymerization with a tris( $\beta$ -diketonato)aluminum/triphenylsilanol system

The results of the previous section implied that the interaction between silanol and aluminum complex was important in order to activate the catalyst. Therefore, the dependence of the structure of aluminum complex on the catalytic activity and relation between the interaction strength and the catalytic activity were investigated. The catalyst activity was first examined with tris( $\beta$ -diketonato)aluminum/triphenylsilanol catalyst system. The resultant initial polymerization rate, a half-value width of SiOH and a weight-average molecular weight are shown in Table 2. The catalyst activity for tris( $\beta$ -diketonato)aluminum with electron withdrawing groups (trifluoromethyl, phenyl, p-fluorophenyl group) was low. Especially, the catalyst activity was negligible for the aluminum complexes with two electron withdrawing groups, such as DFPhPD and PhFBD. The aluminum catalyst had higher activity when electron donating groups were sub-

Table 2 Polymerization of CHO with a Tris( $\beta$ -diketonato)aluminum/ $\text{Ph}_3\text{SiOH}$  Catalyst<sup>a)</sup>

Abbreviation	Ligand	Polymn. rate (mol/min./mol cat.)	Half value width of SiOH (Hz)	$\overline{M}_w \times 10^{-3}$
DFPhPD	$p\text{-FC}_6\text{H}_4\text{COCH}_2\text{CO}p\text{-FC}_6\text{H}_4$	0	—	—
PhFBD	$\text{CF}_3\text{COCH}_2\text{COPh}$	0	13	—
FPD	$\text{CF}_3\text{COCH}_2\text{COCH}_3$	0.6	19	17
PhPD	$\text{CH}_3\text{COCH(Ph)COCH}_3$	2.0	—	15
DMFHD	$(\text{CH}_3)_3\text{CCOCH}_2\text{COCF}_3$	1.4	10	16
acac	$\text{CH}_3\text{COCH}_2\text{COCH}_3$	3.7	24	16
BzBD	$\text{PhCH}_2\text{COCH}_2\text{COCH}_3$	0.8	—	15
TMPD	$(\text{CH}_3)_2\text{CHCOCH}_2\text{COCH}(\text{CH}_3)_2$	4.2	30	17
DPM	$(\text{CH}_3)_3\text{CCOCH}_2\text{COC}(\text{CH}_3)_3$	18.4	—	16
ACH	$\text{CH}_3\text{COCHCO}(\text{CH}_2)_4$	6.4	23	15

a) Polymerization conditions; 40°C, Al compound 0.05 mol%,  $\text{Ph}_3\text{SiOH}$  0.05 mol%

stituted. Moreover, higher catalyst activity was observed when the half value width of the SiOH signals increased (see Table 2). The interaction between aluminum complex and silanol was correlated with the catalytic activity.

#### 4-3 Polymerization with tris( $\beta$ -ketoesterato)aluminum/ triphenylsilanol system

$pK_a$  of ethylacetoacetate is 11.2 and larger than that of acetylacetone (9.76).<sup>2</sup> Therefore electron density of carbonyl oxygen of tris(ethylacetoacetato)aluminum was considered to be larger than that of tris(acetylacetonato)aluminum and high activity was expected. As shown in Table 3, improvement in the catalytic activity was found when tris( $\beta$ -ketoesterato)aluminum was used. The catalyst activity was also enhanced by introducing an electron donating group. It decreased when a phenyl group was introduced to the ligand and increased when a methyl group was substituted. The introduction of an alkyl group to ester moiety of the ligand was also effective for the catalytic activation.

The molecular weight for the polymer obtained with catalysis of tris( $\beta$ -ketoesterato)aluminum/triphenylsilanol was higher than that obtained with tris( $\beta$ -diketonato)-aluminum/triphenylsilanol. The variation in ligand properties did not appreciably change the molecular weight. The  $^1H$ -NMR spectrum of a mixture of tris( $\beta$ -ketoesterato)-



Table 3 Polymerization of CHO with a Tris( $\beta$ -ketoesterato)aluminum/ $\text{Ph}_3\text{SiOH}$  Catalyst<sup>a)</sup>

abbreviation	Ligand	Polymn. rate (mol/min./mol cat.)	$\overline{M}_w \times 10^{-3}$
EtPhPD	$\text{PhCOCH}_2\text{COOC}_2\text{H}_5$	4.2	29
Etaa	$\text{CH}_3\text{COCH}_2\text{COOC}_2\text{H}_5$	7.0	31
nPraa	$\text{CH}_3\text{COCH}_2\text{COOC}_3\text{H}_7$	9.8	30
iBuaa	$\text{CH}_3\text{COCH}_2\text{COOC}_4\text{H}_9$	12.6	31
EtMtaa	$\text{CH}_3\text{COCH}(\text{CH}_3)\text{COOC}_2\text{H}_5$	8.8	31
tBuaa	$\text{CH}_3\text{COCH}_2\text{COOC}(\text{CH}_3)_3$	13.0	30

a) Polymerization conditions; 40°C, Al compound 0.05 mol%,  $\text{Ph}_3\text{SiOH}$  0.05 mol%

aluminum and triphenylsilanol showed that a part of the ligand was free, as shown in Figure 1. This was not observed in case of the tris( $\beta$ -diketonato)aluminum/triphenylsilanol system. The amount of free ligand reached equilibrium values at 15 - 20 mol%, Al(Etaa)<sub>3</sub> : 18 mol%, Al Al(nPraa)<sub>3</sub> : 18 mol%, Al(iBuaa)<sub>3</sub> : 20 mol%, Al(tBuaa) : 15 mol%) within ten minutes after mixing equimoles of tris( $\beta$ -ketoesterato)aluminum with triphenylsilanol at 25°C. The free ligand ratio did not change appreciably by the ligand variation.

#### 4-4 Polymerization with a tris(*ortho*-carbonylphenolato)aluminum/triphenylsilanol catalyst systems

The above results implied that a species of an aluminum compound, obtained after the aluminum complex reacted with triphenylsilanol, was more active in the presence of triphenylsilanol. Therefore, the catalytic activity of a tris(*ortho*-carbonylphenolato)aluminum/triphenylsilanol catalyst system was investigated to determine the relation between the catalytic activity and the molar ratio of the liberated ligand.

Resultant polymerization results are shown in Table 4. The extent of the ligand liberation was measured only in case of tris(salicylaldehydato)aluminum as 25 mol%. The catalytic activity of tris(*ortho*-carbonylphenolato)-aluminum/triphenylsilanol was generally higher than that

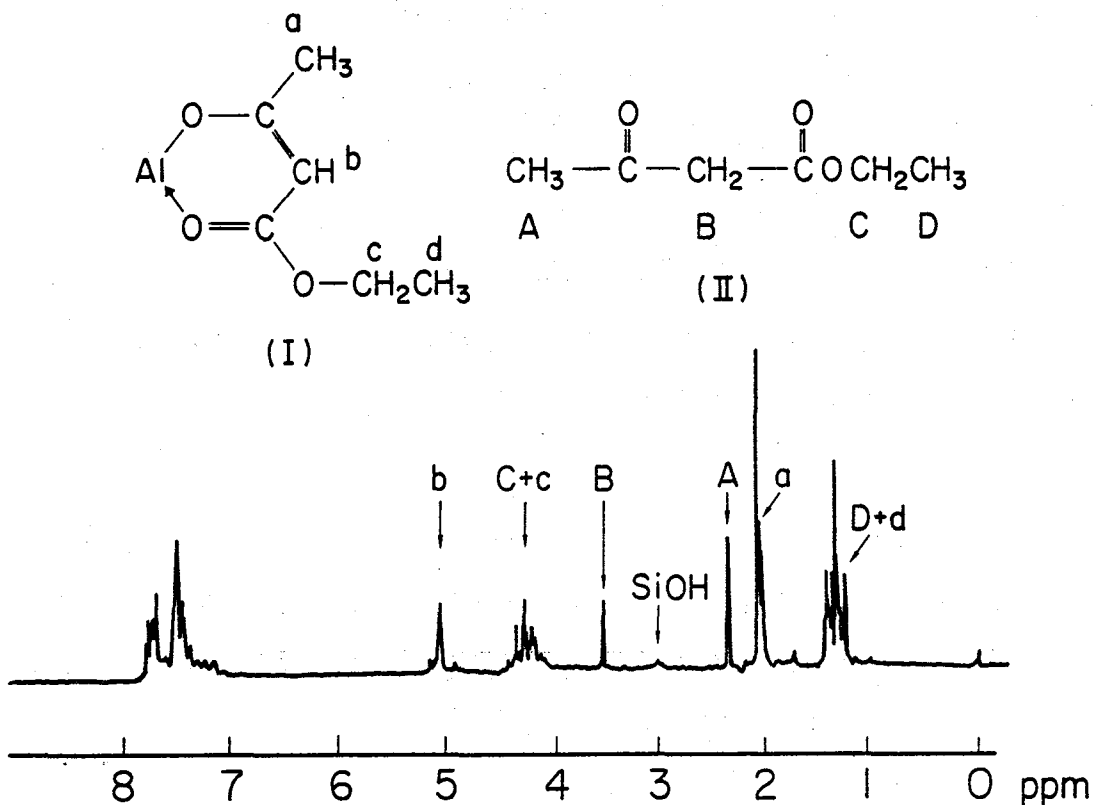
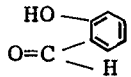
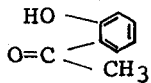
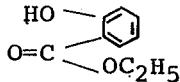
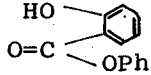


Figure 1  $^1\text{H-NMR}$  spectrum for  $\text{Al}(\text{Etaa})_3/\text{Ph}_3\text{SiOH}$  catalyst system:

Capital letter: signal of liberated ligand.

Small letter: signal of  $\text{Al}(\text{Etaa})_3$ . Refer to the experimental section for the measurement of interaction strength between aluminum complex and silanol.

Table 4 Polymerization of CHO with a Tris(*ortho*-carbonylphenolato) aluminum/Ph<sub>3</sub>SiOH Catalyst<sup>a)</sup>

Abbreviation	Ligand	Polymerization rate (mol/min./mol cat.)	$\overline{M}_w \times 10^{-3}$
SA		59	37
AP		74	35
EtSA		112	37
φSA		109	36

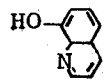
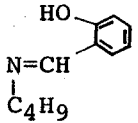
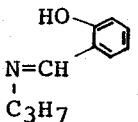
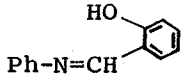
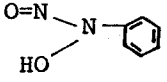
a) Polymerization conditions; 40°C, Al complex 0.05 mol%, Ph<sub>3</sub>SiOH 0.05 mol%

of tris( $\beta$ -ketoesterato)aluminum/triphenylsilanol or tris( $\beta$ -diketonato)aluminum/triphenylsilanol. The same substitution effect was also seen, namely, introduction of an electron donating group activated the catalyst. The weight-average molecular weight for the polymer, obtained with the tris(*ortho*-carbonylphenolato)aluminum/triphenylsilanol, was higher than that obtained with a tris( $\beta$ -ketoesterato)aluminum/triphenylsilanol.

#### 4-5 Polymerization with N, O-chelates of aluminum compound/triphenylsilanol catalyst system

The catalytic activity of N, O-chelates of aluminum compound was considered to be higher than that of O, O-chelating aluminum complex because a SiOH moiety would probably interact with the nitrogen stronger than the oxygen. However, a tris(oxinato)aluminum and a Schiff base-type aluminum complex with an alkyl group bonding to nitrogen did not have catalytic activity. Aluminum complex with a phenyl group, bonding to the coordinating nitrogen, had catalyst activity, as shown in Table 5. The substitution effect on the catalyst activity reversed as compared to the case of the O, O-chelated aluminum complex. This fact implied that the catalyst activity was retarded by strong interaction. A moderate interaction between an aluminum complex and a triphenylsilanol is required for the catalyst activity.

Table 5 Polymerization of CHO with a N,O-chelated Aluminum Complex/Ph<sub>3</sub>SiOH Catalyst<sup>a)</sup>

Abbreviation	Ligand	Polymerization rate (mol/min./mol cat.)
OX		0
SA·nBu		0
SA·nPr		0
SA·A		1.0
NPHA		3.4

a) Polymerization conditions; 40°C, Al complex 0.05 mol%, Ph<sub>3</sub>SiOH 0.05 mol%

#### 4-6 Spin lattice relaxation time ( $T_1$ ) for the $^1\text{H-NMR}$ signal assigned to SiOH Group

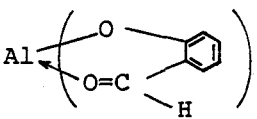
The interaction of a triphenylsilanol with an aluminum complex was considered to occur at the SiOH moiety. The  $T_1$  value for  $^1\text{H-NMR}$  signal assigned to SiOH was found to be influenced by the interaction strength.

The results are shown in Table 6.  $T_1$  value for a triphenylsilanol in  $\text{CDCl}_3$  was 2.5 seconds. On an equimolar addition of a tris( $\beta$ -diketonato)aluminum to the triphenylsilanol in  $\text{CDCl}_3$ , the  $T_1$  value of the SiOH peak decreased to 1.4 - 2.2 seconds. On the other hand, on addition of an equimolar quantity of a tris( $\beta$ -ketoesterato)-aluminum or a tris(salicylaldehydato)aluminum, the  $T_1$  value for the signal due to the SiOH decreased to 0.5 - 0.8 second. Namely, the interaction between a triphenylsilanol and the aluminum complex, which did not liberate the ligand, was smaller than that between a triphenylsilanol and the aluminum complex, which liberated the ligand.

#### 4-7 Reaction scheme

In case of the tris( $\beta$ -diketonato)aluminum, the ligand was not liberated by the reaction with a diphenylsilanediol. In an equimolar mixture of cyclohexene oxide, diphenylsilanediol and  $\text{Al}(\text{acac})_3$ , the copolymer of the cyclohexene oxide and the diphenylsilanediol was obtained. An acetyl-

Table 6 Variation on  $T_1$  Values for an NMR Signal Assigned to the SiOH of the  $\text{Ph}_3\text{SiOH}$  in the Presence of an Aluminum Complex<sup>a)</sup>

Aluminum compound	$T_1$ (sec.)
—	2.5
$\text{Al}(\text{CH}_3\text{COCHCOCH}_3)_3$	1.9 ~ 2.2
$\text{Al}((\text{CH}_3)_2\text{CHCOCHCOCH}(\text{CH}_3)_2)_3$	1.4 ~ 2.2
$\text{Al}(\text{CH}_3\text{COCHCOOC}_2\text{H}_5)_3$	0.5
$\text{Al}(\text{CH}_3\text{COC}(\text{CH}_3)\text{COOC}_2\text{H}_5)_3$	0.7
 $\text{Al} \left( \begin{array}{c} \text{O} \\ \text{O}=\text{C} \\ \text{H} \end{array} \right)_3$	0.8

a)  $T_1$  values were determined with ten different times:

0.05, 0.10, 1.00, 1.50, 1.60, 1.70, 1.80, 1.90, 2.00, 10

second for  $\text{Al}(\text{CH}_3\text{COCHCOOC}_2\text{H}_5)_3/\text{Ph}_3\text{SiOH}$ ,  $\text{Al}(\text{CH}_3\text{COCCOOC}_2\text{H}_5)_3/$

$\text{Ph}_3\text{SiOH}$ ,  $\text{Al} \left( \begin{array}{c} \text{O} \\ \text{O}=\text{C} \\ \text{H} \end{array} \right)_3 / \text{Ph}_3\text{SiOH}$  system. 0.05, 0.10, 0.50,

0.70, 1.00, 1.30, 1.50, 1.70, 2.00, 10 second for  $\text{Ph}_3\text{SiOH}$ ,

$\text{Al}(\text{CH}_3\text{COCHCOCH}_3)_3/\text{Ph}_3\text{SiOH}$ ,  $\text{Al}((\text{CH}_3)_2\text{CHCOCHCOCH}(\text{CH}_3)_2)_3/$

$\text{Ph}_3\text{SiOH}$  system.  $T_1$  values of  $\text{Al}(\text{CH}_3\text{COCHCOCH}_3)_3/\text{Ph}_3\text{SiOH}$

and  $\text{Al}((\text{CH}_3)_2\text{CHCOCHCOCH}(\text{CH}_3)_2)_3/\text{Ph}_3\text{SiOH}$  system were

calculated from null point.



acetone residue was not involved in the copolymer. The signal of the  $\text{Al}(\text{acac})_3$  in the  $^1\text{H-NMR}$  spectrum did not change during the polymerization with 10 mol% of the  $\text{Al}(\text{acac})_3$ /triphenylsilanol catalyst system in  $d_8$ -THF. The catalytic activity correlated with the acidity of a trisubstituted silanol and the electronegativity of the  $\text{C}=\text{O}$  moiety for the aluminum complex. The catalyst activity also correlated with the interaction strength between a silanol and an aluminum complex. Interaction mechanism as shown in Figure 2 is proposed.

The  $\text{SiOH}$  proton is detached from the oxygen when the triphenylsilanol interacts with the tris( $\beta$ -diketonato)-aluminum. The separated proton will cationically polymerize the cyclohexene oxide.

In another initiation mechanism, a silanol interacts with an aluminum with a coordinative unsaturation, as shown in Figure 3.

According to this mechanism, an aluminum complex with electron withdrawing groups should be active because the chelate ring of the aluminum complex will easily be lost. However no such trend was observed.

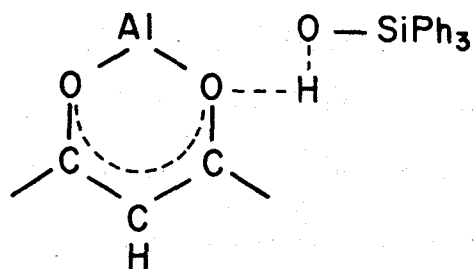
When using a tris( $\beta$ -ketoesterato)aluminum/triphenylsilanol and a tris(*ortho*-carbonylphenolato)aluminum/triphenylsilanol catalyst, a part of the ligand was found to be liberated from the aluminum complex. The following compound was considered to be formed by the reaction be-

tween the catalyst components.



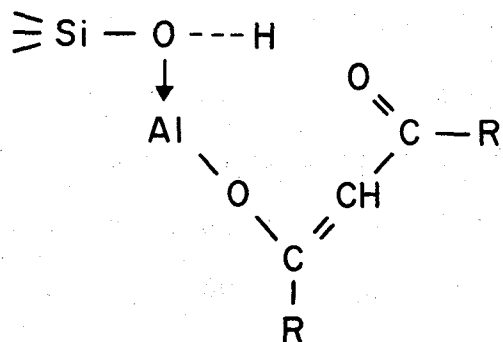
$\text{L}_{3-n}\text{Al}(\text{OSiPh}_3)_n$  formation was confirmed with the IR absorbance of a Si-O-Al linkage ( $1070 \text{ cm}^{-1}$ ) in the product after an ethyl acetoacetate was removed from the reaction mixture of the tris(ethylacetoacetato)aluminum and the triphenylsilanol. However, a compound containing Al-O-SiR<sub>3</sub> linkages, such as  $((\text{CH}_3)_3\text{SiO})_3\text{Al}$ , was not catalytically active at the low catalyst concentration, such as 0.05 mol%. Therefore, a SiOH moiety was considered to be necessary for the catalyst activity. Considering the interaction strength between an aluminum complex and a triphenylsilanol, as inferred with the T<sub>1</sub> measurement, interaction mechanism as shown in Figure 3 was proposed.

Thus, the silanol is activated at two points. The silanol is activated by the interaction of the aluminum with the oxygen of the SiOH and by the interaction of an oxygen in Al-O-Si linkage with the proton of the SiOH. Therefore, the interaction between the silanol and the aluminum complex would be stronger than that in the tris-( $\beta$ -diketonato)aluminum/triphenylsilanol system. The reaction was similar to a silica-aluminum catalyst. The catalyst is considered to be a soluble model system of the silica-alumina catalyst.<sup>3</sup> The following facts suggest the new consideration. SiO<sub>2</sub>-ZrO<sub>2</sub> and SiO<sub>2</sub>-TiO<sub>2</sub>



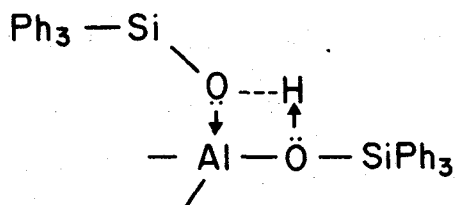
Interaction mechanism I

Figure 2



Interaction mechanism II

Figure 3



Interaction mechanism III

Figure 4

besides  $\text{SiO}_2\text{-Al}_2\text{O}_3$  are as two component metal oxide catalysts containing a strong acidity point.<sup>4</sup> The  $\text{Zr}(\text{acac})_3/\text{silanol}$  and  $\text{TiO}(\text{acac})_2/\text{silanol}$  also polymerized a cyclohexene oxide, however their activity was lower than the  $\text{Al}(\text{acac})_3/\text{silanol}$  system. As an unreacted aluminum compound was also present in the polymerization system, the interaction was considered to be caused by the interaction mechanisms I and III.

Eastham et al. have reported a polymerization of ethylene oxide with a  $\text{BF}_3\text{-H}_2\text{O}$  catalyst system. The polymerization was catalyzed by  $\text{H}^+ \cdot [\text{BF}_4\text{OH}]^-$  species.<sup>5</sup> Russell and Vail reported a  $\text{SnCl}_4$ -phenols catalyst system for a cationic polymerization of a isobutene.<sup>6</sup> Here, the polymerization was catalyzed by the activated proton of phenols and a phenolate anion was present as a counter anion. Termination was considered to be caused by the attack of the phenolate ion or a proton transfer.<sup>6</sup> In the present catalyst, a silanol is considered to play a similar role to that for the phenol. The mechanism of polymerization with the aluminum complex/silanol catalyst could estimate from that with silica-alumina catalyst.

Initiation mechanism as shown in Figure 5 was considered. The initiation caused by  $\text{H}^+$  similar to Brönsted acid was supported by the fact that the polymer structure obtained with the aluminum complex/silanol was atactic as mentioned the following section. The silanolate anion

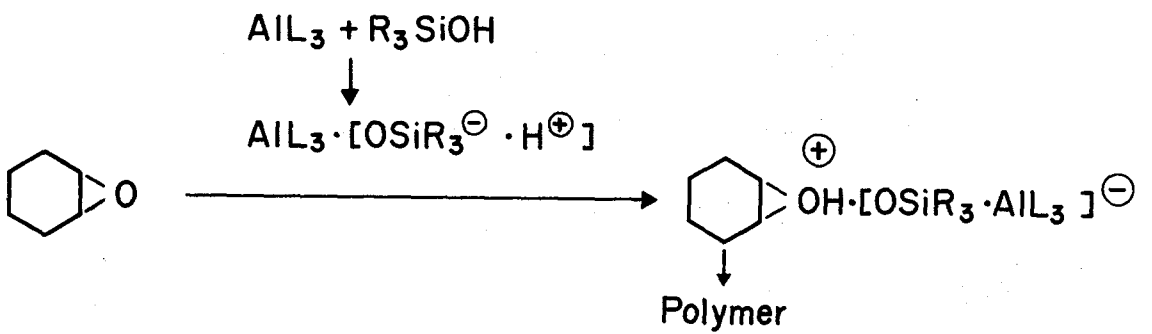


Figure 5 Polymerization mechanism

will be present as a counter anion.

The termination was considered to be caused by the silanolate anion addition to a polymer end. The presumption on the termination was supported by the following factors.

a) When a cyclohexene oxide was polymerized by 100 mol% of the  $\text{Al}(\text{acac})_3/\text{Ph}_2\text{Si}(\text{OH})_2$  catalyst, a copolymer of cyclohexene oxide and  $\text{Ph}_2\text{Si}(\text{OH})_2$  was obtained. When a polymeric silanol, such as SH6018 (Toray silicone, molecular weight, about 1600), was used, a GPC curve of the polymer had two peaks. The higher molecular weight peak disappeared after NaOH treatment. This fact shows that the polymer had a C-O-Si $\equiv$  linkage due to the termination.

b) When the cyclohexene oxide was polymerized with the  $\text{Al}(\text{acac})_3$ /trisubstituted silanol catalyst, the amount of silanol with less bulky substituents decreased with polymerization time in the polymerization system. However no such trend was observed when a silanol with bulky substituents was used. The molecular weight of the polymer was lower than that obtained with the silanol with bulky substituents.

c) When the silanol with bulky substituents was used, the polymerization activity was higher than that observed with the less bulky substituent. Silanols have been known to react with epoxide to form the C-O-Si linkage.<sup>7</sup>

The polymerization proceeded with a considerable

chain transfer, which was indicated by the fact that the molecular weight of the polymer obtained by  $\text{Al}(\text{acac})_3/\text{Ph}_2\text{Si}(\text{OH})_2$  catalyst system did not depend on polymerization time. To obtain the information about the chain transfer step, the  $^1\text{H}$ -nmr spectrum of the oligomer, obtained with an equimolar quantity of the  $\text{Al}(\text{acac})_3/\text{Ph}_2\text{Si}(\text{OH})_2$  catalyst, was examined. Olefinic proton signals at  $4.5 \sim 4.8$  ppm<sup>6</sup> indicated the reaction as shown in Figure 6. The chain transfer reaction was considered to contain a proton transfer from the polymer end to the catalyst anion.<sup>6</sup>

#### 4-8 Conclusion

The followings are found to be important for the present catalytic polymerization.

- 1)  $\alpha$ -position of carbonyl group in ligand is substituted with electron donating groups.
- 2) The ratio of reaction between aluminum complex and silanol is about  $20 \sim 25$  mol%, where an equimolar aluminum complex is used with silanol.

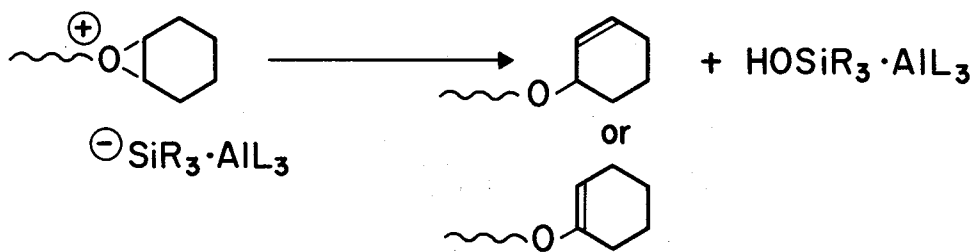


Figure 6 Termination mechanism



## References

1. R. M. Salinger and R. West, *J. Organometal. Chem.* 11, 631 (1968)
2. M. Calvin, K. W. Wilson, *J. Am. Chem. Soc.*, 67, 2003 (1945)
3. M. W. Tamele, *Dis. Faraday Soc.*, 8, 270 (1960)
4. K. Shibata, T. Kiyoura, J. Kitagawa, T. Sumiyoshi and K. Tanabe, *Bull. Chem. Soc. Japan*, 47, 1064 (1974)
5. D. J. Worsford and A. M. Eastham, *J. Am. Chem. Soc.* 79, 900 (1957); A. E. Bastham, "The Chemistry of Cationic Polymerization", P. H. Plesch, ed., Pergamon Press, New York, 1963, Chapter 10; G. A. Latremouille, G. T. Merrall, and A. M. Eastam, *J. Am. Chem. Soc.*, 82, 120 (1960), *ibid.*, *Can. J. Chem.*, 38, 1967 (1960)
6. K. E. Russel and L. G. M. C. Vail, *Can. J. Chem.*, 57, 2355 (1979); R. F. Bauer, R. T. LaFair and K. E. Russell, *Can. J. Chem.*, 48, 1251 (1970)
7. H. M. Banc, U. S. Pat. 3971747

## Chapter 5 Catalyst Supported on Zeolite and Porous Silica

### 5-1 Introduction

SiOH and Al-O-Si moieties are also found on the surfaces of zeolite and SiO<sub>2</sub>. Therefore it is expected that a combination of zeolite/silanol and silica gel/aluminum compound will polymerize cyclohexene oxide. Porous silica interacts with silanol compounds to result in a change of silanol properties, which in turn will influence catalytic activity.

### 5-2 Aluminum compound/silicagel catalyst

Figure 1 shows the polymer conversion-time curve for the cyclohexene oxide polymerization with Al(acac)<sub>3</sub>/silica gel catalyst. The behavior of the catalyst was similar to that of Al(acac)<sub>3</sub>/diphenylsilanediol catalyst; that is, after fast polymerization, the rate subsided. It was found that 0.36 wt% of hydrogen was contained in this silica gel by hydrogen analysis in dry N<sub>2</sub>. If water is eliminated by heat, SiOH is considered present. The amount of SiOH in silica gel calculated using this value was 2 mol % to the cyclohexene oxide. When the polymer yield was compared under the same catalyst concentration, the catalytic activity of Al(acac)<sub>3</sub>-silica gel was about 1/100 that of the Al(acac)<sub>3</sub>-diphenylsilanediol catalyst system.

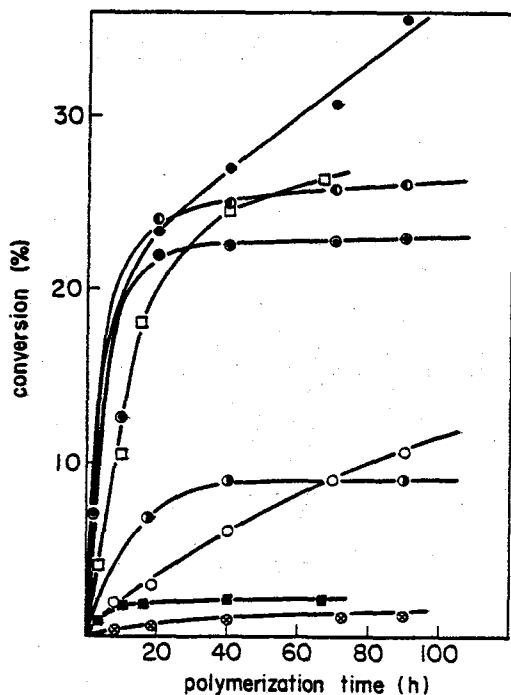


Figure 1 Polymerization of cyclohexene oxide by various catalysts\*: polymerization temperature 40°C; catalyst (—□—)  $\text{Al}(\text{acac})_3\text{-MePhSi}(\text{OH})_2\text{-silica C}$ , (—■—)  $\text{Al}(\text{acac})_3\text{-MePhSi}(\text{OH})_2$ , (—●—)  $\text{Al}(\text{acac})_3\text{-Ph}_2\text{Si}(\text{OH})_2\text{-silica C}$ , (—●—)  $\text{Al}(\text{acac})_3\text{-Ph}_2\text{Si}(\text{OH})_2\text{-9F}$ , (—⊙—)  $\text{Al}(\text{acac})_3\text{-Ph}_2\text{Si}(\text{OH})_2$ , (—●—)  $\text{Al}(\text{acac})_3\text{-silica gel}$ , (—⊗—) 9F, (—○—) 9F- $\text{Ph}_2\text{Si}(\text{OH})_2$ ; concentration  $\text{Al}(\text{acac})_3$ , 0.05 mol%; inorganic compound, 5 wt%,  $\text{Ph}_2\text{Si}(\text{OH})_2$ , 0.15 OH equivalent %.<sup>†</sup>

\*  $\text{Al}(\text{acac})_3$  and silica C have low catalyst activity in cyclohexene oxide polymerization. The time-polymer conversion curves shown in Figure 1 were corrected by the amount of polymer obtained by catalysis of  $\text{Al}(\text{acac})_3\text{-silica C}$ .

† OH equivalent, the molecular weight of silanol compound divided by the amount of SiOH in the silanol compound; (mol%), (mol of catalyst/mol of monomer) x 100; OH equivalent %, (OH equivalent of catalyst/mol of monomer) x 100.

### 5-3 Zeolite/silanol catalyst system

The zeolites used were 4A, 5A, 6A, and 9F. These zeolites by themselves gave only a low amount of polymer at 40°C. However, the zeolite-silanol system polymerized cyclohexene oxide. The polymer conversion-time curve is presented in Figure 1, and shows that this catalyst resisted deactivation more than the diphenylsilanediol- $\text{Al}(\text{acac})_3$  catalyst did. The effect of pore size on polymer yield was examined, and the results are shown in Figure 2. There is a large increase between 4A and 5A. The molecular weight of polymer obtained with zeolite 5A-diphenylsilanediol catalyst was three times as was obtained with  $\text{Al}(\text{acac})_3$ -diphenylsilanediol catalyst (Fig. 3).

We suggest that the activity of this catalyst is due to the stability of silanol during the polymerization process. In order to examine this possibility, the thermal stability of diphenylsilanediol supported by zeolite was studied in THF with GPC. Silanol compounds readily form siloxane by self-condensation; consequently a substantial amount of silanol in the polymerization system will be lost and catalytic activity will decrease. Thus it is expected that stabilization of silanol enhances catalytic activity. As shown in Figure 4, the stability of diphenylsilanediol supported by zeolites decreased in the order 5A >> 3A >  $\text{Al}(\text{acac})_3$ .

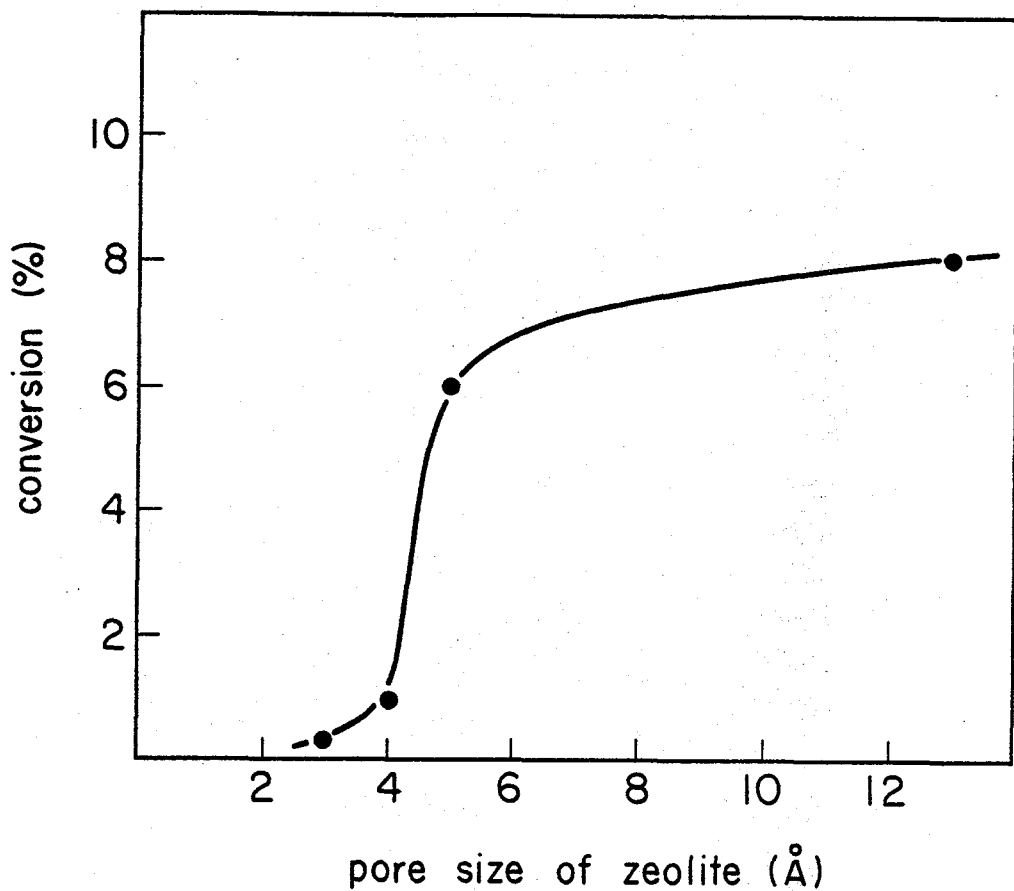


Figure 2 Polymerization of cyclohexene oxide with  $\text{Ph}_2\text{Si}(\text{OH})_2$  supported on zeolites: catalyst concentration,  $\text{Ph}_2\text{Si}(\text{OH})_2$ , 0.15 OH equivalent %; zeolite, 5 wt%; polymerization conditions, 40°C, 70 h.

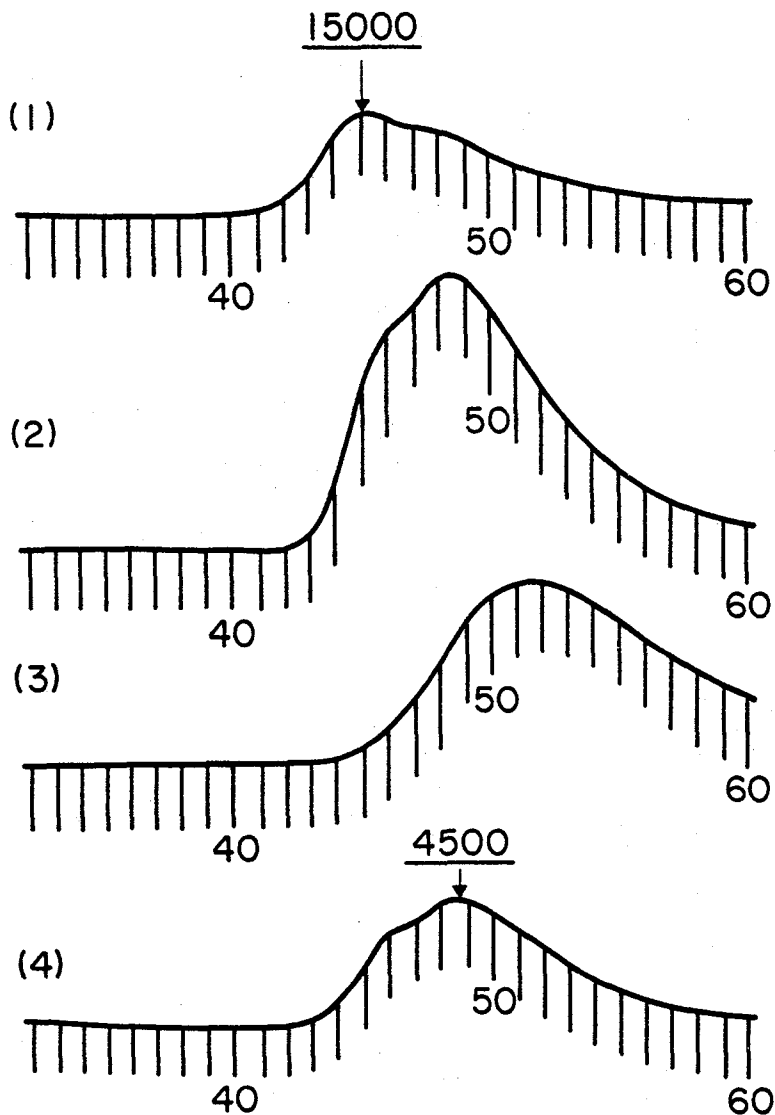


Figure 3 GPC curves for polymers obtained by various catalysts: (1) zeolite 5A- $\text{Ph}_2\text{Si}(\text{OH})_2$ , (2)  $\text{Al}(\text{acac})_3$ - $\text{Ph}_2\text{Si}(\text{OH})_2$ -silica C, (3)  $\text{Al}(\text{acac})_3$ -silica gel, (4)  $\text{Al}(\text{acac})_3$ - $\text{Ph}_2\text{Si}(\text{OH})_2$ .

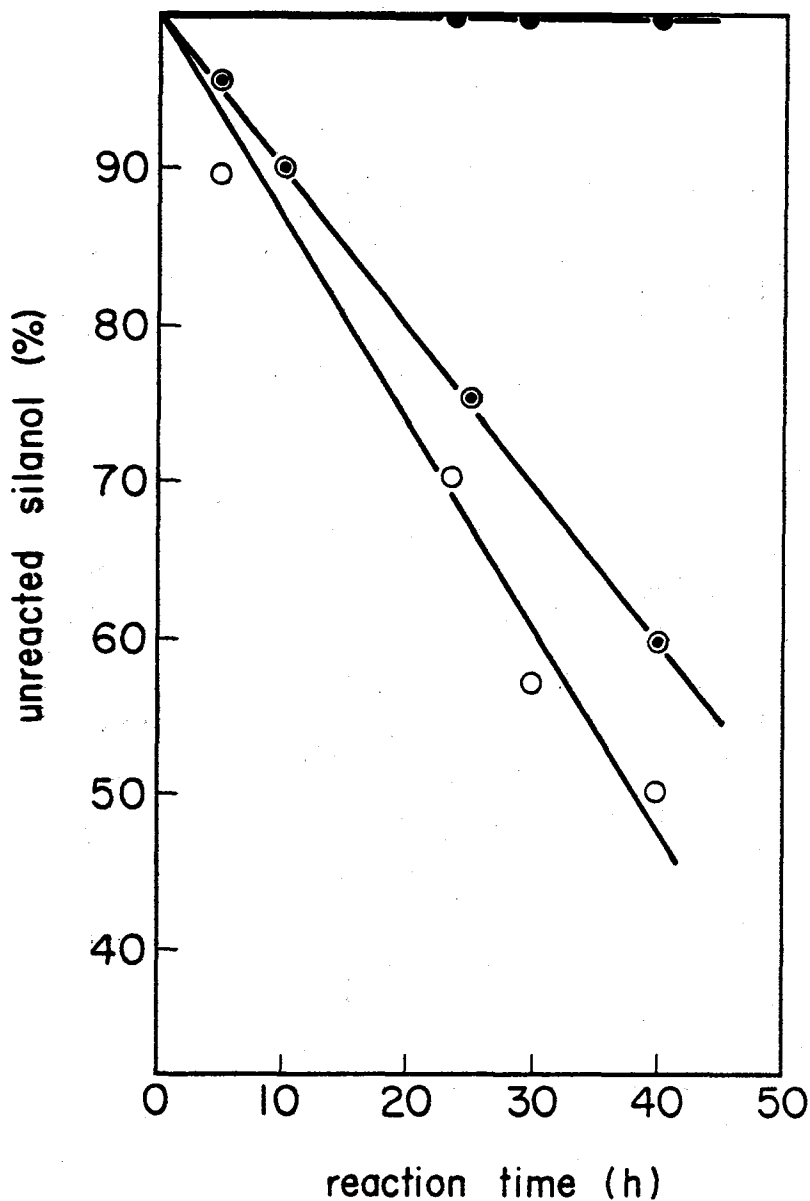


Figure 4 Stability of  $\text{Ph}_2\text{Si}(\text{OH})_2$  supported by zeolites at  $40^\circ\text{C}$ : solvent, THF;  $\text{Al}(\text{acac})_3/\text{Ph}_2\text{Si}(\text{OH})_2 = 1$  (mol/OH equivalent);  $\text{Ph}_2\text{Si}(\text{OH})_2$ , 2.4 wt% to THF; zeolite, 5 wt% to THF; (—○—)  $\text{Ph}_2\text{Si}(\text{OH})_2\text{-Al}(\text{acac})_3$  (—●—)  $\text{Ph}_2\text{Si}(\text{OH})_2\text{-5A}$ , (—⊙—)  $\text{Ph}_2\text{Si}(\text{OH})_2\text{-3A}$ .

To investigate the interaction between zeolite and diphenylsilanediol in detail, NMR spectra of diphenylsilanediol were measured in the presence of zeolite in  $d_8$ -THF. The SiOH difference in chemical shift between diphenylsilanediol only and diphenylsilanediol in the presence of zeolite will be proportional to the magnitude of the interaction between the silanol and the zeolite. The interaction between zeolite and diphenylsilanediol decreased in the sequence,  $9F > 5A > 4A > 3A$ , which relates to catalytic activity as shown in Figure 5. From these results it appears that, in the zeolite/diphenylsilanediol catalyst system, the silanol is activated by interaction with zeolite and catalytic activity is enhanced.

Figure 1 also shows the polymer conversion-time curve for the zeolite  $9F/Al(acac)_3/Ph_2Si(OH)_2$  catalyst system. Polymerization conversion did not level off but continued to increase, and the polymer was obtained at high yield. Moreover, molecular weight of this polymer was higher than that polymerized by an  $Al(acac)_3-Ph_2Si(OH)_2$  catalyst, as shown in Table 1.

#### 5-4 $Al(acac)_3$ /silanol compound catalyst system supported by porous silica

As mentioned before, polymer conversion is changed by using silanol compound as cocatalyst, as follows: (i) Silanols with a phenyl group, e.g.,  $Ph_2Si(OH)_2$ , were more



Table 1 Polymerization of Cyclohexene Oxide<sup>a)</sup>

Run	Al(acac) <sub>3</sub> (mol%)	Ph <sub>2</sub> Si(OH) <sub>2</sub> (mol%)	Polymer- ization time (h)	Adsor- bent	(wt%)	Polymer conversion (%)	M <sub>n</sub>	M <sub>w</sub>
1	0.05	0.075	40	3A	5	20	2600	5400
2	0.05	0.075	40	4A	5	18	2900	5800
3	0.05	0.075	40	5A	5	26	5400	9700
4	0.05	0.075	40	9F	5	28	4400	8600
5	...	0.150	40	5A	5	8	7500	13,000
6	...	0.225	40	5A	5	10	7000	12,500
7	...	0.300	40	5A	5	18	6300	11,700
8	0.05	0.150	20	5A	5	35	4400	8700
9	0.05	0.225	20	5A	5	43	3900	7800
10	0.05	0.300	20	5A	5	60	3300	6900
11	0.05	0.075	40	...	...	22	2300	4500

a) Polymerization temperature 40°C.

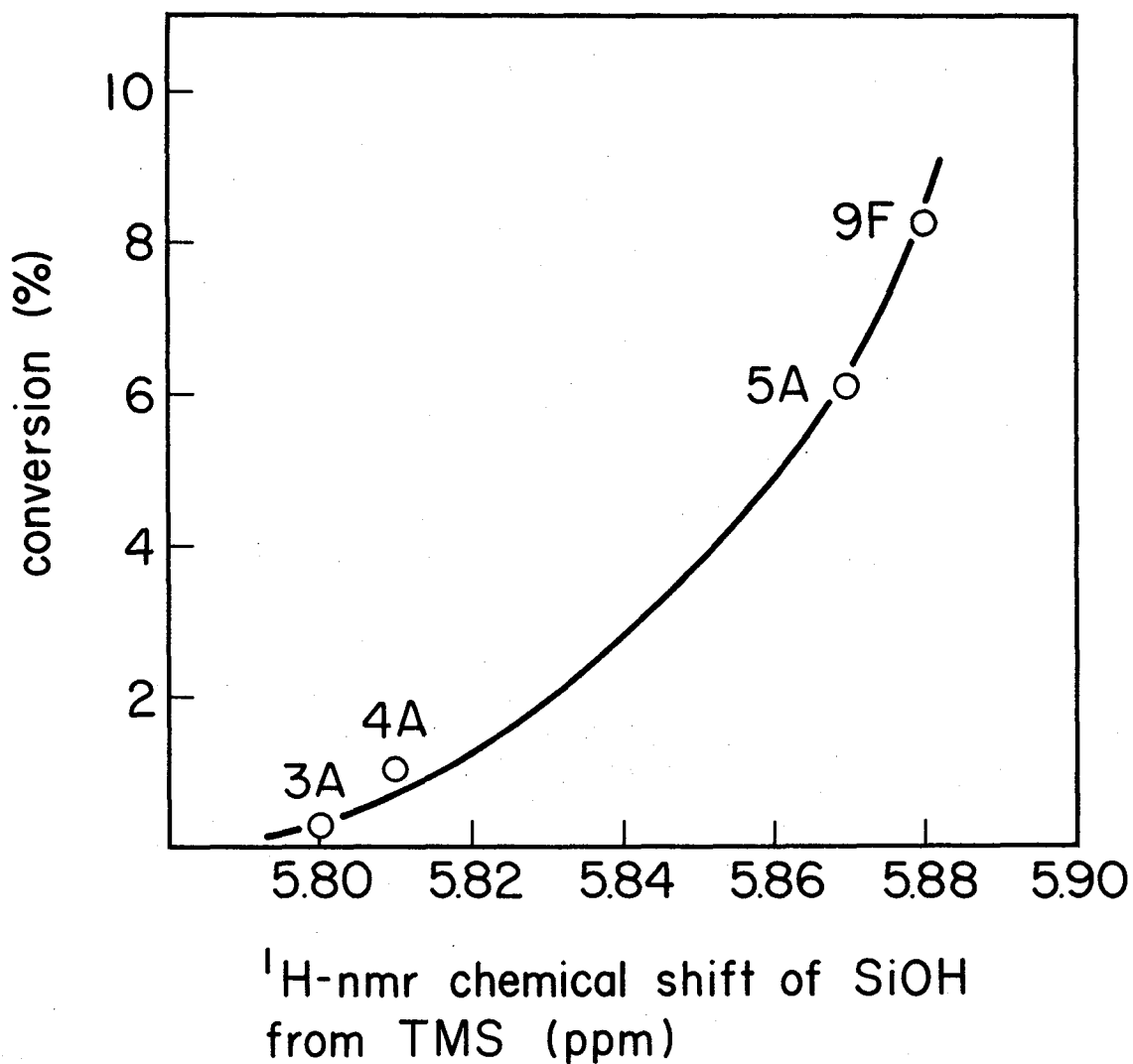


Figure 5 Relationship between polymer yield and chemical shift of SiOH. Polymerization conditions are the same as in Fig. 2. NMR spectra for  $\text{Ph}_2\text{Si}(\text{OH})_2$  were measured in  $d_8$ -THF in the presence of dispersed zeolite.

active than silanols with a methyl group. (ii) Monomeric silanol compound was less active than polymeric silanol compound.

These phenomena may be attributed to the stability and acidity of the silanol compound, which may be explained by substitution and aggregation of silanols. If these two effects could be achieved by another method, polymer conversion would increase. It is known that OH compounds are strongly adsorbed on the surface of porous silica by strong hydrogen bonding.<sup>1</sup> The chemical properties of silanol may be strongly influenced by the presence of porous silica. Therefore catalytic activity may be affected by using porous silica as a support.

The stability of silanol against self-condensation in the presence of  $\text{Al}(\text{acac})_3$  combined with porous silica was examined by GPC and compared with that observed in the presence of  $\text{Al}(\text{acac})_3$  only. The amount of unreacted silanol was plotted with time as shown in Figure 6 using diphenylsilanediol or methylphenylsilanediol as the silanol compound. The figure shows that these silanol compounds are stable on the porous silica.

Figure 1 also shows the polymer conversion-time curve in cyclohexene oxide polymerization with the catalyst systems  $\text{Al}(\text{acac})_3$ -diphenylsilanediol and  $\text{Al}(\text{acac})_3$ -methylphenylsilanediol, respectively, in the presence and absence of porous silica. The effect of porous silica was espe-

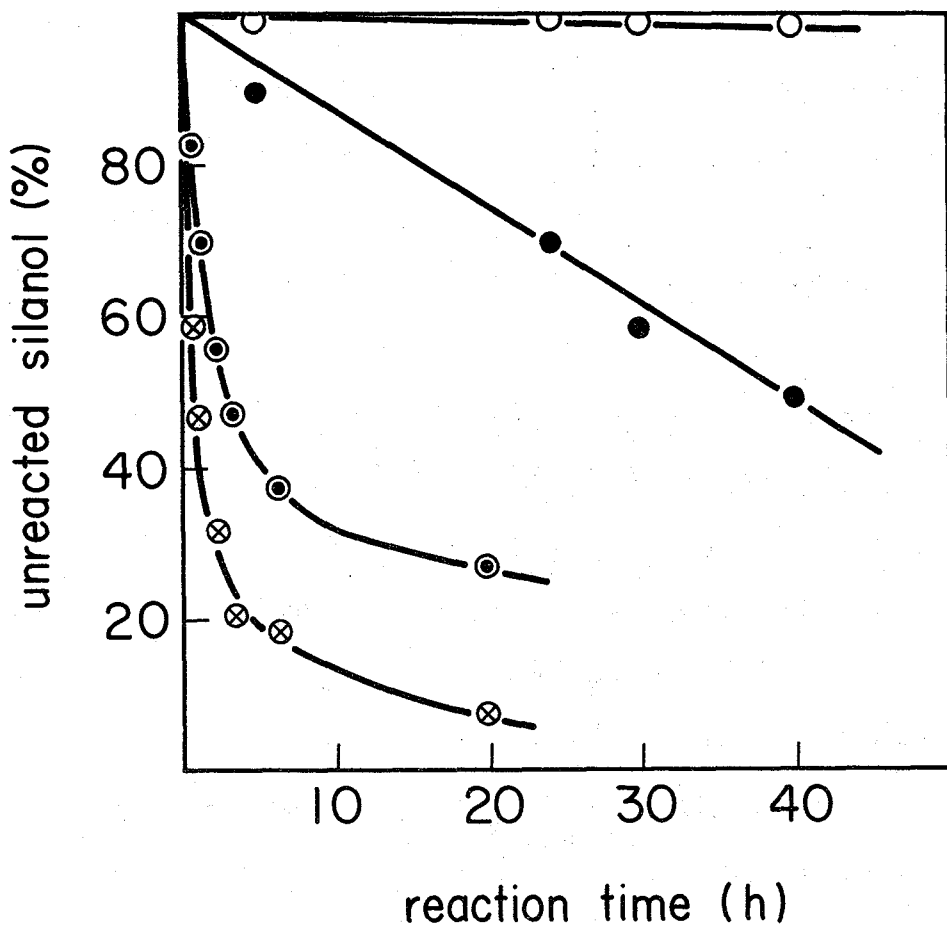


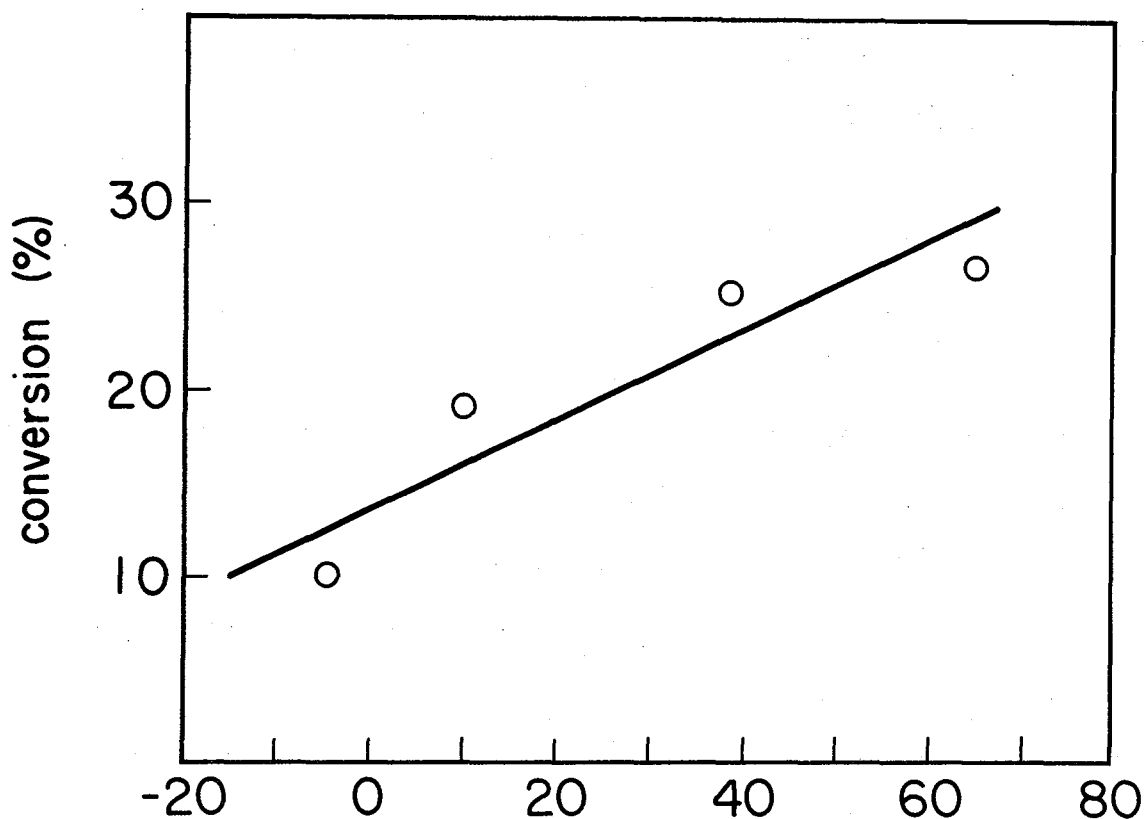
Figure 6 Stability of  $\text{Ph}_2\text{Si}(\text{OH})_2$  and  $\text{MePhSi}(\text{OH})_2$  supported by silica-C. Reaction conditions are the same as in Fig. 4; silica C, 5 wt% to THF: (—○—)  $\text{Al}(\text{acac})_3\text{-Ph}_2\text{Si}(\text{OH})_2\text{-silica C}$ , (—●—)  $\text{Al}(\text{acac})_3\text{-Ph}_2\text{Si}(\text{OH})_2$ , (—●—)  $\text{Al}(\text{acac})_3\text{-MePhSi}(\text{OH})_2\text{-silica C}$ , (—⊗—)  $\text{Al}(\text{acac})_3\text{-MePhSi}(\text{OH})_2$ .

cially pronounced for the  $\text{Al}(\text{acac})_3$ -methylphenylsilanediol catalyst as compared with the  $\text{Al}(\text{acac})_3$ -diphenylsilanediol catalyst. This phenomenon may be explained as follows: Catalyst activation on porous silica would be due to the stability and acidity of the silanol compound. The effect of porous silica on methylphenylsilanediol stabilization against self-condensation was not large enough to explain the effect of porous silica on polymer conversion, compared with the effect on diphenylsilanediol stabilization. Therefore the increase in acidity and stabilization against the addition to epoxide by aggregation would be important. Methylphenylsilanediol with its methyl group would have lower acidity and lower stabilization against addition to epoxide than diphenylsilanediol with its phenyl groups. Diphenylsilanediol would have strong acidity and stabilization against addition to epoxide to some degree in itself. When methylphenylsilanediol and diphenylsilanediol interact with porous silica, the increase in acidity and stability would be greater in methylphenylsilanediol than in diphenylsilanediol.

The interaction between silanol and porous silica was examined by NMR. Among many silicas, some activated the  $\text{Al}(\text{acac})_3$ /silanol compound catalyst, some had no effect, and others deactivated. When the NMR spectrum of diphenylsilanediol was measured in  $d_8$ -THF in the presence of porous silica-C, which activated the catalyst, the SiOH signal was

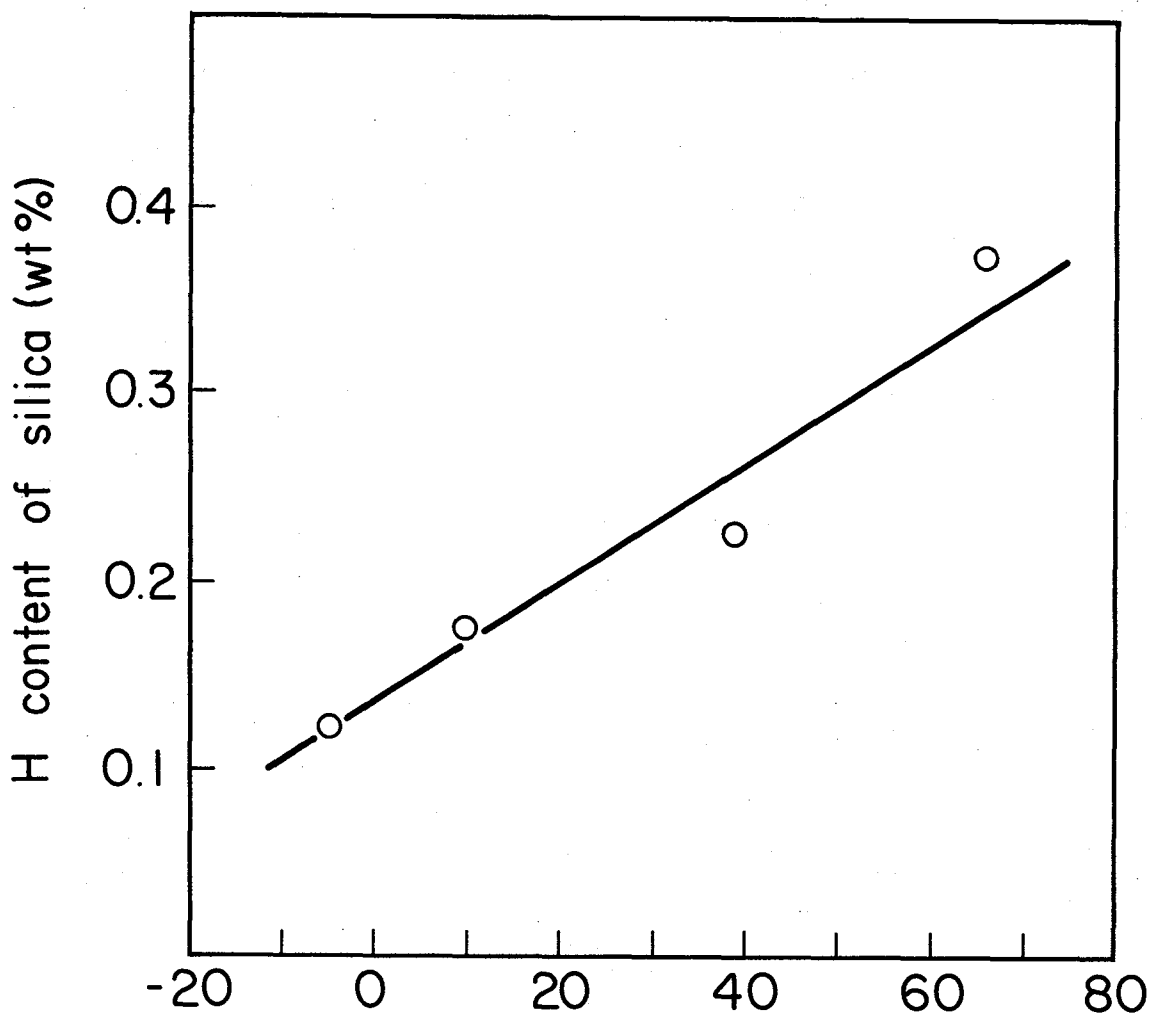
broad and shifted high field. This fact shows that the diphenylsilanediol SiOH formed hydrogen bonds with the silica surface. On the other hand, the SiOH signal measured in presence of porous silica-F, which did not activate the catalyst, hardly changed compared with the absence of porous silica. In Figure 7, the abscissa shows the difference between the half-value width of the SiOH signal and the half-value width of CH<sub>2</sub> in THF, and gives the relative strength of interaction. The ordinate shows polymer conversion. Figure 7 shows that the greater the interaction with silica, the higher the polymer conversion.

The amount of SiOH on surface of porous silica was estimated from the elemental analysis of H after removal of the adsorbed water (in dry N<sub>2</sub>). This amount of H was associated with the relative strength of the interaction between diphenylsilanediol and silica, as shown in Figure 8. It is believed that the interaction was between diphenylsilanediol and SiOH on the silica surface. As seen above, the increase in catalytic activity in the presence of porous silica was caused by the stabilization of organosilanol and the increase in organosilanol acidity, which were due to the hydrogen bond between organosilanol and the SiOH on the porous silica surface.



difference between signal width of the  $^1\text{H}$ -nmr SiOH signal and that of the lower field  $\text{CH}_2$  signal for THF (Hz)

Figure 7 Relation between polymer yield and signal width of  $^1\text{H}$ -NMR. Polymerization conditions are the same as in Fig. 1. Polymerization time, 15 h; NMR spectra for  $\text{Ph}_2\text{Si}(\text{OH})_2$  were measured in  $d_8$ -THF in the presence of dispersed porous silica (90 MHz).



difference between signal width of the  $^1\text{H}$ -nmr SiOH signal and that of the lower field  $\text{CH}_2$  signal for THF (Hz)

Figure 8 Relation between H content of porous silica and signal width of  $^1\text{H}$ -NMR. Polymerization conditions and NMR measurement conditions are the same as in Fig. 7.



## 5-5 Molecular weight distribution of the polymer

The molecular weight distribution of the polymer obtained from  $\text{Al}(\text{acac})_3/\text{Ph}_2\text{Si}(\text{OH})_2/\text{porous silica}$  was the same as that obtained from  $\text{Al}(\text{acac})_3/\text{Ph}_2\text{Si}(\text{OH})_2$  alone, as shown in Figure 3. When cyclohexene oxide was polymerized in the presence of porous silica, polymer conversion increased, while the molecular weight distribution was the same.

Figure 3 also shows the molecular weight distribution of the polymer obtained from  $\text{Al}(\text{acac})_3/\text{silica gel}$ . In this case, the molecular weight of polymer was lower than that obtained from  $\text{Al}(\text{acac})_3/\text{Ph}_2\text{Si}(\text{OH})_2$ .

In the zeolite/ $\text{Ph}_2\text{Si}(\text{OH})_2$  catalyst system, the molecular weight of the polymer changed with the pore size of the zeolite used; the largest-molecular-weight polymer was obtained from zeolite5A/ $\text{Ph}_2\text{Si}(\text{OH})_2$  catalyst. The polymer obtained with zeolite/ $\text{Al}(\text{acac})_3/\text{Ph}_2\text{Si}(\text{OH})_2$  catalyst had a molecular weight intermediate between that of the polymer made with  $\text{Al}(\text{acac})_3/\text{Ph}_2\text{Si}(\text{OH})_2$  and that made with zeolite/ $\text{Ph}_2\text{Si}(\text{OH})_2$  (Table 1).

## Reference

1. A. W. Baker and A. T. Shulgin, *J. Am. Chem. Soc.*, 81, 1523 (1959); R. West and C. S. Kraihanzel, *J. Am. Chem. Soc.*, 81, 765 (1961); R. West, *ibid.*, 81, 1614 (1959), M. R. Basila, *J. Chem. Phys.*, 35, 1151 (1961); S. Kohama, *Nippon Kagaku Kaishi*, 81, 69 (1960)



## Chapter 6 Microstructure of Poly(Cyclohexene Oxide)

### 6-1 Introduction

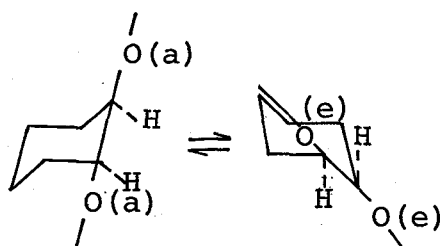
Microstructure of poly(cyclohexene oxide) was investigated by Bacskai<sup>1</sup> and Malhotra<sup>2</sup> using <sup>1</sup>H-NMR spectroscopy. Bacskai concluded that poly(cyclohexene oxide) polymerized by AlEt<sub>3</sub> had stereoregular all-trans structure and Malhotra concluded that a polymer polymerized by triphenylmethyl cation had cis-trans mixed structure.

Microstructure of poly(cyclohexene oxide) might be varied by the polymerization catalyst and will reflect the properties of the catalysts. The microstructure might also be varied by use of a catalyst supported on porous silica or zeolite. In this Chapter, structure of the polymers is described in detail.

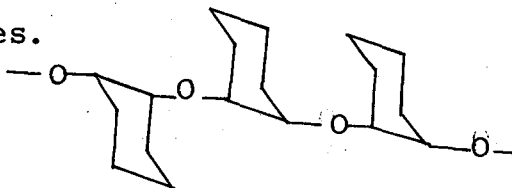
### 6-2 Structure of poly(cyclohexene oxide) polymerized by catalysis of Al(acac)<sub>3</sub>/silanol system

Figure 1 shows the <sup>13</sup>C-NMR spectrum of poly(cyclohexene oxide) obtained by catalysis of the Al(acac)<sub>3</sub>/Ph<sub>2</sub>Si(OH)<sub>2</sub>. Three peaks were found for each carbon and this may be interpreted by either of the following:

- (1) Mixture of cis and trans structure.
- (2) Equilibrium mixtures of diaxial and diequatorial structure of the main chain.



(3) Mixture of diisotactic and disyndiotactic structures.



In regard to the first possibility Elderfield reported<sup>3</sup> that alicyclic epoxide gave the trans form by cationic catalyst. Bacskai concluded<sup>1</sup> that a polymer by  $\text{AlEt}_3$  had an all-trans structure by comparing the  $^1\text{H-NMR}$  spectra of the polymer with that of cis- and trans-1,2-cyclohexane diol. By comparing the  $^{13}\text{C-NMR}$  spectra the C-1 signal of the polymer was shown to have chemical shift differences of only 0.61 and 1.80 ppm, but the difference in the C-1 chemical shift between cis- and trans-1,2-cyclohexane diol was 4.75 ppm (Table 1). From the above it is impossible to regard the structure of the polymer as cis and trans. In regard to the second possibility the  $^{13}\text{C-NMR}$  spectra were measured at 30, 60, and 90°C (Fig. 1), but the spectral pattern was the same. Therefore these chemical shift changes are not caused by the equilibrium

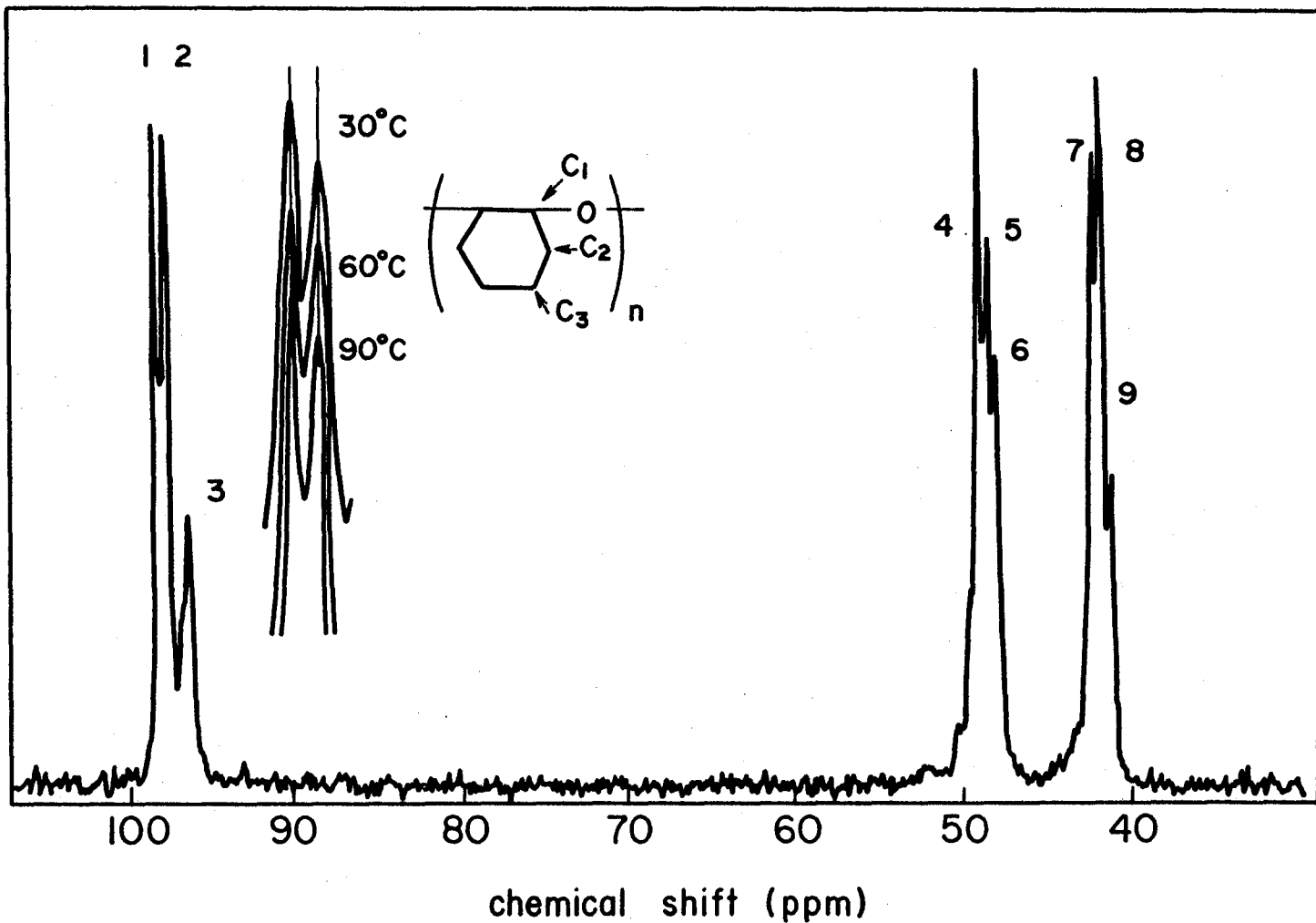


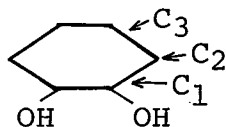
Figure 1  $^{13}\text{C}$ -NMR spectrum for poly(cyclohexene oxide):  
measured at 30°C in  $\text{C}_6\text{D}_6$ .

Table 1 Assignment and Spin-Lattice Relaxation Time for Poly(cyclohexene oxide) and 1,2-Cyclohexane Diol(cis-trans Mixture) in  $^{13}\text{C}$ -NMR spectrum<sup>a</sup>

Signal	Carbon	Polymer <sup>a</sup>		Cyclohexanediol <sup>b</sup>	
		Chemical Shift (ppm)	$T_1$ (s)	Chemical Shift (ppm)	$T_1$ (s)
1	C <sub>1</sub>	98.68	0.30	95.98	3.45
2	C <sub>1</sub>	98.07	0.30	91.23	3.7 <sub>1</sub>
3	C <sub>1</sub>	96.89	0.30	—	—
4	C <sub>2</sub>	50.25	0.14	53.56	1.88
5	C <sub>2</sub>	49.65	0.15	50.59	2.00
6	C <sub>2</sub>	49.34	0.14	—	—
7	C <sub>3</sub>	43.53	0.16	44.89	1.78
8	C <sub>3</sub>	43.15	0.16	42.23	1.9 <sub>3</sub>
9	C <sub>3</sub>	42.42	0.15	—	—

<sup>a</sup> Measured at 60°C in C<sub>6</sub>D<sub>6</sub>.

<sup>b</sup>



mixtures. Spin-lattice relaxation time ( $T_1$ ) can be used for peak assignments. In this case the  $T_1$ s were measured to distinguish the properties of individual carbons (Table 1). Because the  $T_1$ s for C-1 signals were almost the same, these signals were assignable as carbons in the main chain of polymer, but the first possibility could not be studied by  $T_1$  measurement because the  $T_1$  difference was too small even for a monomeric compound like 1,2-cyclohexane diol.

According to the above, the chemical shift changes are due to the third possibility. Vandenberg reports<sup>4</sup> that the complexities in the  $^{13}\text{C}$ -NMR of the 2,3-epoxybutenes are due to atactic structure. Oguni et al., also report<sup>5</sup> that the three signals of the methine carbon in amorphous poly(propylene oxide) are due to triad tacticity. Thus the three signals of C-1 are due to the same triad tacticity and the polymer will have an atactic structure. This conclusion is supported by the x-ray diffraction curve. No change in the x-ray diffraction curve and half-value width were observed between the polymer treated at 40°C for 1 week (crystallization process) and the polymer treated at 80°C and immediately cooled to -196°C (quenching process). These polymers are essentially amorphous because of its atactic structure.

$^{13}\text{C}$ -NMR spectra of poly(cyclohexene oxide) polymerized with  $\text{Al}(\text{acac})_3/\text{silanol}$ , zeolite/silanol compound, and



Al(acac)<sub>3</sub>/silanol compound/porous silica were almost the same. Figure 2 shows the <sup>13</sup>C-NMR spectral pattern for polymers prepared with various catalysts. As polymerized on the surface of inorganic compounds, these polymers would have a random structure.

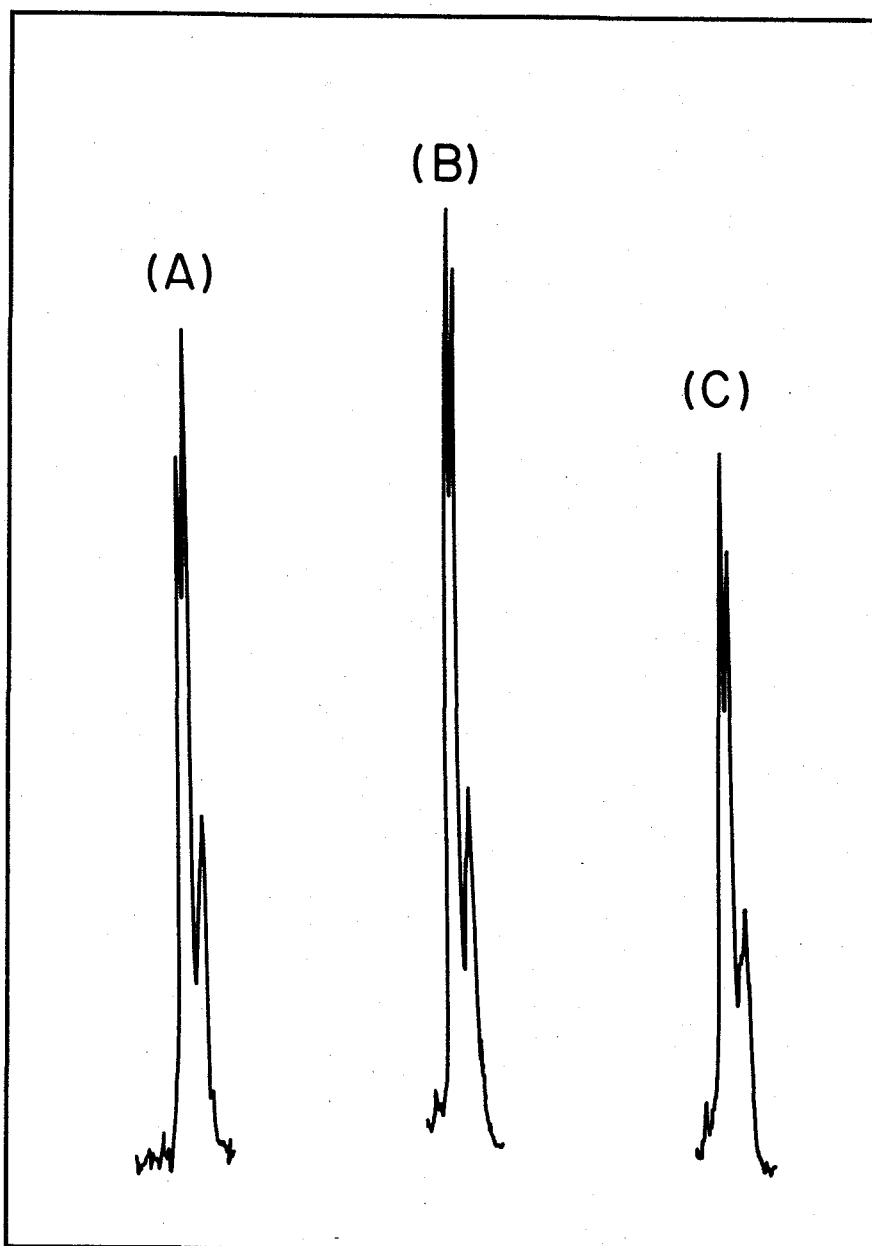


Figure 2  $^{13}\text{C}$ -NMR spectra assignable to C-1 of poly-(cyclohexene oxide). Catalysts: (A)  $\text{Ph}_2\text{Si}(\text{OH})_2$  zeolite 5A, (B)  $\text{Al}(\text{acac})_3\text{-Ph}_2\text{Si}(\text{OH})_2\text{-silica}$ , (C)  $\text{Al}(\text{acac})_3\text{-Ph}_2\text{Si}(\text{OH})_2$ ; C-1, carbon bonding to oxygen.

## References

1. R. Bacskai, J. Polymer Sci., A-1, 2777 (1963)
2. S. L. Malhotra, J. Macromol. Sci. Chem., A-12, 1379 (1978)
3. R. C. Elderfield, Ed., Heterocyclic Compounds, Vol. 1, Wiley, New York, 1953, p30
4. C. E. Foll, Soc. Chem. Ind. Monogr. No. 26, 103-138; E. J. Vandenberg, J. Polymer Sci., A-1, 7, 525 (1969); *ibid.*, J. Polymer Sci., 47, 489 (1960)
5. N. Oguni, K. Lee and H. Tani, Macromolecules, 5, 819 (1972); *ibid.*, Polymer J., 11, 755 (1979)

## Chapter 7 Effect of Intramolecular Hydrogen Bonds of Silanol on the Catalyst Activity

### 7-1 Introduction

Aggregation of silanol was found to be important for the catalyst activation with porous silica. The effect of aggregation was also implied in the polymerization with  $\text{Al}(\text{acac})_3/\text{SH6018}$  described in Chapter 2.

In order to examine the effect of intramolecular hydrogen bond, first, an oligomer of diphenylsilanediol was used as silanol. Because the oligomer is more suitable for consideration of the reaction mechanism, as compared to the polymer of silanol. Then, the effects of silanol polymers were investigated.

### 7-2 Aluminum complex/ $\text{HO}(\text{Ph}_2\text{SiO})_n\text{H}$ catalyst system

(n; 1, 2, 3 and 4)

Catalytic activity of an aluminum complex/ $\text{HO}(\text{Ph}_2\text{SiO})_n\text{H}$  system was investigated as a function of n in order to examine the effect of intramolecular hydrogen bonding of silanols, because the hydrogen bonding varied with the number on n.

Table 1 gives the polymerization results. The catalytic activity for  $\text{Al}(\text{acac})_3/\text{HO}(\text{Ph}_2\text{SiO})_n\text{H}$  (0.05 mol%/0.05 mol%) varied with the number of n as follows.  $1 > 4 > 3 > 2$ . The diphenylsilanediol is distinct from the others in

Table 1 Polymerization of Cyclohexene Oxide with Aluminum  
Complex/ $\text{HO}(\text{Ph}_2\text{SiO})_n\text{OH}$  Catalyst.a)

Aluminum complex		n of silanol		Ligand liberation (mol%)	Solvent CHO/ $\text{PhCH}_3$ <sup>1)</sup> (v/v)	Polymer conversion (%) ( ): polymerization time (min.)		
Al(acac) <sub>3</sub>	0.05	1	0.05	—	1/0	12(2)	30(10)	37(20)
	0.05	2	0.05	—	1/0	3(2)	9(10)	12(21)
	0.05	3	0.05	—	1/0	8(2)	12(3)	23(10)
	0.05	4	0.05	—	1/0	9(2)	27(10)	34(20)
Al(Etaa) <sub>3</sub>	0.025	2	0.025	30	1/0	19(3)	27(8)	32(15)
	0.025	3	0.025	43	1/0	14(3)	24(8)	30(15)
	0.025	4	0.025	33	1/0	24(3)	35(8)	39(15)
	0.05	1	0.05	30	7/3	19(2)	30(5)	34(10)
	0.05	2	0.05	30	1/0	5(2)	12(5)	14(10)
	0.05	3	0.05	43	7/3	3(2)	8(5)	8(10)
	0.05	4	0.05	33	7/3	25(2)	35(5)	39(10)
Al(SA) <sub>3</sub>	0.025	1	0.025	42	1/0	90(3)	—	100(10)
	0.025	2	0.025	50	1/0	90(3)	—	100(10)
	0.025	3	0.025	65	1/0	16(3)	20(8)	22(14)
	0.025	4	0.025	41	1/0	90(3)	—	100(10)

a) Polymerization temperature, 40°C 1) CHO: cyclohexene oxide

view of its acidity and bulkiness. The catalytic activity due to the intramolecular hydrogen bond should be compared among the Dimer, the Trimer and the Tetramer. The SiOH group of diphenylsilanediol oligomers can form the intramolecular hydrogen bond if they are longer than the Trimer.<sup>1</sup> It is well-known that hydrogen bonding between OH groups makes the acidity strong.<sup>2</sup> As mentioned in Chapter 3, catalytic activity increased with an increase in the silanol acidity. The catalytic activity variation depending on the value of n is explained in term of the acidity increment due to the intramolecular hydrogen bonding.

Catalytic activity in the presence of other aluminum complexes was also examined.

Followings are described in Chapter 4. Both  $\text{Al}(\text{Etac})_3$  and  $\text{Al}(\text{SA})_3$  interacted with silanols to liberate a part of the ligand from the aluminum chelate. The resultant aluminum compound had Si-O-Al linkage. The ratio of reaction was estimated from the ratio of ligand liberation. The resultant aluminum compound which had no catalytic activity by itself interacted with the residual silanol and showed higher catalytic activity.

When the aluminum complex was mixed with an equimolar amount of oligosilanols, the aluminum complex also reacted with the oligosilanols as shown in Table 1 as the ratio of ligand liberation. Ligand liberation from the aluminum

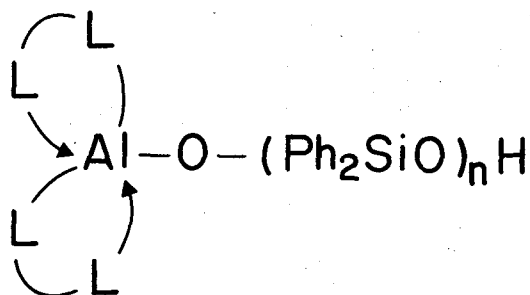
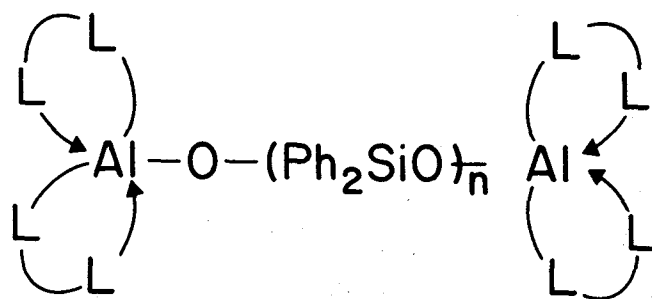
complex was greatest when the trimer was used. Fig. 1 and 2 shows the probable reaction products.

The structures of the products were confirmed as follows.  $\text{Al}(\text{Etaa})_3$  was mixed with an equimolar amount of the Dimer or the Trimer. The resultant ethyl acetoacetate from the  $\text{Al}(\text{Etaa})_3$  was removed under reduced pressure. The structure of the residual reaction mixture was estimated with  $^1\text{H-NMR}$  and IR spectroscopy. The peak at  $1070\text{ cm}^{-1}$  in the IR spectra showed the presence of Al-O-Si linkage. The  $^1\text{H-NMR}$  spectra showed that the reaction product from the Trimer and  $\text{Al}(\text{Etaa})_3$  had one ethyl acetoacetate group, however that from the Dimer and the  $\text{Al}(\text{Etaa})_3$  had two ethyl acetoacetate groups. The probable structures of reaction products are shown in Fig. 1 and 2 (IA and IIA structure).

The catalytic activity of  $\text{Al}(\text{Etaa})_3/\text{HO}(\text{Ph}_2\text{SiO})_n\text{H}$  (0.025 mol% / 0.025 mol%) or (0.05 mol% / 0.05 mol%) varied with  $n$  as follows.

$$4 > 1 > 2 > 3$$

The catalytic activity of  $\text{Al}(\text{SA})_3/\text{HO}(\text{Ph}_2\text{SiO})_n\text{H}$  (0.025 mol% / 0.025 mol%) was also lowest for  $n = 3$ . The results are explained by the fact that the Trimer reacts with the aluminum complex readily and the amount of SiOH group decreased in the polymerization system. Because catalyst activity is due to the amount of Al-O-Si linkage and the amount of Si-OH in polymerization system, catalyst activity



I L = Ligand n = 1, 2, 4

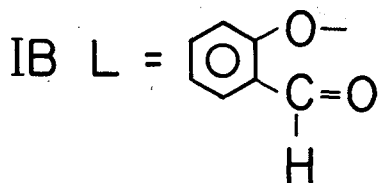
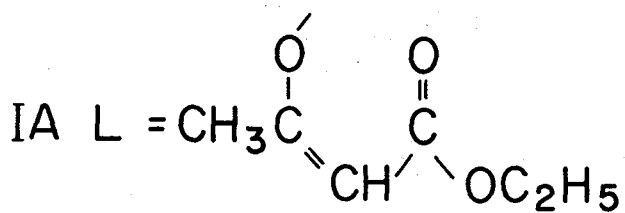
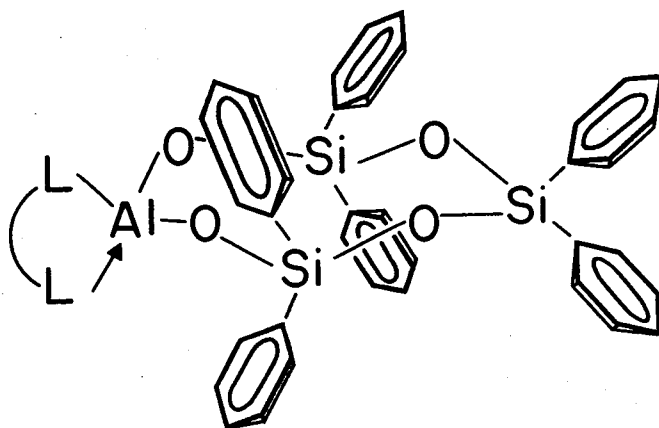


Figure 1 Structure of residual aluminum complex.





$n = 3$

II L = Ligand

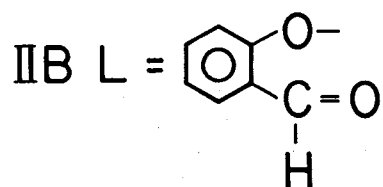
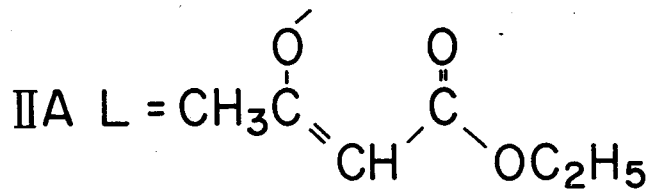


Figure 2. Structure of residual aluminum complex.

at  $n = 3$  will be lowest. A suitable extent of reaction between aluminum complex and silanol will be important for the catalyst activation.

### 7-3 $\text{Al}(\text{SA})_3$ /Trimer + Dimer or Monomer catalyst system

If the ratio of Trimer to Dimer or Monomer + Trimer is changed gradually from 0 to 1 under the same  $\text{SiOH}$  concentration, the ratio of reaction between  $\text{Al}(\text{SA})_3$  and the oligosilanol will change gradually, then the catalytic activity may have a maximum at a ratio of Trimer to Dimer or Monomer + Trimer. The catalytic activity of mixed silanol systems, Trimer/Dimer, and Trimer/Monomer was examined, where the silanol concentration in the polymerization system was constant at 0.05 mol% to cyclohexene oxide, and  $\text{Al}(\text{SA})_3$  was used as the aluminum component. Table 2 shows the results. Ligand liberation from the aluminum complex did indeed gradually increase and the maximum polymer conversion and the maximum molecular weight were obtained at the ratio of 1 : 9 mol (Trimer:Dimer or Trimer:Monomer).

Instead of the ratio of the ligand liberation, it was also considered that the structure of IIB was more active than that of IB in the presence of silanol. Because IIB had two Si-O-Al linkage in a molecule. Where, II and I mean aluminum complex only, not containing additional silanol.

Table 2 Dependence of Conversion on the Ratio of Trimer/Dimer or Trimer/Monomer. a)

the ratio of HO(Ph <sub>2</sub> SiO) <sub>3</sub> OH/ HO(Ph <sub>2</sub> SiO) <sub>n</sub> OH+ HO(Ph <sub>2</sub> SiO) <sub>3</sub> OH (mol/mol)	n	Polymer conver- sion (%)	Ligand <sup>b)</sup> libera- tion (%)	Molecular weight	
				M <sub>w</sub>	M <sub>n</sub>
0	1	38	40		
0.1	1	64	41		
0.3	1	61	41		
0.5	1	54	44		
0.7	1	39	46		
0.9	1	20	48		
1.0	1	18	50		
0	2	35	43	41600	19100
0.1	2	39	43	69700	31900
0.3	2	33	45	63100	26300
0.5	2	30	45	64500	29400
0.7	2	22	47	57300	26300
0.9	2	21	48	55700	23700
1.0	2	20	50	64700	27200

a) Polymerization conditions: Al(SA)<sub>3</sub> 0.05 mol% to CHO, the trimer + the dimer or the monomer 0.05 mol% to CHO, at 40°C for 50 minutes, CHO/toluene 2/1(v/v)

b) Al(SA)<sub>3</sub>(0.16M) and silanol (0.16M) in the mixture of d<sub>8</sub>-THF and d<sub>6</sub>-acetone(1/1(v/v)).

The catalytic activity of IA or IIA/triphenylsilanol (0.02 mol% / 0.05 mol%) system instead of IB or IIB/triphenylsilanol was examined. The results are shown in Table 3. IA or IIA had a slight catalytic activity by itself. However, when 0.05 mol% of triphenylsilanol was added, IIA/triphenylsilanol became a more active catalyst than IA/triphenylsilanol, as shown in Table 3.

The results of the catalyst activity on the ratio of Trimer/Monomer or Dimer + Trimer was explained from the three points. 1) ratio of Si-O-Al linkage 2) the amount of resultant silanol 3) difference in catalyst activity between I and II aluminum structures in presence of silanol. Namely, when the ratio of the Trimer increased under the constant silanol concentration, the ratio of II aluminum structure increased and the concentration of the SiOH group decreased, then the polymer yield also decreased. However, when an appropriate amount of II structure was present in the polymerization system, namely, a small amount of the active species formed, the polymer conversion was maximum.

#### 7-4 Aluminum complex/1,4-bis(hydroxydimethylsilyl)benzene system

1,4-bis(hydroxydimethylsilyl)benzene (HMSB) has a similar molecular length of the Trimer (molecular length between SiOH oxygen: HMSB, 9.96 Å; the trimer, 9.90 Å). However, HMSB can not hydrogen bond intramolecularly

Table 3 Polymerization of CHO with Aluminum Complex/ $\text{Ph}_3\text{SiOH}$  Catalyst<sup>a)</sup>

Catalyst	Polymeri- zation time (min.)	Polymer conversion (%)			Molecular weight	
		25	50	80	$M_w$	$M_n$
IA/ $\text{Ph}_3\text{SiOH}$		39	42	45	56400	29800
IA only		0	1	1	53100	25900
IIA/ $\text{Ph}_3\text{SiOH}$		53	57	61	69500	36700
IIA only		1	2	3	48500	25200

a) Polymerization conditions: Aluminum complex 0.02 mol% to CHO,  $\text{Ph}_3\text{SiOH}$  0.05 mol% to CHO, CHO/toluene; 5/4.5 (v/v) 40°C

because it has a benzene ring. Therefore, the catalytic activity of the aluminum complex/HMSB system was compared with that of the aluminum complex/dimethylphenylsilanol (monomer unit of HMSB) system to explain the effect of the intramolecular hydrogen bond on the catalytic activity.

Table 4 shows the relative acidity of the silanols and ratio of the ligand liberation. The acidity of HMSB was slightly higher than that of dimethylphenylsilanol.  $\text{Al}(\text{Etac})_3$  reacted with the two silanol compounds, liberating almost the same amount of the ligand.  $\text{Al}(\text{SA})_3$  reacted with dimethylphenylsilanol, liberating 27 mol% of salicylaldehyde, however, the reaction of  $\text{Al}(\text{SA})_3$  with HMSB gave a precipitate and 33 mol% of the salicylaldehyde was liberated in the system. The large value could be explained in terms of shift of equilibrium caused by precipitation. Therefore, the ratio of the ligand liberation of  $\text{Al}(\text{SA})_3$ /dimethylphenylsilanol system probably will also be the same as that on the  $\text{Al}(\text{SA})_3$ /HMSB system, if they are compared in solution.

The catalytic activity of  $\text{Al}(\text{acac})_3$ /HMSB was higher than that of  $\text{Al}(\text{acac})_3$ /dimethylphenylsilanol. The catalytic activity of the HMSB system was also higher when  $\text{Al}(\text{SA})_3$  was used instead of  $\text{Al}(\text{acac})_3$ . The catalyst deactivation seen in  $\text{Al}(\text{SA})_3$ /Trimer system was not observed. The results are reasonable when the intramolecular hydrogen bonding is considered. (Table 5).

Table 4 Relative acidity of 1,4-Bis(hydroxydimethylsilyl)benzene and Phenyldimethylsilanol and Ligand Liberation

Silanol	Relative acidity			Al complex	Ratio of ligand liberation (%)
	(B) in CDCl <sub>3</sub> from TMS (Hz)	(A) in d <sub>6</sub> -DMSO from TMS (Hz)	(A) - (B)		
Phenyldimethyl silanol	190	528	338	Al(Etaa) <sub>3</sub>	15
			(3.77 ppm)	Al(SA) <sub>3</sub>	27
1,4-bis(hydroxy dimethylsilyl) benzene	184	526	342	Al(Etaa) <sub>3</sub>	17
			(3.82 ppm)	Al(SA) <sub>3</sub>	-

Table 5 Polymerization of CHO with Aluminum Complex/  
Ph(CH<sub>3</sub>)<sub>2</sub>SiOH and Aluminum Complex/HMSB<sup>1)</sup>  
Catalyst

Catalyst	Polymer conversion (%)		
	20 min. <sup>2)</sup>	63 min.	175 min.
Al(acac) <sub>3</sub> /Ph(CH <sub>3</sub> ) <sub>2</sub> SiOH	1.2	1.4	1.5
Al(acac) <sub>3</sub> /HMSB	2.2	2.8	3.0
Al(Etaa) <sub>3</sub> /Ph(CH <sub>3</sub> ) <sub>2</sub> SiOH	1.6	1.8	1.9
Al(Etaa) <sub>3</sub> /HMSB	3.6	3.9	4.0
Al(SA) <sub>3</sub> /Ph(CH <sub>3</sub> ) <sub>2</sub> SiOH	2.2	2.5	2.5
Al(SA) <sub>3</sub> /HMSB	9.2	10.0	10.5

Polymerization conditions: 40°C, Al complex, 0.05 mol%  
silanol compound, 0.05 mol% to CHO on Ph(CH<sub>3</sub>)<sub>2</sub>SiOH,  
0.025 mol% to CHO on HMSB

1) HMSB: 1,4-bis(hydroxydimethylsilyl)benzene

2) Polymerization time.



7-5 Aluminum complex/diphenyl(4-vinylphenyl)silanol  
(DVPS) catalyst system

From the experiment using silanol oligomers, a dependence on an effect of silanol chain length was anticipated in the  $\text{Al}(\text{acac})_3/\text{silanol}$  catalyst system. However in the  $\text{Al}(\text{Etac})_3/\text{silanol}$  or the  $\text{Al}(\text{SA})_3/\text{silanol}$  system, the following silanol was considered to give the polymer effects.

- a) the silanol with intramolecular hydrogen bond.
- b) the silanol which reacts with an appropriate amount of aluminum complex.

Table 6 shows the polymer conversion of cyclohexene oxide when  $\text{Al}(\text{acac})_3/\text{mono}(\text{DVPS})$  and  $\text{Al}(\text{acac})_3/\text{poly}(\text{DVPS})$  were used. The polymer conversion with  $\text{Al}(\text{acac})_3/\text{poly}(\text{DVPS})$  catalyst system increased about five times, compared with that with  $\text{Al}(\text{acac})_3/\text{mono}(\text{DVPS})$  catalyst system. The catalyst would be activated by the acidity increment due to the aggregation of the silanol (intramolecular hydrogen bonding). The consideration was supported by the following experiment. When the DVPS copolymerized with styrene was used under the same  $\text{SiOH}$  concentration for preventing the silanol from the aggregation, the polymer conversion decreased.

The catalytic activity of  $\text{Al}(\text{SA})_3/\text{poly}(\text{DVPS})$  was higher than that of  $\text{Al}(\text{SA})_3/\text{mono}(\text{DVPS})$ . In the case of DVPS, the deactivation seen in the  $\text{Al}(\text{SA})_3/\text{Trimer}$  catalyst system was not observed. The results are supported by the

Table 6 Polymerization of CHO with Aluminum Complex/polymeric Silanol and the Ligand Liberation.

catalyst	concentration <sup>1)</sup> of silanol to CHO (mol%)	solvent CHO/PhCH <sub>3</sub> (v/v)	polymer conversion				the ratio of ligand liberation (%)	Mw	Mn
			2) 5min.	10min.	15min.	20min.			
Al(acac) <sub>3</sub> /monoDVPS	0.05	3/1	5	8	11	13	-	-	-
Al(acac) <sub>3</sub> /polyDVPS (Mw8000)	0.05	3/1	35	50	60	65	-	-	-
Al(acac) <sub>3</sub> /polyDVPS (Mw8000)	0.035	neat	58	64	66	67*	-	40000	13000
Al(acac) <sub>3</sub> /poly (DVPS:styrene(1:1))(Mw12000)	0.035	neat	53	58	63	65*	-	46000	18000
Al(acac) <sub>3</sub> /poly (DVPS:styrene(1:2))(Mw11000)	0.035	neat	49	54	57	62*	-	41000	20000
Al(acac) <sub>3</sub> /poly (DVPS:styrene(1:4))(Mw10000)	0.035	neat	45	51	55	60*	-	46400	21000
Al(acac) <sub>3</sub> /poly (DVPS:styrene(1:8))(Mw9000)	0.035	neat	40	46	50	53*	-	47000	21000
Al(acac) <sub>3</sub> /poly (DVPS:styrene(1:16))(Mw9000)	0.035	neat	14	25	30	33*	-	22000	7000
			2) 5min. 10min. 20min.						
Al(SA) <sub>3</sub> /monoDVPS	0.02	3/1	21	25	28*		25	45000	15000
Al(SA) <sub>3</sub> /poly (DVPS:styrene(1:2))	0.02	3/1	45	54	58*		25	75200	29000
Al(SA) <sub>3</sub> /poly (DVPS:styrene(1:4))	0.02	3/1	43	49	54*		26	76000	35000
Al(SA) <sub>3</sub> /poly (DVPS:styrene(1:8))	0.02	3/1	37	45	48*		26	63000	31000
Al(SA) <sub>3</sub> /poly (DVPS:styrene(1:16))	0.02	3/1	10	12	13*		26	44000	19000
Al(SA) <sub>3</sub> /polyDVPS	0.02	3/1	51	56	62*		26	75000	30000
			2) 5min. 20min. 40min. 60min.						
Al(acac) <sub>3</sub> /SH6018 <sup>4)</sup>	0.05 <sup>3)</sup>	neat	23	37	42	43*	0	62000	33000
Al(Etaa) <sub>3</sub> /SH6018 <sup>4)</sup>	0.05 <sup>3)</sup>	neat	28	47	50	53*	23	81000	41000
Al(SA) <sub>3</sub> /SH6018 <sup>4)</sup>	0.05 <sup>3)</sup>	neat	13	18	22	25*	35	44000	23000

polymerization conditions: 40°C 1) The concentration of aluminum complex was the same as that of silanol compound,

2) polymerization time, 3) equivalent %, OH equivalent of SH6018/mol of monomer,

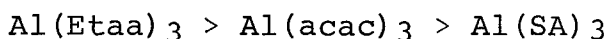
4) polymerization temperature, 45°C.

\* Molecular weight of this polymer was measured.

fact that the ligand liberation of  $\text{Al}(\text{SA})_3$  did not change with the DVPS used, mono(DVPS) and poly(DVPS), as shown in Table 6. Table 6 also shows the molecular weight of the polymer. Maximum value was obtained when 1 : 1 ~ 1 : 4 DVPS : styrene polymers were used.

#### 7-6 Aluminum complex/SH6018 catalyst system

When poly(DVPS) was used as a silanol component, the catalytic activity of  $\text{Al}(\text{SA})_3/\text{poly}(\text{DVPS})$  was higher than that of  $\text{Al}(\text{acac})_3/\text{poly}(\text{DVPS})$ . However, when a silicone resin containing  $\text{SiOH}$  (SH6018, Toray silicone, Mw 1600, OH equivalent about 400) was used as a silanol component, the catalytic activity and molecular weight varied with the aluminum compound as follows. (Table 6)



The ratio of the ligand liberation of  $\text{Al}(\text{SA})_3$  was especially high in case of  $\text{Al}(\text{SA})_3/\text{SH6018}$  catalyst system, as shown in Table 6. The phenomenon could be explained by the facts obtained in the experiment of aluminum complex/oligosilanol catalyst system, namely, poly(DVPS) could make the intramolecular hydrogen bond with an appropriate ratio of the reaction between aluminum complex and silanol, however, SH6018 could do it with large ratio of the reaction. The difference would be due to the silanol structure, that is, the rigidity of polymer chain, and bulkiness around the  $\text{SiOH}$  group, and position of  $\text{SiOH}$ .

## References

1. G. I. Harris, J. Chem. Soc. (B), 1970, 492
2. A. W. Baker and A. T. Shulgin, J. Am. Chem. Soc., 81, 1523 (1959); R. West and C. S. Kraihanzel, J. Am. Chem. Soc., 81, 765 (1961); R. West, *ibid.*, 81, 1614 (1959), M. R. Basuka, J. Chem. Phys., 35, 1151 (1961); S. Kohama, Nippon Kagaku Kaishi, 81, 69 (1960)



## Chapter 8 Polymerization under UV Irradiation

### 8-1 Introduction

In Chapter 4 and 5 it was shown that interaction between aluminum complex and silanol was important for the catalyst activation. The interaction was considered to be induced by UV-radiation, because it is known that under UV-radiation acid dissociation was promoted to strengthen the hydrogen bonding, for example, between cytosine and guanine.<sup>1</sup>

### 8-2 Polymerization profiles

The results on polymerization under UV-radiation are shown in Figures 1, 2 and 3. The catalyst activity of the  $\text{Al}(\text{acac})_3$ /triphenylsilanol system increased about 3-4 times under UV-radiation, especially 254 nm radiation. However the catalyst,  $\text{Al}(\text{Etaa})_3$  or  $\text{Al}(\text{SA})_3$ /triphenylsilanol system was not activated.

The difference in polymerization behavior under UV-radiation implied the difference in the mechanism of interaction as mentioned in Chapter 5. Namely, interaction between  $\text{Al}(\text{acac})_3$  and triphenylsilanol will be one between carbonyl oxygen and  $\text{SiO-H}$ . Chelation will weaken the double bonding of carbonyl, however, the properties as carbonyl will remain yet. The interaction between cytosine and guanine occurs between the N-H and the

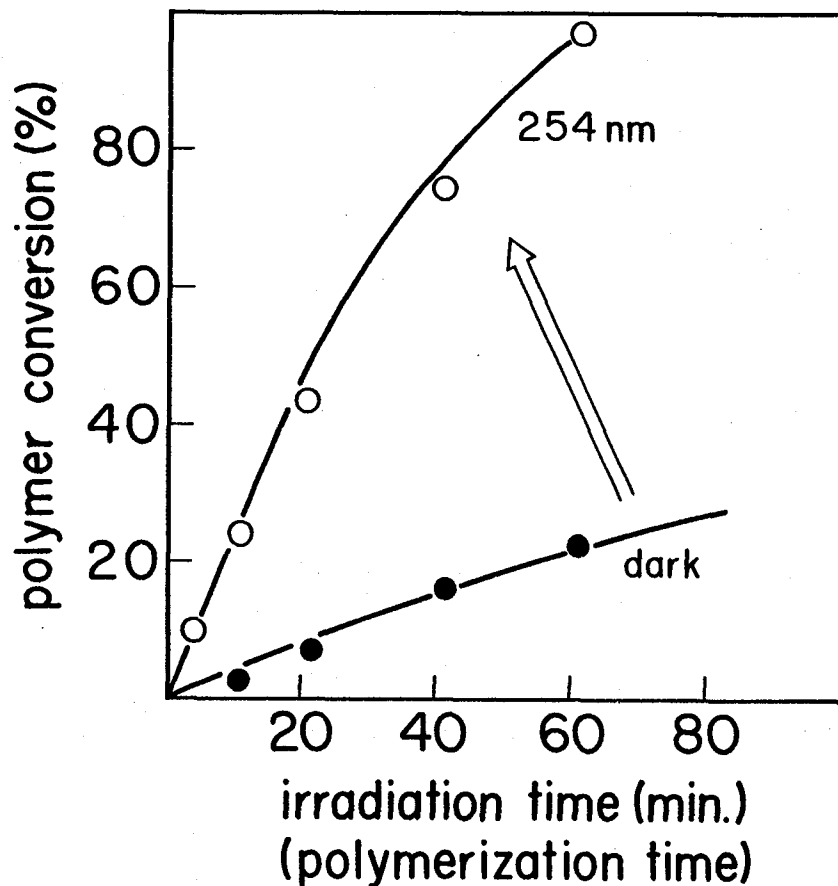


Figure 1 Polymerization of cyclohexene oxide under UV radiation: polymerization conditions: 40°C, 400W-high pressure mercury lamp, Al(acac)<sub>3</sub> 0.03 mol%, Ph<sub>3</sub>SiOH 0.03 mol%.

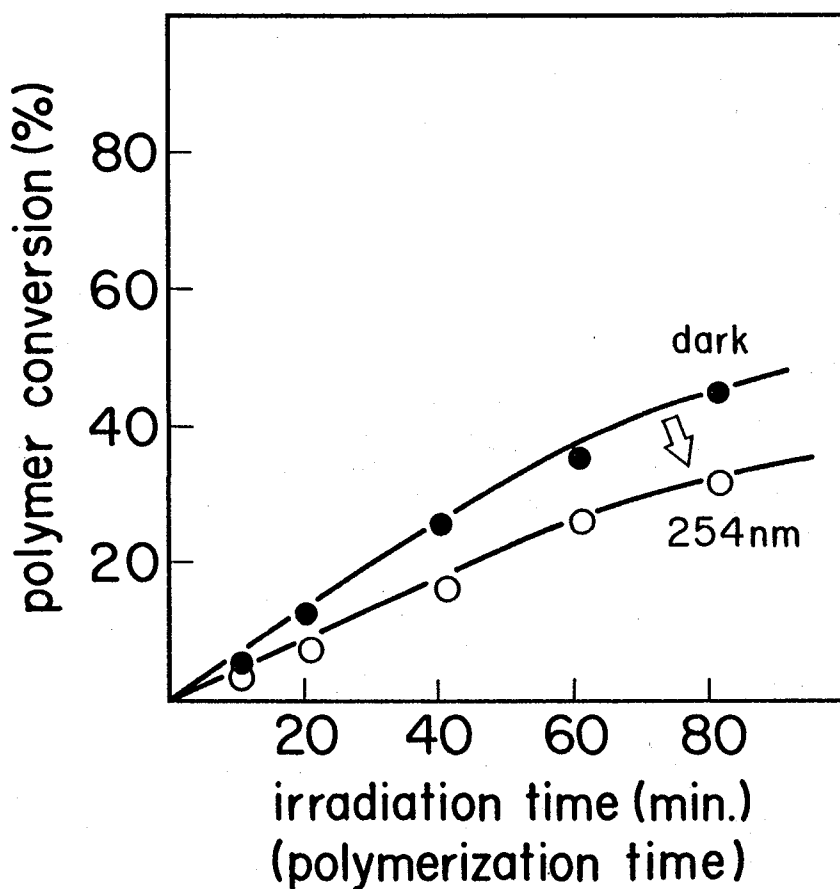


Figure 2 Polymerization of cyclohexene oxide under UV radiation. Polymerization conditions are the same as in Figure 1.  $\text{Al}(\text{Etac})_3$  0.015 mol%,  $\text{Ph}_3\text{SiOH}$  0.015 mol%.



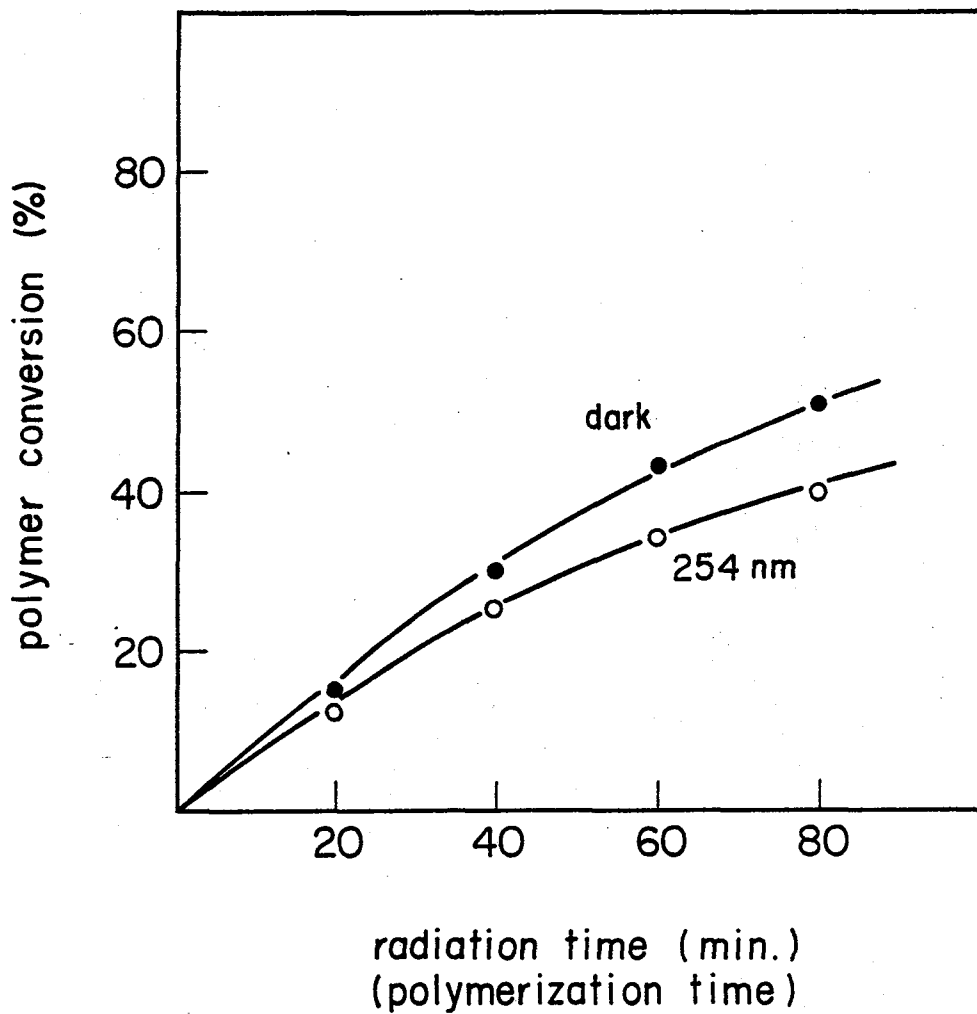


Figure 3 Polymerization of cyclohexene oxide under UV radiation.  $\text{Al}(\text{SA})_3/\text{Ph}_3\text{SiOH}$  (0.01 mol%/0.01 mol/%) low pressure mercury lamp.

carbonyl oxygen. Therefore it is anticipated that the interaction between  $\text{Al}(\text{acac})_3$  and triphenylsilanol is strengthened under UV-radiation.

However, in case of  $\text{Al}(\text{Etac})_3$ /triphenylsilanol or  $\text{Al}(\text{SA})_3$ /triphenylsilanol, interaction between aluminum complex and silanol is caused between oxygen of Si-OH and aluminum, and between oxygen of Al-O-Si and proton of SiO-H. Probably, such an interaction is not strengthened under UV-radiation. Another reason has to be considered. Since aluminum complex becomes labile under UV-radiation, ligand exchange reaction between aluminum chelate and triphenylsilanol will become to occur easily. Therefore, it is considered that the amount of effective SiOH decreases in polymerization system, and catalyst activity also decreases.

## Reference

1. P. Suppan, Principles of Photochemistry, The Chemical Society Monographs, No. 22, The Chemistry Society Publication (1972); T. Matuura, "Yuki Hikari Kagaku", Chemistry Monograph No. 20, p. 179, Kagaku Dojin, Kyoto (1976)

Chapter 9 Thermal and Electrical Properties of Epoxy  
Resin Cured by Aluminum Complex/Silanol  
Catalyst

9-1 Introduction

The present catalyst is developed for the epoxy resin to be used in electrical appliances. In order to examine the effect of the catalyst, electrical properties of the epoxy resin cured with the present catalyst were measured. The results especially at high temperature were unexpectedly good. The reason of such excellent electrical properties will be discussed.

9-2 Difference in electrical properties between epoxy resin cured with  $\text{BF}_3$  complex catalyst and that cured with tris(salicylaldehydato)aluminum/diphenylsilanediol catalyst

The electrical properties of bisphenol A type epoxy resin (I) Epikote 828 cured with tris(salicylaldehydato)-aluminum/diphenylsilanediol ((I)- $\text{Al}(\text{SA})_3/\text{DP}$ ) were compared with that cured with  $\text{BF}_3$  monoethylamine complex catalyst ((I)- $\text{BF}_3 \cdot \text{MEA}$ ). Figure 1 shows the relation between electrical dissipation factor ( $\text{Tan } \delta$ ) and temperature. The dissipation factor of (I)- $\text{BF}_3 \cdot \text{MEA}$  increased remarkably at the temperature above  $130^\circ\text{C}$ . However in case of (I)- $\text{Al}(\text{SA})_3/\text{DP}$ , the value had a maximum at about  $150^\circ\text{C}$  and

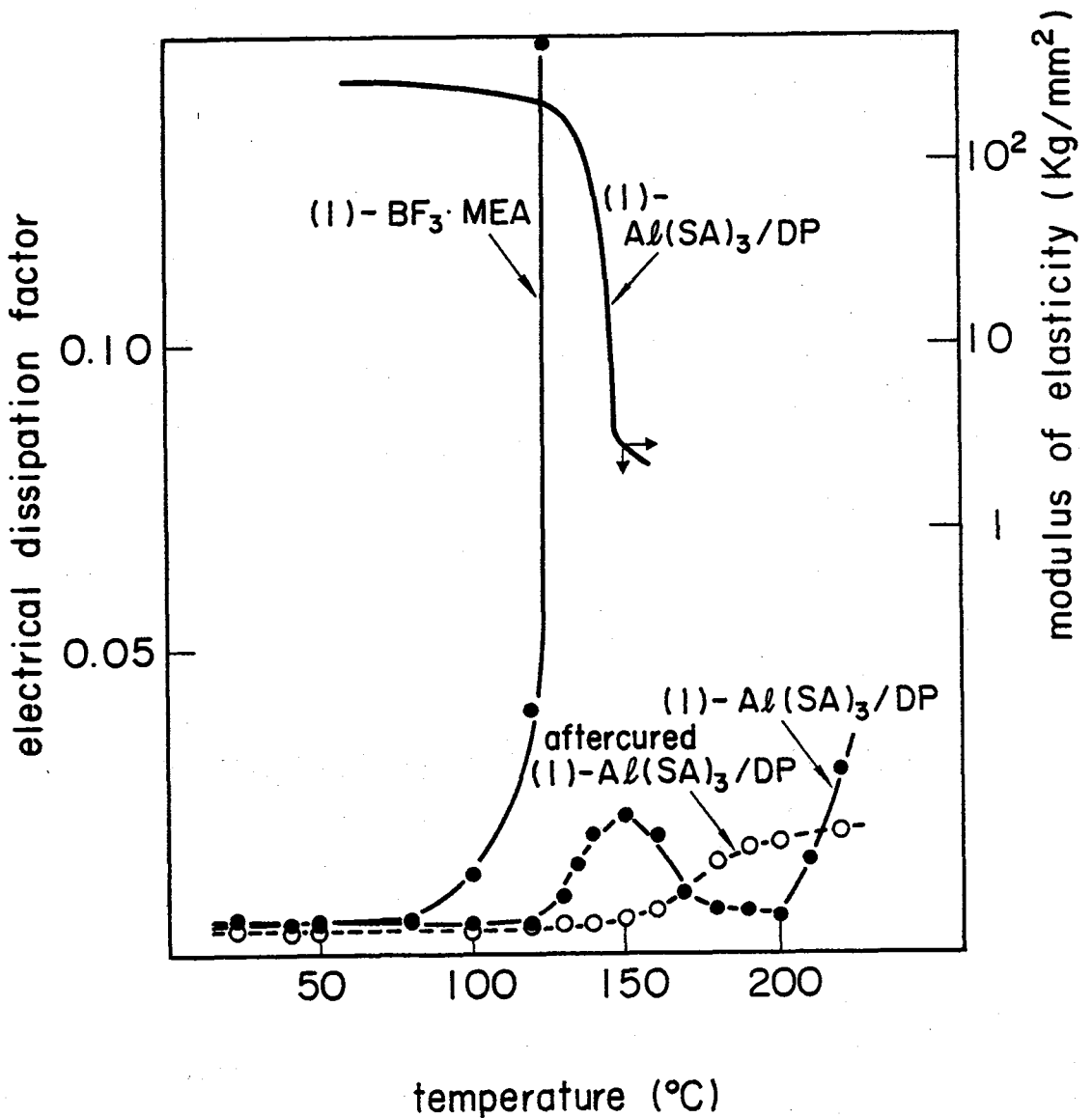


Figure 1 Relation between electrical dissipation factor and temperature, and relation between modulus of elasticity and temperature. Sample, thickness 1 mm, (I)-Al(SA)<sub>3</sub>/DP, Al(SA)<sub>3</sub>, 2 phr, DP 2 phr: (I)-BF<sub>3</sub>·MEA, BF<sub>3</sub>·MEA, 3 phr, 150°C, 15 h, aftercure 180°C for 15 h.

increased again gradually at temperature above 200°C. The maximum point shifted to higher temperature and the height of peak diminished when (I)-Al(SA)<sub>3</sub>/DP was after-cured at 180°C for 15 hours. Figure 1 also shows the modulus of elasticity. T<sub>g</sub> of (I)-Al(SA)<sub>3</sub>/DP coincided with the maximum temperature for Tan δ - temperature curve. Therefore, the peak is considered to be due to the mobility of main chain of epoxy resin cured. The dissipation factor for (I)-BF<sub>3</sub>·MEA did not have such a maximum. This could be explained as follows. The conductance loss became a dominant factor at temperature above 130°C, therefore, the peak of Tan δ due to the motion of the dipoles on the main chain was considered to be buried by the increase in the conductance loss. The explanation was supported by the fact that the relation between ε'' and frequency in the logarithmic scale becomes to have a straight line with slope equal to -1 at temperature above 130°C, as shown in Figure 2. The following equation is known between A.C. conductivity and angular frequency.<sup>1</sup>

$$\sigma_a(\omega) = \omega \left\{ \frac{1}{\omega} \sigma_{a0} + \epsilon_0 \epsilon''(\omega) \right\} = \sigma_{a0} + \epsilon_0 \epsilon''(\omega) \cdot \omega$$

where      $\sigma_a(\omega)$  : A.C. conductivity  
           $\sigma_{a0}$     : D.C. conductivity  
           $\omega$         : angular frequency  
           $\epsilon_0$        : dielectric constant in vacuum

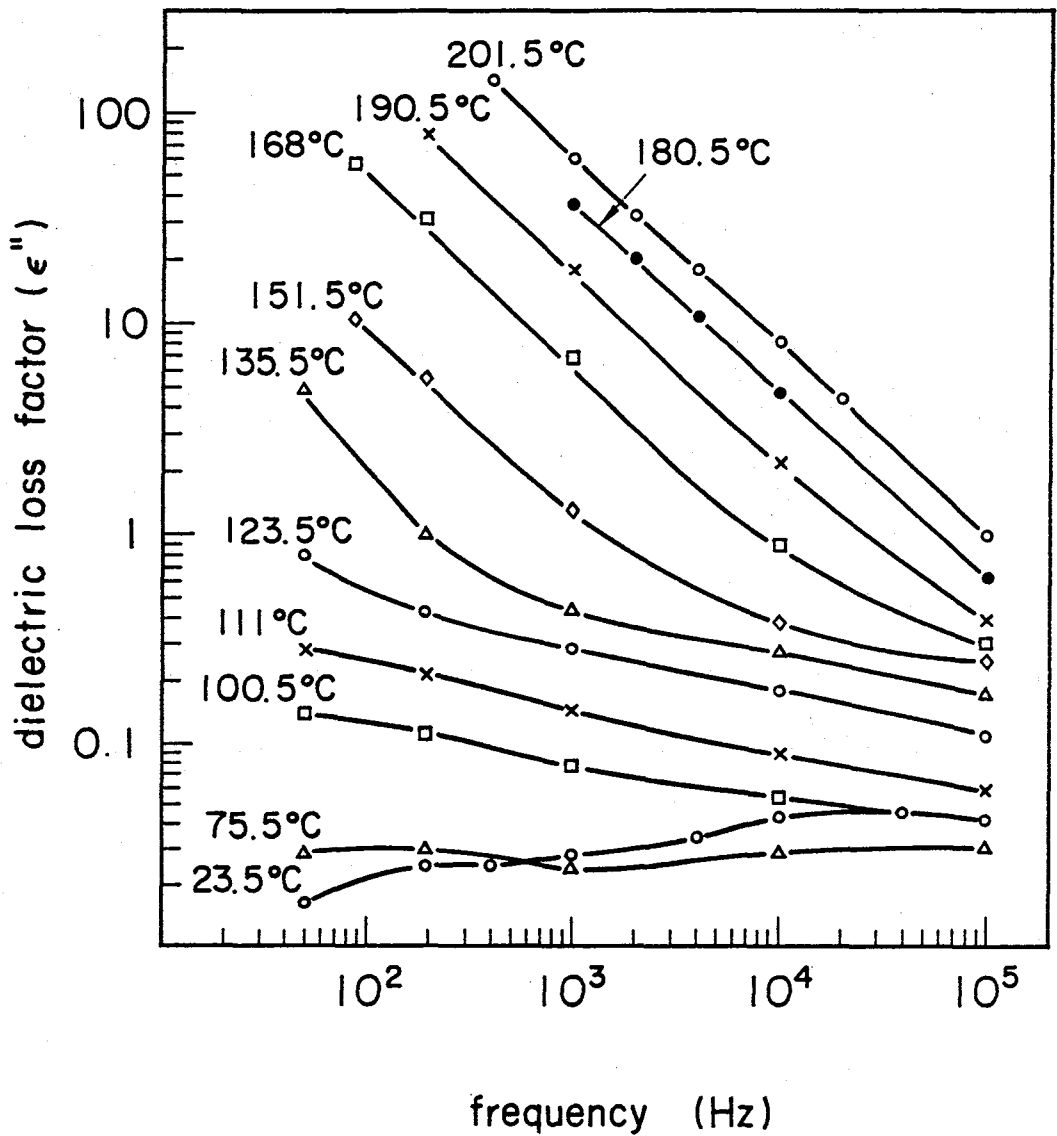


Figure 2 Relation between dielectric loss factor and frequency: sample, (I)-BF<sub>3</sub>·MEA.

Therefore, if conductance loss is predominant,  $\log \epsilon''$  would be inversely proportional to  $\log f$  (frequency), and the slope would be -1.

The difference in the electrical properties between (I)-Al(acac)<sub>3</sub>/SH6018 and (I)-BF<sub>3</sub>·MEA was investigated by means of thermal depolarization current method. Figure 3 shows the depolarization current-temperature curve. The curve had a maximum at about 120°C. Figure 4 shows the relation between the depolarization charge (Q) and the polarizing field (E<sub>p</sub>). The depolarization charge for (I)-Al(acac)<sub>3</sub>/SH6018 was about 10<sup>-8</sup> coul/cm<sup>2</sup> and that for (I)-BF<sub>3</sub>-MEA was about 10<sup>-6</sup> ~ 10<sup>-7</sup> coul/cm<sup>2</sup>. Generally speaking, polarization of dielectrics is classified into heterogeneous polarization and homogeneous polarization<sup>3</sup>. In the former, there are hetero charge which is caused by the macroscopic shift of ionic impurity in dielectrics, and homocharge which is caused by the injection of charge from electrode to dielectric. In the latter, there are orientational polarization charge and hetero charge which is caused by the microscopic displacement of ionic impurity. In the present experiment, the charge was hetero. The depolarization charge was directly proportional to the polarizing field. Therefore, the charge was considered to be due to homogeneous polarization.<sup>4</sup> If the polarization is attributed to the thermal disorder for orientational dipole only, maximum value for orientational



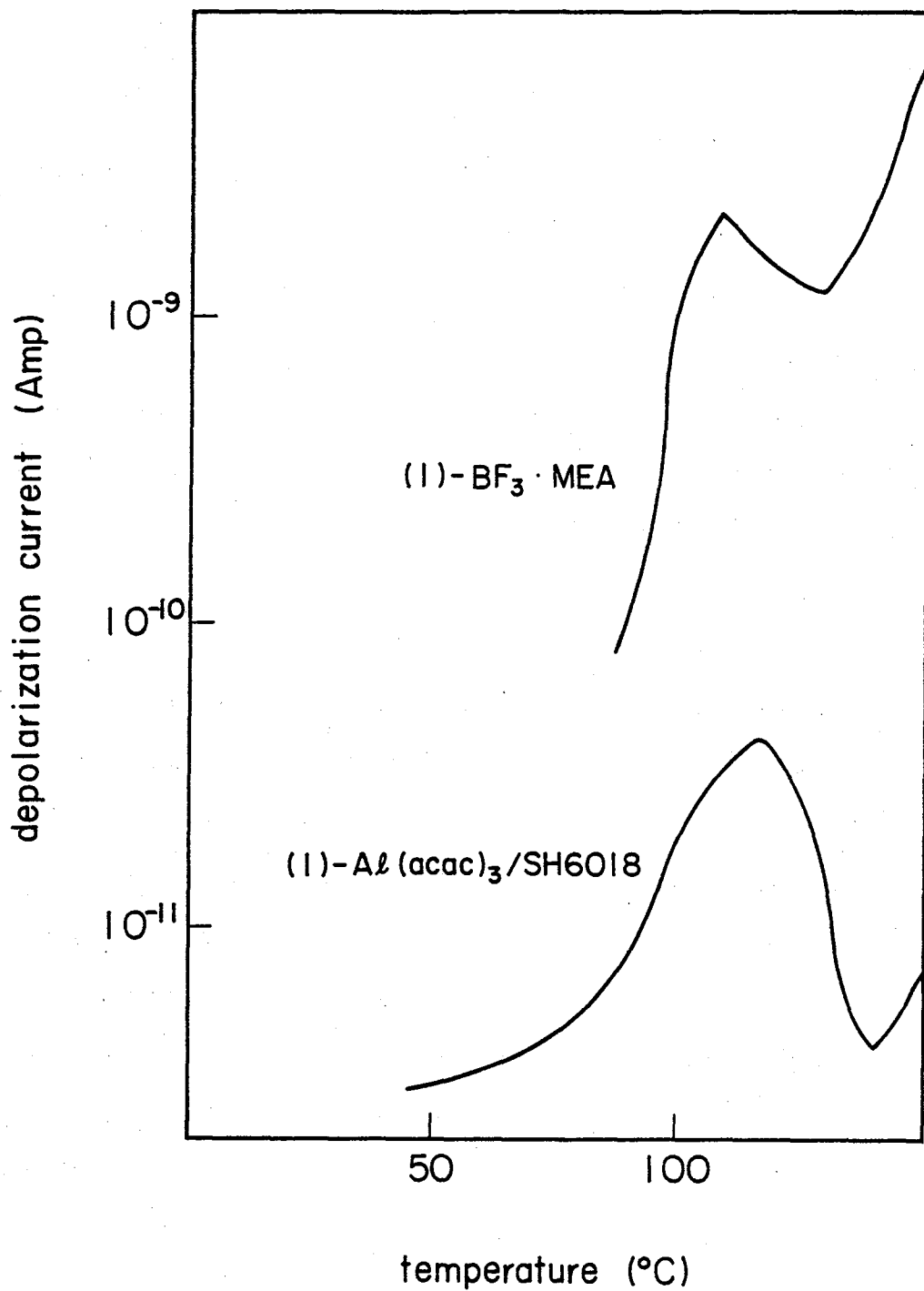


Figure 3 Depolarization current curve.  
Condition, see Figure 4.

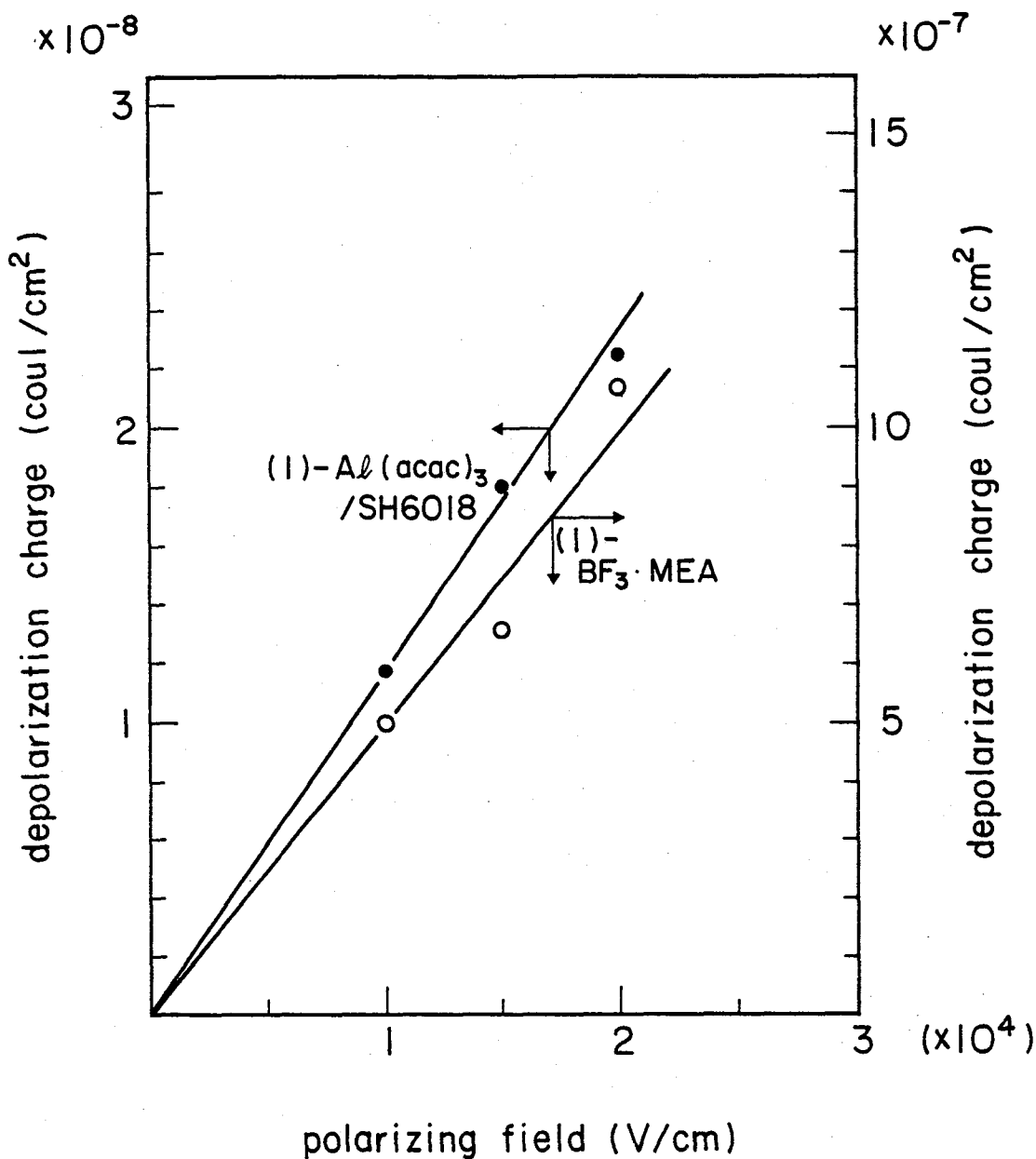


Figure 4 Relation between depolarization charge and polarizing field. Thickness 1 mm, (I)-Al(acac)<sub>3</sub>/SH6018, Al(acac)<sub>3</sub> 2 phr, SH6018 3 phr, 150°C, 15 h, electrode 10 mmφ,  $2 \times 10^4$  V/cm at 150°C.

polarization charge would be obtained from the following equation by use of Debye's polarization orientation theory.<sup>5</sup>

$$P = \frac{N\mu_{\text{eff}}^2 E_p}{3kT_p}$$

Where

- N : the number of dipole in 1 cm<sup>3</sup>
- $\mu_{\text{eff}}$ : effective dipole moment
- $E_p$  : polarizing field
- k : Boltzmann's constant
- $T_p$  : depolarization temperature

Hydroxide and ether linkage are present as the dipole in the cured epoxy resins. Group moment for alcohol and ether is about 1.6 - 1.7 Debye. The calculated orientational polarization charge was about 10<sup>-10</sup> coul/cm<sup>2</sup>, even if dipole moved freely. The measured depolarization charge was more than the calculated depolarization charge by a factor of about 10<sup>2</sup> in case of (I)-Al(acac)<sub>3</sub>/SH6018 and by a factor of about 10<sup>3</sup> ~ 10<sup>4</sup> in case of (I)-BF<sub>3</sub>·MEA. Therefore the depolarization charge could not be explained in terms of thermal disordering of dipoles only. However, when microscopic displacement and trap for ionic impurity were considered, the experimental results could be explained. Both of (I)-Al(acac)<sub>3</sub>/SH6018 and (I)-BF<sub>3</sub>·MEA had ionic impurity, however, it was found that the amount of ionic impurity in (I)-Al(acac)<sub>3</sub>/SH6018 was smaller

than that in (I)-BF<sub>3</sub>·MEA.

Dielectric constant for (I)-Al(SA)<sub>3</sub>/DP was relatively constant throughout the temperature from 25°C to 220°C. However dielectric constant for (I)-BF<sub>3</sub>·MEA changed remarkably at the temperature above 130°C, as shown in Figure 5.

Figure 6 shows the relation between volume resistivity and temperature. The volume resistivity of (I)-Al(SA)<sub>3</sub>/DP was higher than that of (I)-BF<sub>3</sub>·MEA by a factor of about 10<sup>4</sup> times at 150°C. The volume resistivity for (I)-Al(SA)<sub>3</sub>/DP hold the value of 10<sup>12</sup> Ωcm at even 200°C.

Break down voltage for (I)-Al(acac)<sub>3</sub>/SH6018 was compared with that for (I)-BF<sub>3</sub>·MEA. Figure 7 shows the results. Break down voltage for (I)-Al(acac)<sub>3</sub>/SH6018 increased gradually with temperature, however, that for (I)-BF<sub>3</sub>·MEA decreased remarkably at 120°C. These results show that Al(acac)<sub>3</sub>/SH6018 catalyst system is "clean" electrically, compared with BF<sub>3</sub>·complex catalyst.

The polymerization was considered to be caused cationically by the proton formed by the interaction between aluminum complex and silanol as mentioned in Chapter 5. Diphenylsilanediol was consumed by self condensation reaction, condensation with secondary alcohol in epoxy resin, and addition to the epoxide as shown in Figure 8. The cationic site is made by the interaction between aluminum complex and silanol. If the silanol is consumed in

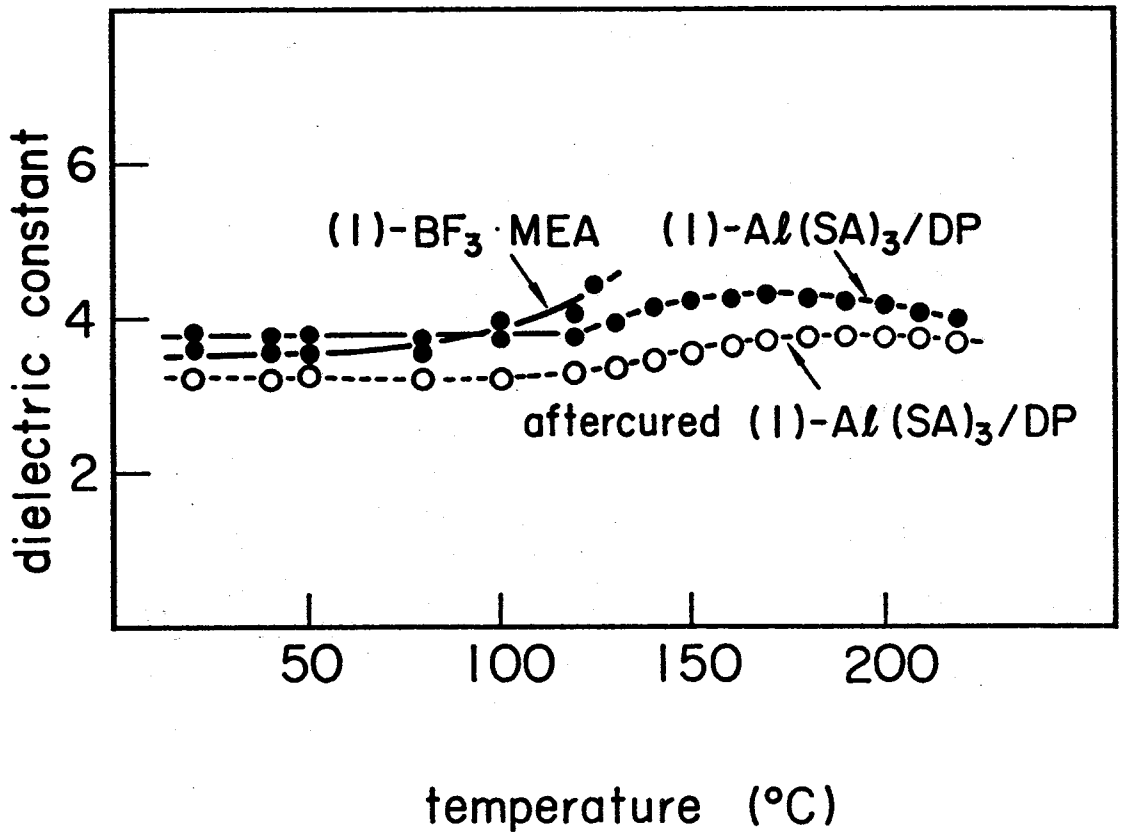


Figure 5 Relation between dielectric constant and temperature: aftercure, 180°C for 15 h.

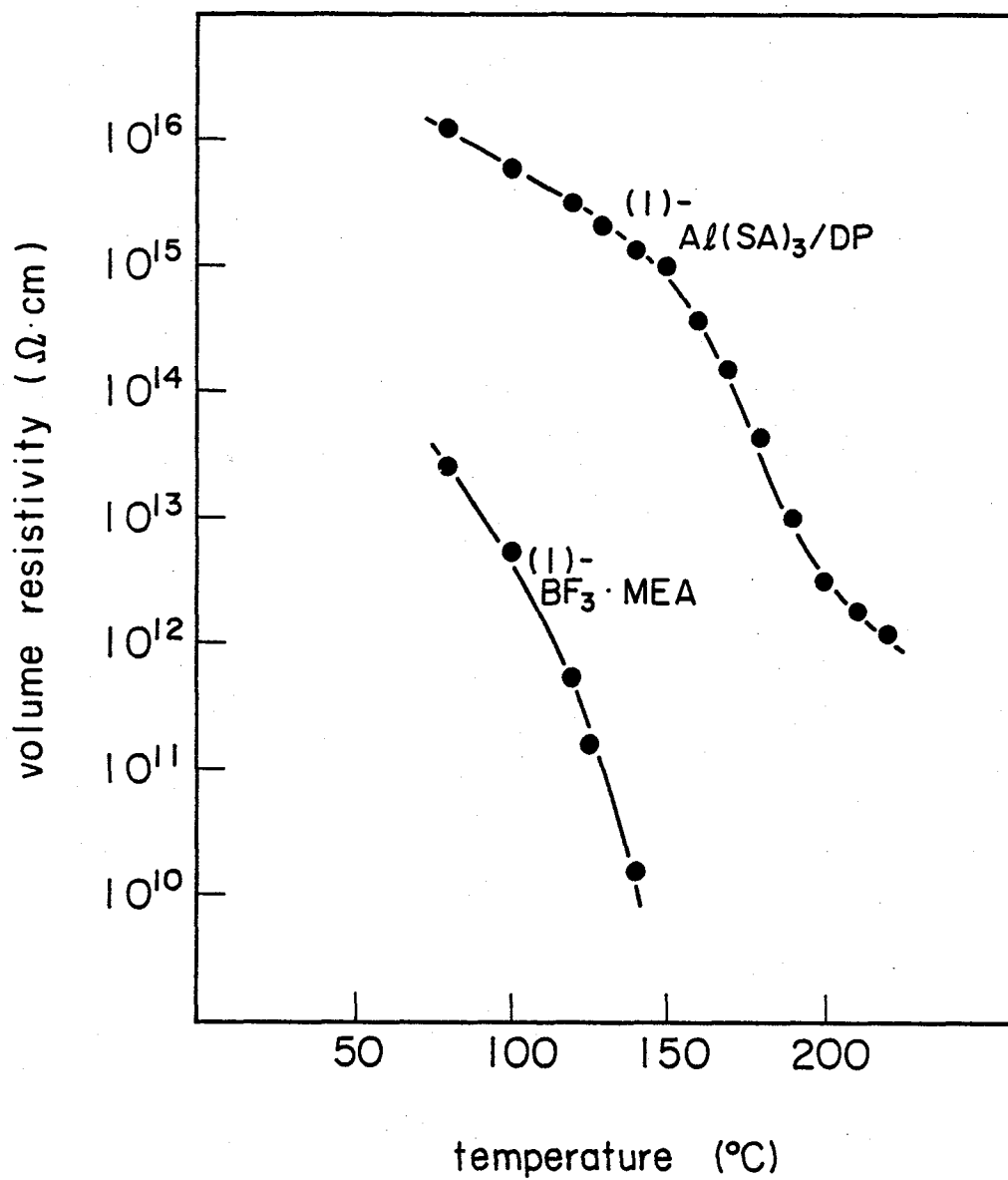


Figure 6 Relation between volume resistivity and temperature.

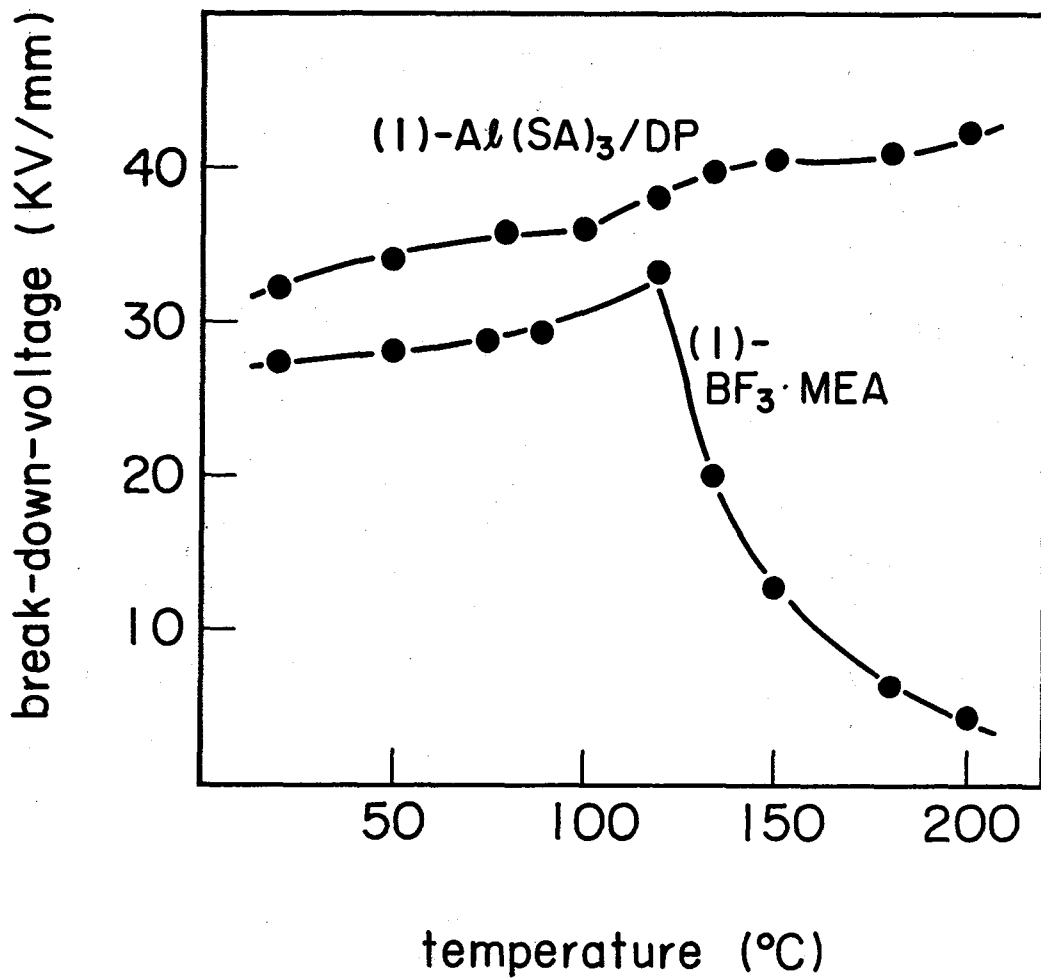
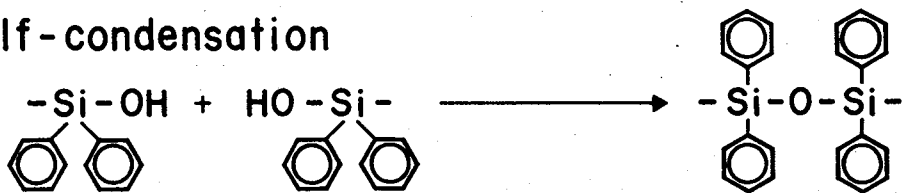
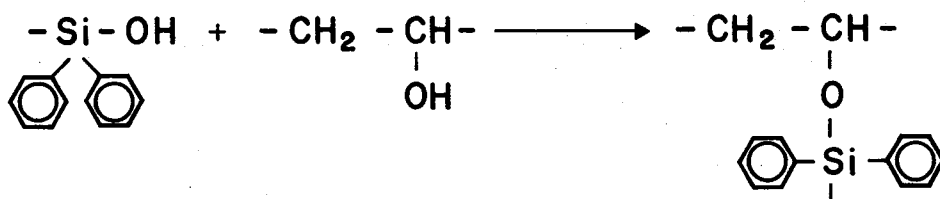


Figure 7 Relation between break-down-voltage and temperature.

self-condensation



condensation with secondary alcohol of epoxy resin



addition to epoxide

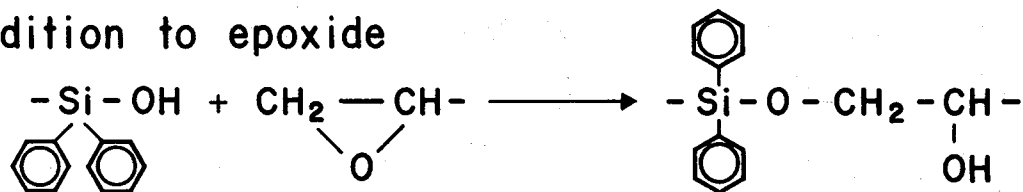


Figure 8



the polymerization reaction, no cationic site exists in the polymerization system. Therefore, the absence of any appreciable ionic species after polymerization will be important for the excellent electrical properties.

The presence of the cationic site in the cured resin matrix was considered to affect the thermal stability. Relation between weightloss of cured resin plate and aging time at 225°C was shown in Figure 9. The ratio of weightloss for (I)-BF<sub>3</sub>·MEA was larger than that for (I)-Al(SA)<sub>3</sub>/SH6018 (Toray silicone, silicone resin containing SiOH, OH equivalent 400). Ionic species in (I)-BF<sub>3</sub>·MEA would accelerate the degradation of the polymer chain.

### 9-3 Dependence of the electrical properties on structure of catalyst

The electrical properties depend on the structure of catalyst, as shown in Table 1. When triphenylsilanol was used as the silanol component, the electrical properties at 220°C deteriorated depending on the structure of catalyst, as follows, Al(SA)<sub>3</sub> > Al(Etaa)<sub>3</sub> > Al(acac)<sub>3</sub>. Gelation of the epoxide occurred depending on the catalyst, in the following order, Al(SA)<sub>3</sub>/Ph<sub>3</sub>SiOH > Al(Etaa)<sub>3</sub>/Ph<sub>3</sub>SiOH > Al(acac)<sub>3</sub>/Ph<sub>3</sub>SiOH. The electrical properties improved as curing proceeds.

When Al(SA)<sub>3</sub> was used as the aluminum component, the dependence of the electrical properties on silanol struc-

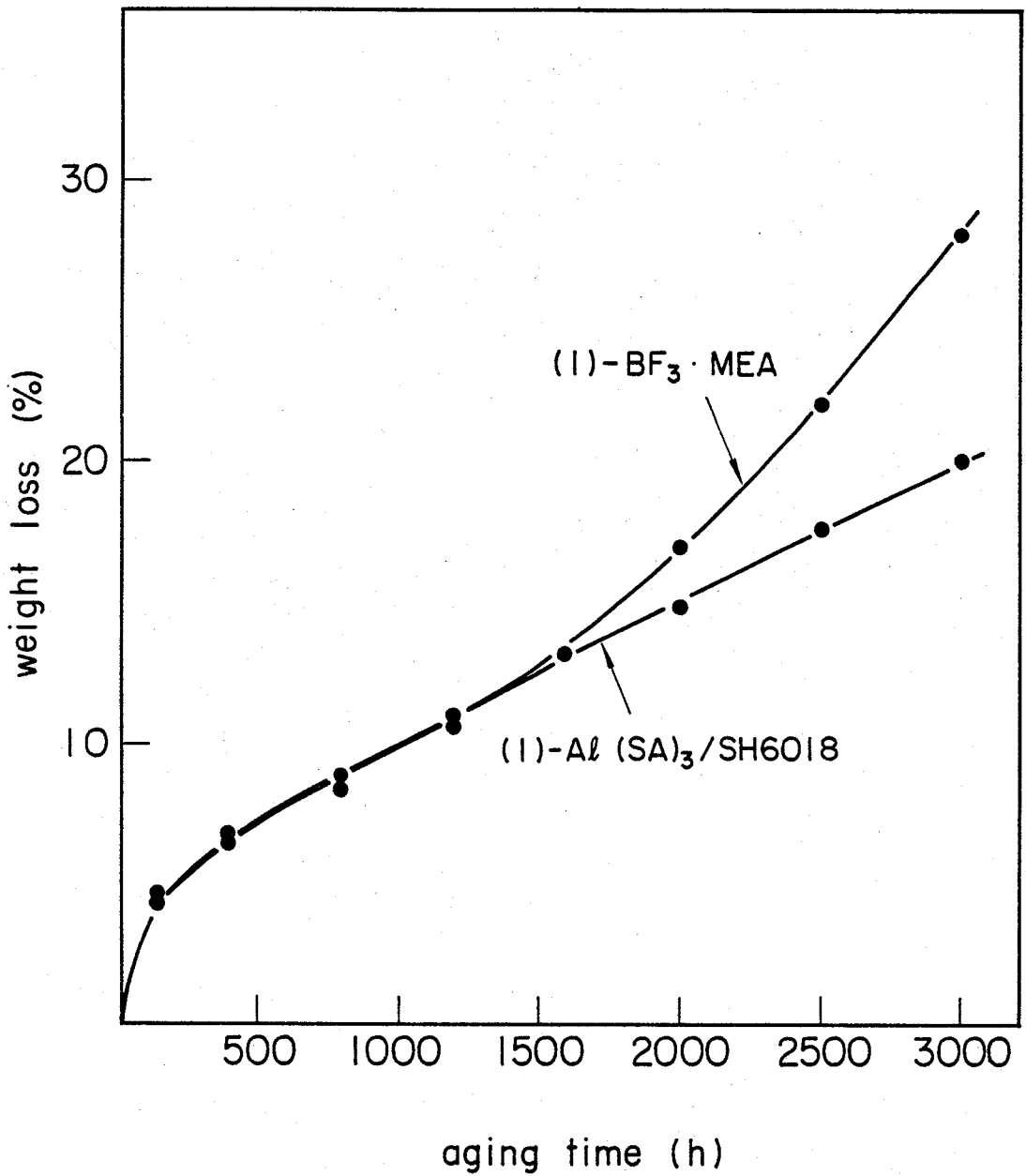


Figure 9 Relation between weight loss and aging time at 225°C Sample, (I)-Al(SA)<sub>3</sub>/SH6018, Al(SA)<sub>3</sub> 2 phr, SH6018 2 phr, 150°C, 15 h.

ture was examined. The electrical properties at 220°C lowered as follows,  $\text{Ph}_3\text{SiOH} > \text{SH6018} > \text{Ph}_2\text{Si}(\text{OH})_2$ . The order could be explained as the same way.

Dependence of the electrical properties on the amount of the catalyst was examined. When the amount of the silanol increased, the gellation time of the epoxy resin was faster. However, best electrical properties were obtained in case of aluminum complex/silanol(1/3) (mol/mol). When the ratio of the silanol was too large, silanol would remain in the matrix of the cured epoxy resin, therefore, the electrical properties would deteriorate.

Table 1 Electrical Properties for Epoxy Resin Cured with Aluminum Complex/Silanol Catalysts<sup>a)</sup>

Al complex (phr)	Silanol (phr)	Dissipation factor (%)		Dielectric constant		Volume resistivity ( $\Omega\text{cm}$ )		
		25°C	220°C	25°C	220°C	220°C		
Al(SA) <sub>3</sub>	2.4	Ph <sub>3</sub> SiOH	3.8	0.5	1.2	3.7	3.8	7.2 x 10 <sup>12</sup>
Al(Etaa) <sub>3</sub>	2.6	Ph <sub>3</sub> SiOH	3.8	0.4	2.9	3.9	4.1	3.0 x 10 <sup>12</sup>
Al(acac) <sub>3</sub>	2.0	Ph <sub>3</sub> SiOH	3.8	0.5	6.0	3.7	4.4	9.5 x 10 <sup>11</sup>
Al(SA) <sub>3</sub>	2.4	SH6018	5.6	0.5	2.5	3.8	3.9	5.0 x 10 <sup>12</sup>
Al(SA) <sub>3</sub>	2.4	Ph <sub>2</sub> Si(OH) <sub>2</sub>	3.0	0.5	3.0	3.8	4.0	1.1 x 10 <sup>12</sup>
Al(acac) <sub>3</sub>	2.0	Ph <sub>2</sub> Si(OH) <sub>2</sub>	1.5	0.8	12.4	3.9	6.1	-
"	"	"	3.0	0.6	8.0	3.7	4.9	-
"	"	"	4.5	0.7	6.2	3.7	4.5	-
"	"	"	6.0	0.7	4.9	3.7	4.0	-
"	"	"	7.5	0.5	5.7	3.9	4.7	-
"	"	"	9.0	0.9	10.0	4.1	5.7	-

a) 150°C for 15 h cure

## References

1. H. Mikawa, and S. Kusabayashi, *Kobunshi Handotai*, p. 248, Kodan-sha, printed in Japan (1977);  
Y. Toriyama, *Hoden Hand Book*, Denki-Gakkai, p.390, printed in Japan.
2. P. K. C. Pillai and M. Goel, *J. Electrochem. Soc.*, 120, 395 (1973)
3. G. Gross, *Phys. Rev.*, 54, 57 (1940)
4. M. M. Perlman, *J. Appl. Phys.*, 42, 2645 (1971)
5. P. Debye, "Polar Molecules" Reinhold Pub. Co., (1929)

## Chapter 10 Latent Catalyst

### 10-1 Introduction

In this way, "clean" and active catalyst for epoxide polymerization was obtained. For practical use, epoxy resins are provided as a composition containing catalyst. The epoxy resin composition must be stable before use. It must be cured rapidly. Therefore, molecular design is necessary for the active catalyst which is generated by a trigger. Heat or UV-radiation is usually used as the trigger. The catalyst is called as a latent catalyst.

The following latent catalyst were investigated.

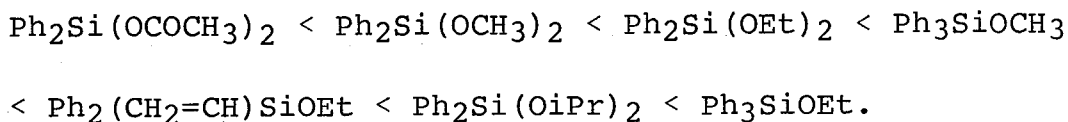
- 1) Aluminum complex/hydrolyzable silicon compound system.
- 2) Aluminum complex/thermally generated silicon compound system.
- 3) Aluminum complex/photogenerated silicon compound system.

### 10-2 Aluminum complex/hydrolyzable silicon compound system

Active site of aluminum complex/silanol catalyst is SiO-H. If the SiOH is protected with alkoxy group, the catalyst activity at room temperature will be inhibited. However, the alkoxy silane will be hydrolyzed by small amount of water contained in epoxy resin monomer at higher temperature, then the catalyst will be active.

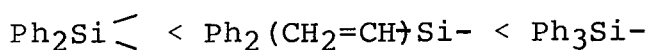


The temperature at which the reaction is carried out ( $T_h$ ) was examined. Alicyclic epoxy resin (II) shown in Figure 1 was used. Temperature of epoxy resin (II) containing the catalyst was raised at 1.5°C/min and the rise in temperature caused by reaction heats was examined. Table 1 shows the results. The  $T_h$  rised in the following order, depending on the structure of alkoxyasilane.

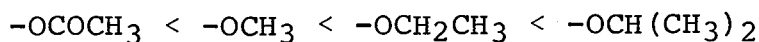


The  $T_h$  changed by following factor.

1) Substituent bonding to Si



2) Alkoxide (or esterate)



Ease in hydrolyzability for Si-O is determined by bulkiness neighbour Si and O. The tendency of  $T_h$  was coincident with that of hydrolyzability.

Table 2 shows the activation energy of gelation from 150°C to 200°C, when Epikote 828 epoxy resin [I] type was

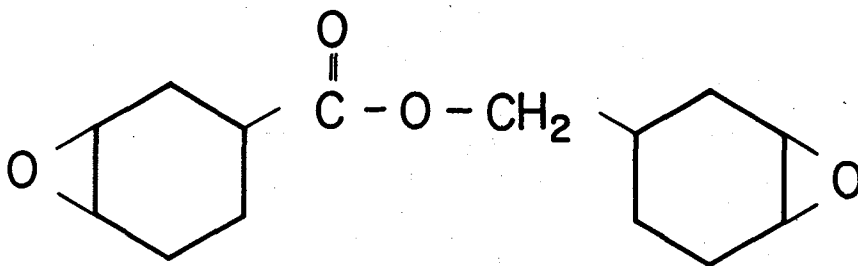


Figure 1 Structure of alicyclic epoxide.  
(ERL 4221, UCC)

Table 1 Variation of Catalytic Activity of  
Al(acac)<sub>3</sub>/alkoxysilane.<sup>a)</sup>

Alkoxysilane	phr <sup>b)</sup>	Temperature (°C)
Ph <sub>2</sub> Si(OMe) <sub>2</sub>	0.37	73
Ph <sub>2</sub> Si(OEt) <sub>2</sub>	0.41	85
Ph <sub>2</sub> Si(OiPr) <sub>2</sub>	0.45	123
Ph <sub>2</sub> Si(OCOCH <sub>3</sub> ) <sub>2</sub>	0.45	50
Ph <sub>3</sub> SiOMe	0.44	95
Ph <sub>3</sub> SiOEt	0.46	130
Ph <sub>2</sub> (CH <sub>2</sub> =CH)SiOEt	0.39	100

a) Program rate 1.5°C/min. epoxide aliphatic epoxide  
(see Figure 1), Al(acac)<sub>3</sub> 0.19 mol%, alkoxysilane  
0.38 mol%

b) weight % to epoxy resin.

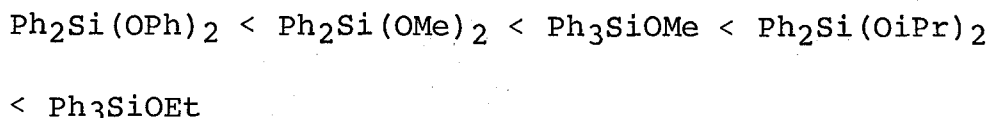


Table 2    Activation Energy Obtained Using  
 Various Silane Catalysts<sup>a)</sup>

Alkoxysilane	Activation energy (kcal/mol)
$\text{Ph}_2\text{Si}(\text{OMe})_2$	23.7
$\text{Ph}_2\text{Si}(\text{OEt})_2$	28.4
$\text{Ph}_2\text{Si}(\text{OiPr})_2$	25.6
$\text{Ph}_2\text{Si}(\text{OPh})_2$	23.3
$\text{Ph}_2\text{SiOEt}$	26.0
$\text{Ph}_3\text{SiOMe}$	25.5

a)  $\text{Al}(\text{SA})_3$  2.4 phr, alkoxysilane 0.123 mol/1000 ml  
 of epoxide, measurement of gelation by curast  
 meter method.

cured with  $\text{Al}(\text{SA})_3$ /alkoxysilane catalyst. The activation energy increased in the following order.

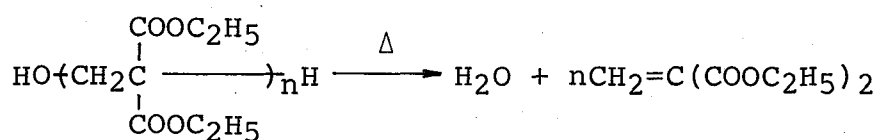


The tendency of order of activation energy was the same as that of  $T_h$ .

In the aluminum complex/alkoxysilane catalyst, the alkoxysilane was gradually hydrolyzed even at room temperature and the epoxy resin was gradually reacted. In order to prevent the reaction at room temperature, water in the epoxy resin was eliminated with zeolite 4A. Figure 2 shows the results. The composition was more stable in presence of zeolite. However above  $100^\circ\text{C}$ , gelation of the composition in presence of the zeolite was faster.

### 10-3 Aluminum complex/thermally generated silicon compound system

The silicone compound liberating silanol thermally without  $\text{H}_2\text{O}$  was investigated. It is known that the organic compound decomposes by means of  $\beta$ -elimination as follows.<sup>1</sup>



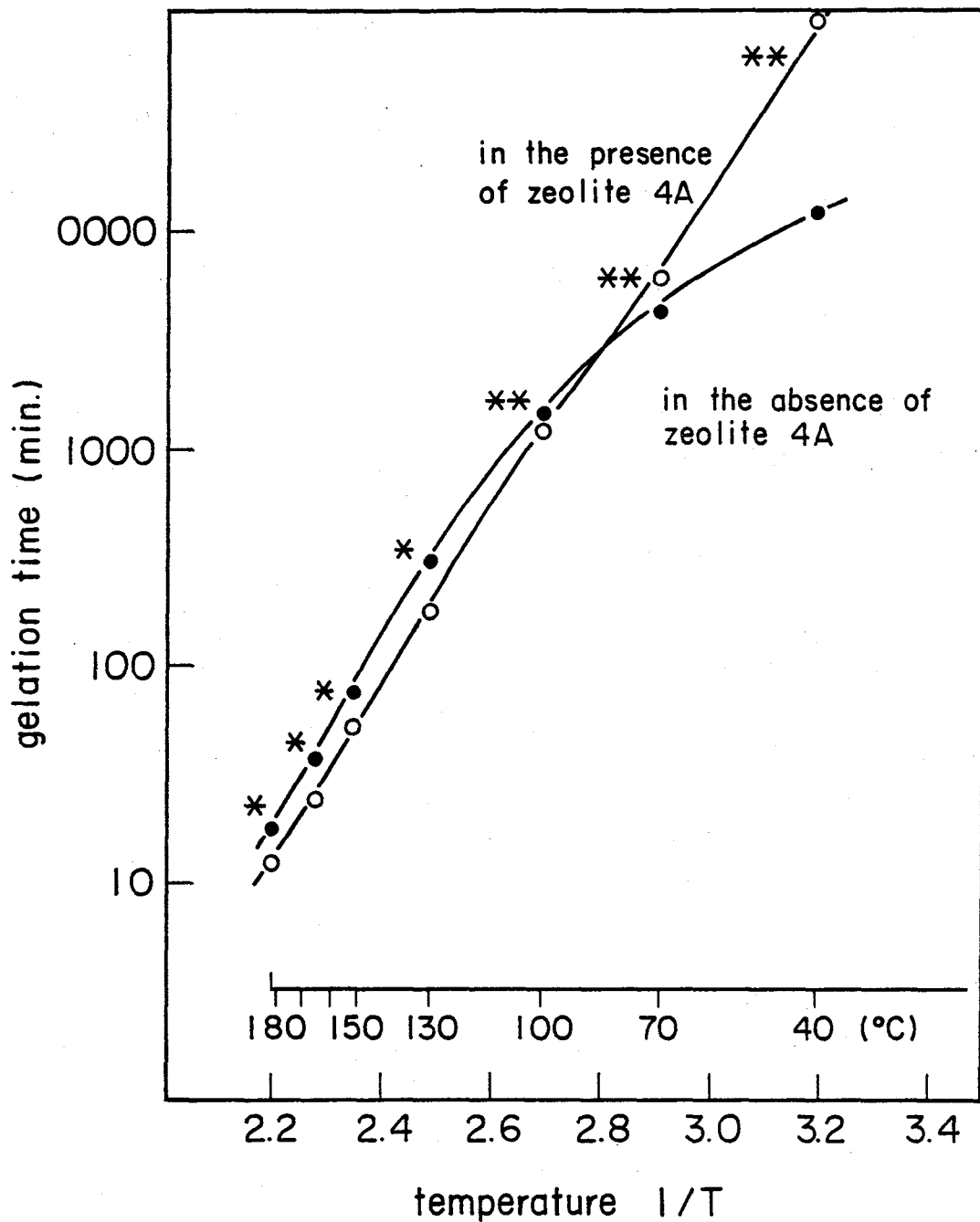
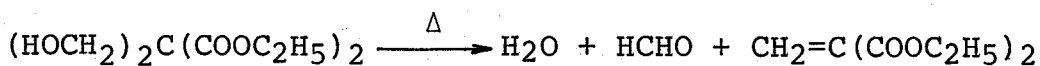
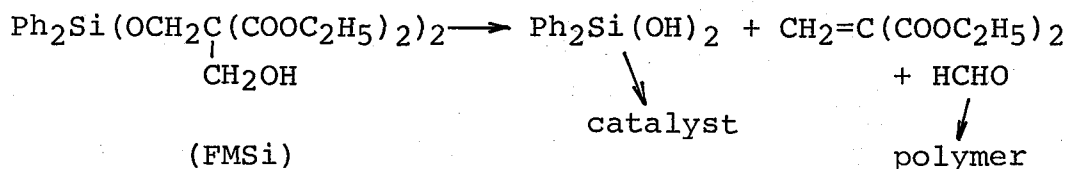


Figure 2 Relation between gelation time and temperature.  
 $\text{Al}(\text{SA})_3$  4.8 phr,  $\text{Ph}_2\text{Si}(\text{OMe})_2$  2.0 phr, Epikote 828 epoxy resin, zeolite 4A 10 phr.

\* curast meter method, \*\* test tube method.



Decomposition of silicon compound by means of the  $\beta$ -elimination was examined. The following compound was found to satisfy the purpose.



The aluminum complex/FMSi catalyst was more latent than the aluminum complex/hydrolyzable silicon compound catalyst. The results are shown in Table 3. Decomposition of FMSi was slow by itself. However, the aluminum complex accelerated the decomposition. FMSi decomposed within 15 min. at 130°C completely in the presence of  $\text{Al}(\text{SA})_3$ .

#### 10-4 Photogenerated catalyst (I): Aluminum complex/ Ph<sub>3</sub>SiCOPh/alcohol system

The catalyst curing epoxy resin with UV radiation have recently attracted interest due to the processability and to the energy saving. The photo-generated catalyst will be most important as latent catalyst, because reaction starts at low temperature, however long pot life is expected in the absence of UV-radiation.

Diazonium salts and some onium salts are known to be effective for the UV curing of the epoxy resins.<sup>2</sup> However

Table 3 Gelation Time of FMSi/Al(SA)<sub>3</sub> Latent Catalyst<sup>a)</sup>

temperature (°C)	Gelation time (min.)							
	40	100	130	140	150	160	170	180
reference Ph <sub>2</sub> Si(OEt) <sub>2</sub> /Al(SA) <sub>3</sub>	1.4 x 10 <sup>4</sup>	4.3 x 10 <sup>3</sup>	9.5 x 10 <sup>2</sup>	-	60	30	20	17
FMSi/Al(SA) <sub>3</sub>	7.0 x 10 <sup>5</sup>	1.1 x 10 <sup>3</sup>	5.0 x 10 <sup>2</sup>	1.5 x 10 <sup>2</sup>	60	31	20	17

a) Al(SA)<sub>3</sub> 4.8 phr, Silyl compound 3 phr, test tube method.

diazonium salts had problems that N<sub>2</sub> gas was evolved, and these catalyst gave ionic species which disturbed insulation.

The UV-curable epoxy resins with good electrical properties may be obtained by use of compounds which produce a component of the present catalyst by photo-reaction. Such photolabile component is implied since A. G. Brook reported that Ph<sub>3</sub>SiCOPh had n- $\pi^*$  absorption (424 nm ( $\epsilon = 292$ )) and  $\pi$ - $\pi^*$  absorption (257 nm (16200)), and photo-decomposed to Ph<sub>3</sub>SiOH in the presence of H<sub>2</sub>O or alcohols.<sup>3</sup> A new catalyst system (aluminum complex/Ph<sub>3</sub>SiCOPh/alcohol) was thus investigated.

Figure 3 shows the time-conversion and time-molecular weight curve; the dashed line indicates the polymer conversion curve under UV irradiation and the solid lines indicate conversion curves after UV irradiation was stopped at the point where the dashed line connects with the solid lines. Both polymerization rate and molecular weight increased with photopolymerization time. The polymerization also continued after UV irradiation was stopped. The polymerization rate increased with UV irradiation time. Cyclohexene oxide did not polymerize in the absence of UV irradiation and did not polymerize in the absence of a catalyst component, even under UV irradiation. These facts imply that the catalyst activity results from the interaction between the aluminum complex

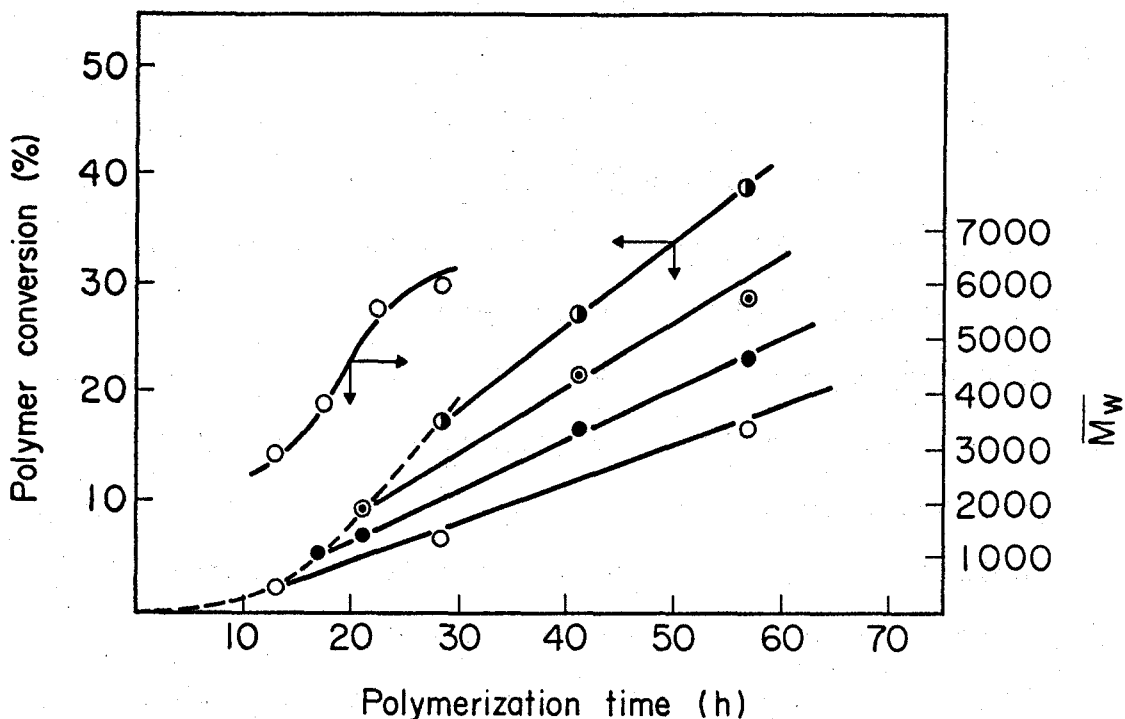


Figure 3 Photopolymerization of cyclohexene oxide.

Polymerization conditions:  $\text{Al}(\text{acac})_3$ , 0.1 mol%,  $\text{Ph}_3\text{SiCOPh}$ , 0.5 mol%,  $\text{H}_2\text{O}$ , 1 mol%, polymerization temperature,  $40^\circ\text{C}$ . (—○—) molecular weight-polymerization time curve (under UV irradiation); (—○—●—○—●—) polymer conversion-polymerization time curve (under UV irradiation); (—○—) polymer conversion-polymerization time curve after UV irradiation was stopped at 13 h; (—●—) polymer conversion-polymerization time curve after UV irradiation was stopped at 17 h; (—○—) polymer conversion-polymerization time curve after UV irradiation was stopped at 22 h; (—●—) polymer conversion-polymerization time curve after UV irradiation was stopped at 28 h.

and the  $\text{Ph}_3\text{SiOH}$  which is a photodecomposition product of  $\text{Ph}_3\text{SiCOPh}$ .

The fact that the molecular weight and polymerization rate increased with photopolymerization time could be explained by the presence of alcohol in the polymerization system. In thermal polymerization with  $\text{Al}(\text{acac})_3/\text{Ph}_3\text{SiOH}$  catalyst the polymerization rate was almost constant or decreased with polymerization time and the molecular weight was almost constant. Table 4 shows the polymer conversion and molecular weight in thermal polymerization with  $\text{Al}(\text{acac})_3/\text{Ph}_3\text{SiOH}$  catalyst in the presence of *i*-PrOH. Addition of 2 mol% of *i*-PrOH decreased the polymerization rate to 40 % and decreased the molecular weight of the polymer obtained. The polymerization behavior in Figure 3 can be explained as follows: in the initial stage of photopolymerization a large amount of alcohol was present in the polymerization system, but the alcohol diminished as the photodecomposition of  $\text{Ph}_3\text{SiCOPh}$  proceeded. Therefore the molecular weight and polymerization rate probably increased with photopolymerization time.

#### Influence of the structure of alcohol on photopolymerization catalyst activity

In  $\text{Al}(\text{n-Pr})_3/\text{Ph}_3\text{SiCOPh}/i\text{-PrOH}$  catalyst the photodecomposition rate of  $\text{Ph}_3\text{SiCOPh}$  became greater and polymer conversion increased by increasing the amount of *i*-PrOH.



Table 4 Influence of Polymer Conversion and Molecular Weight on the Amount of i-PrOH

i-PrOH (mol%)	Polymerization rate ( $\times 10^{-5}$ ) (mol/min)	$M_w$	$M_n$
0	0.20(1.00) <sup>1</sup>	—	—
0.1	0.14(0.70)	29,000	14,000
0.5	0.11(0.55)	24,000	11,000
1.0	0.09(0.45)	18,000	8,000
2.0	0.08(0.40)	15,000	7,300

Note: Polymerization conditions: 40°C, Al(acac)<sub>3</sub> 0.05 mol%, Ph<sub>3</sub>SiOH 0.05 mol%, cyclohexene oxide 1 mL.

<sup>1</sup>The values in parenthesis show the relative polymerization rate when the polymerization rate in the absence of i-PrOH was 1.00.

However, the molecular weight decreased because the amount of *i*-PrOH in the polymerization system increased (Figure 4). Polymer conversion also varied with the identity of the alcohol (Table 5). The catalyst activity decreased in the following order for the OH component: *i*-PrOH > *n*-PrOH > *i*-BuOH > EtOH > MeOH > *t*-BuOH > H<sub>2</sub>O. Three reasons are given for the maximum polymer conversion when using Al(*n*-praa)<sub>3</sub>/Ph<sub>3</sub>SiCOPh/*i*PrOH catalyst.

(a) Photodecomposition rate of Ph<sub>3</sub>SiCOPh in THF is influenced by the structure of OH compound and decreased as follows:

MeOH > EtOH > *i*-PrOH > H<sub>2</sub>O > *t*-BuOH (Table 5, decomposition rate).

(b) Addition of OH compound inhibited the polymerization of cyclohexene oxide with aluminum complex/silanol catalyst. The degree of inhibition varied with the structure of the OH compound and decreased in the following order:

*t*-BuOH > *i*-PrOH > EtOH > MeOH > H<sub>2</sub>O (Table 5, model thermal polymerization rate).

(c) Ph<sub>3</sub>SiCOPh has been known to be photodecomposed to Ph<sub>3</sub>SiOH, Ph<sub>3</sub>SiOR, Ph<sub>3</sub>SiOCH(OR)Ph, and other products.<sup>3</sup> Among them only Ph<sub>3</sub>SiOH became the active catalyst component by interaction with aluminum complex. The formation rate of Ph<sub>3</sub>SiOH decreased in the following order:

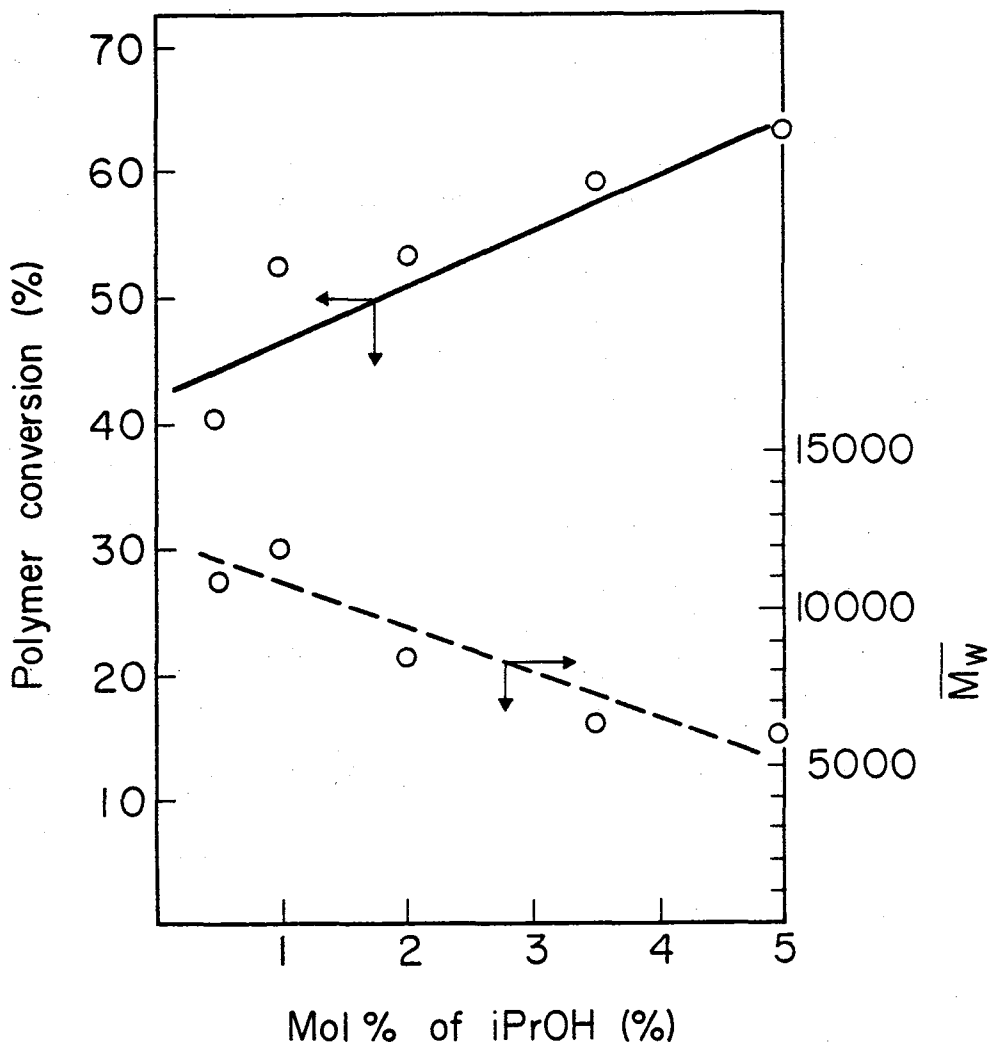


Figure 4 Influence of the amount of i-PrOH on polymer yield and molecular weight. Polymerization conditions:  $\text{Al}(\text{n-Pr}aa)_3$ ; 0.1 mol%,  $\text{Ph}_3\text{SiCOPh}$ ; 0.5 mol%, polymerization time; 12 h, polymerization temperature,  $40^\circ\text{C}$ .

Table 5 Influence of polymer conversion on alcohol

OH compound	Polymerization time (h)	$\overline{M}_w$	Conversion (%)	Decomposition 1) rate $\times 10^{-8}$ (mol/min)	Model 2) reaction rate $\times 10^{-5}$ (mol/min)	Ratio of Ph <sub>3</sub> SiOH(%)
H <sub>2</sub> O	12.5	—	14.3	0.95 (1)	0.54 (1.0)	35
MeOH	10.0	8,800	19.9	6.18 (6.5)	0.92 (1.7)	16
EtOH	10.0	12,000	27.1	2.95 (3.1)	1.08 (2.0)	55
n-PrOH	11.0	8,400	39.4	— (-)	— (-)	-
i-BuOH	11.0	8,500	32.9	— (-)	— (-)	-
t-BuOH	11.0	14,000	14.6	0.38 (0.4)	1.62 (3.0)	43
i-PrOH	11.0	10,500	50.6	0.95 (1.0)	1.24 (2.3)	69

Polymerization conditions ; Al(nPraa)<sub>3</sub> 0.1 mol%, Ph<sub>3</sub>SiCOPh 0.5 mol%, OH compound, 0.1 mol%, 40°C

1) Ph<sub>3</sub>SiCOPh  $1.23 \times 10^{-5}$  mol, OH compound  $1.83 \times 10^{-3}$  mol, THF 2.5 cc

2) Al(acac)<sub>3</sub> 0.05 mol%, Ph<sub>3</sub>SiOH 0.05 mol%, OH compound 1 mol%, cyclohexene oxide 1.0 ml, 40°C

$i\text{-PrOH} > \text{EtOH} > t\text{-BuOH} > \text{H}_2\text{O} > \text{MeOH}$  (Table 5, ratio of  $\text{Ph}_3\text{SiOH}$ ).

In a combination of these three different orders the best selection was  $i\text{-PrOH}$ . The molecular weight was also influenced mainly, by alcohols and decreased in the following order:  $t\text{-BuOH} > \text{EtOH} > i\text{-PrOH} > \text{MeOH}$ , which was similar to the order of the polymerization rate with  $\text{Al}(\text{acac})_3/\text{Ph}_3\text{SiOH}$  catalyst in the presence of alcohol.

#### Dependence of Polymer Conversion and Molecular Weight on the Amount of $\text{Ph}_3\text{SiCOPh}$

When the amount of  $\text{Ph}_3\text{SiCOPh}$  was changed from 1 to 4 mol% under the condition that  $\text{Al}(\text{n-Praa})_3$  and  $i\text{-PrOH}$  were 1 mol% the polymer conversion increased (Fig. 5). The degree of increase was large from 1.0 to 2.0 mol% and small from 2.0 to 4.0 mol%. This molecular weight decreased from 12,000 to 9,000 linearly.

#### Influence of the Structure of Aluminum Complex on Polymer Conversion

Table 6 shows the dependence of polymer conversion on the structure of the aluminum complex. The complexes used were in the following three categories:

(a)  $\beta$ -diketonato aluminum:  $\text{Al}(\text{acac})_3$ ,  $\text{Al}(\text{DPM})_3$ ,  
 $\text{Al}(\text{DMH})_3$ .

(b)  $\beta$ -ketoesterato aluminum:  $\text{Al}(\text{Etaa})_3$ ,  $\text{Al}(\text{n-Praa})_3$ ,

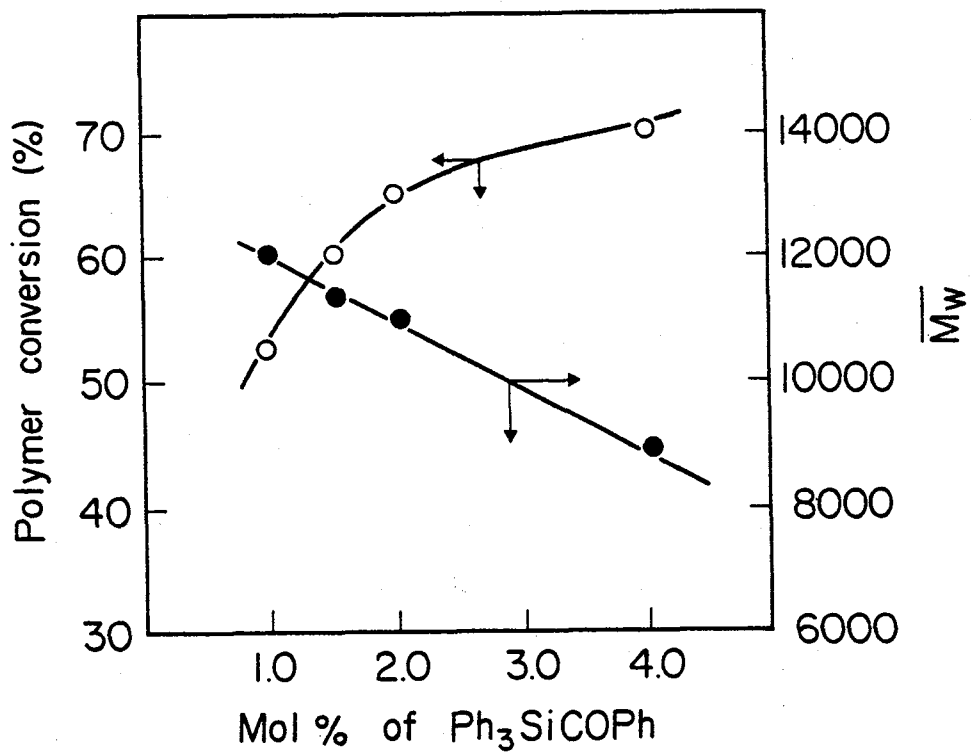


Figure 5 Influence of amount of  $\text{Ph}_3\text{SiCOPh}$  on polymer yield and molecular weight, Polymerization conditions:  $\text{Al}(\text{n-Pr}aa)_3$ , 0.1 mol%, *i*-PrOH, 1.0 mol%, polymerization time, 12 h, polymerization temperature, 40°C.

Table 6 Influence of Aluminum Compound on Polymer Conversion

Aluminum compound	Polymer conversion (%)	$\bar{M}_w$	Decomposition rate of $\text{Ph}_3\text{SiCOPh}^{\text{a}}$ ( $\times 10^{-8}$ ) (mol/min)
$\text{Al}(\text{acac})_3$	3.1	5300	0.95
$\text{Al}(\text{DMH})_3$	4.5	—	—
$\text{Al}(\text{DPM})_3$	5.1	8200	0.94
$\text{Al}(\text{Etaa})_3$	15.5	8000	0.98
$\text{Al}(\text{nPraa})_3$	19.3	8000	0.95
$\text{Al}(\text{iBuaa})_3$	22.6	—	—
$\text{Al}(\text{SA})_3$	11.0	8300	0.85
$\text{Al}(\text{ASA})_3$	14.0	—	—

Note: Polymerization conditions: aluminum compound, 0.1 mol%,  $\text{Ph}_3\text{SiCOPh}$ , 0.5 mol%, *i*-PrOH, 1.0 mol%, polymerization temperature, 40°C, polymerization time, 9.5 h.

a)  $\text{Ph}_3\text{SiCOPh}$   $4.92 \times 10^{-3}\text{M}$ , *i*-PrOH 0.73M and aluminum complex,  $1.85 \times 10^{-3}$  in THF. See Experimental section, photolysis.

$\text{Al}(\text{iBuaa})_3$ .

(c) Orthocarbonylphenolato aluminum:  $\text{Al}(\text{SA})_3$ ,  $\text{Al}(\text{ASA})_3$ .

Although the catalyst system that contained  $\beta$ -diketonato aluminum had low activity, activity in the catalyst system that contained  $\beta$ -ketoesterato aluminum was high. Among the catalyst systems that contained  $\beta$ -diketonato aluminum the catalyst activity decreased in the sequence  $\text{Al}(\text{DPM})_3 > \text{Al}(\text{DMH})_3 > \text{Al}(\text{acac})_3$ , which was coincident with the activity order of the aluminum complex in the thermal polymerization with aluminum complex/ $\text{Ph}_3\text{SiOH}$  catalyst. Among the catalyst systems that contained  $\beta$ -ketoesterato aluminum the same trend was recognized:  $\text{Al}(\text{i-Buaa})_3 > \text{Al}(\text{n-Praa})_3 > \text{Al}(\text{Etaa})_3$ .

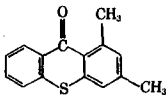
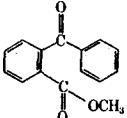
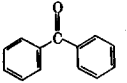
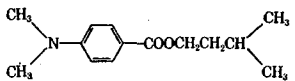
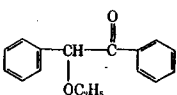
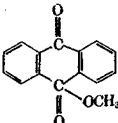
Orthocarbonylphenolato aluminum had high activity in thermal polymerization with  $\text{Ph}_3\text{SiOH}$ . In photopolymerization, however, the activity was not high. The lower photoactivity can be explained: orthocarbonylphenolato aluminum has strong absorption in the UV region. Therefore photodecomposition of  $\text{Ph}_3\text{SiCOPh}$  would be inhibited to some extent in the presence of orthocarbonylphenolato aluminum. As shown in Table 6 (decomposition rate), the photodecomposition rate of  $\text{Ph}_3\text{SiCOPh}$  in the presence of orthocarbonylphenolato aluminum was slower than that in the presence of the other aluminum complexes.



## The Photosensitizer

A. G. Brook reported that pyridine was effective as a sensitizer in photodecomposition of  $\text{Ph}_3\text{SiCOPh}$ .<sup>3</sup> In the present experiment the following three categories of sensitizers were used in the  $\text{Ph}_3\text{SiCOPh}/\text{Al}(\text{nPr})_3/\text{i-PrOH}$  catalyst system (Table 7): (a) benzophenones, (b) amines, (c) benzoin ether. Among them, benzophenone derivatives were the most useful for the photodecomposition of  $\text{Ph}_3\text{SiCOPh}$  and catalytic polymerization. Compared with the decomposition rate in the absence of sensitizer, photodecomposition was accelerated 10.7 times in the presence of methyl benzoylbenzoate and polymer conversion was 2.6 times larger. Benzophenone was most effective and polymer conversion increased 3.2 times. When the amount of benzophenone was large the polymer conversion increased with no decrease in molecular weight. Amines were not effective and the decomposition rate was only 1.2 or 1.3 times larger. Moreover, the polymer conversion was lower than that in the absence of amines. The effects of amines can be explained: (a) the polymerization is probably cationic; therefore the presence of amine would retard the polymerization. (b) When amine was used as a sensitizer the amount of  $\text{Ph}_3\text{SiOH}$  in the photodecomposition products of  $\text{Ph}_3\text{SiCOPh}$  was extremely low. When the amine with low basicity was used at low concentration inhibition of polymerization was negligible

Table 7 Dependence of Photosensitizer on Polymer Conversion

Sensitizer	Mole %	Polymerization time (h)	Polymer conversion	$\bar{M}_w$	Decomposition rate of $\text{Ph}_3\text{SiCOPh}^a$ ( $\times 10^{-8}$ ) (mol/min)
—	—	7	8.5	4,200	0.95 (1.0) <sup>b</sup>
	0.5	7	13.8	3,700	4.47 (4.7)
	0.5	7	22.0	3,400	10.17 (10.7)
	0.5	7	26.8	3,400	—
NEt <sub>3</sub>	0.4	12	3.5	—	0.95 (1.0)
Pyridine	0.4	12	3.1	—	1.24 (1.3)
	0.01	9	12.2	—	1.14 (1.2)
"	0.05	9	6.6	—	—
"	0.10	9	5.5	—	—
	0.5	7	11.5	3,500	3.14 (3.3)
	0.08	7	18.1	3,500	—
"	0.41	7	20.0	3,400	—
"	0.83	7	23.2	3,600	—
"	1.67	7	25.1	3,600	—

Note: Polymerization conditions: 40°C, Al(*n*-Pr)<sub>3</sub>, 0.1 mol %,  $\text{Ph}_3\text{SiCOPh}$ , 0.5 mol %, *i*-PrOH, 1.0 mol %.

<sup>a</sup>  $\text{Ph}_3\text{SiCOPh}$   $4.92 \times 10^{-2} M$ , *i*-PrOH, 0.73M in THF. See Experimental section, photolysis.

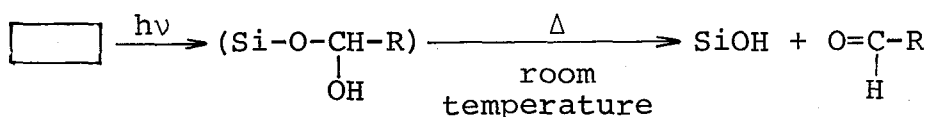
<sup>b</sup> The values in parentheses show the relative decomposition rate of  $\text{Ph}_3\text{SiCOPh}$  when the rate in the absence of sensitizer was 1.0.

but became apparent as the concentration increased.

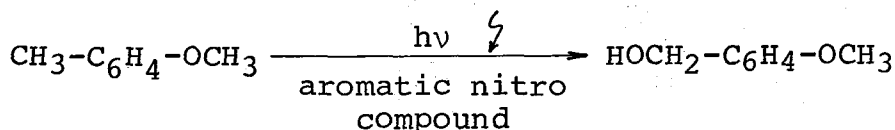
Benzoin ether photodecomposed at the fastest rate but the decomposition rate of Ph<sub>3</sub>SiCOPh in the presence of benzoin ether was not larger than that in the presence of benzophenone. Therefore polymer conversion with benzoin ether was lower than that with benzophenone.

10-5 Photogenerated catalyst (II): Aluminum complex/  
ortho-nitrobenzylsilyl ether system

Some silicon compounds which isomerize to silanols directly under UV radiation were also investigated. A compound with a hemiacetal structure, SiOCH(OH)-, formed by photolysis was considered to be suitable for the present purpose. If the hemiacetal is formed under UV-radiation, the silicon compound will decompose rapidly even at room temperature, forming silanol, as follows.



The hemiacetal compound might be produced by photo-oxidation of Si-O-CH<sub>2</sub>-Ph with an aromatic nitro compound, since it is known that p-methoxytoluene is photodecomposed to p-methoxybenzylalcohol, as follows.<sup>4</sup>



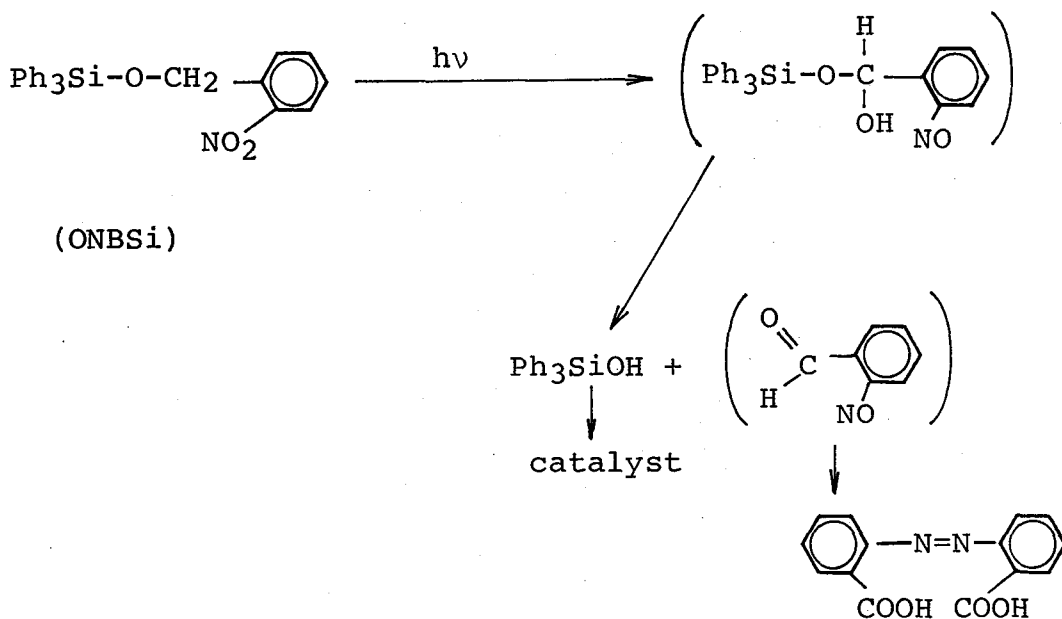
The photo-polymerization catalyst, aluminum complex/triphenylbenzyl ether/aromatic nitro compound system, polymerized cyclohexene oxide under UV-radiation. Table 8 shows the results. The catalytic activity increased with introduction of a methoxy group to the benzene ring of the benzyl ether group, and increased with introduction of a nitro group to nitrobenzene. It is known that photodecomposition rate of methoxytoluene is increased by introduction of a methoxy group to the benzene ring of the benzyl ether group. The reason is explained by the fact that introduction of the methoxy group increases electron density of methoxytoluene, then, the electron transfer from methoxytoluene to nitrobenzene readily takes place<sup>4</sup>. The substitution effect on the catalyst activity could be explained in the same way.

When the amount of nitrobenzene was varied, maximum yield was obtained at 2.0 mol%. Nitrobenzene in concentration higher than 2.0 mol% will retard the thermal polymerization after photolysis because of prevention of the interaction between aluminum complex and silanol.

Introduction of a nitro group to benzene ring of nitrobenzene increased the catalyst activity. The reason could be explained by the above donor-acceptor theory.

Thus, the aluminum complex/methoxybenzyl(triphenyl)silyl ether/nitrobenzene catalyst was found to have catalyst activity.

In order to obtain more active catalyst, ortho-nitrobenzylsilyl ether, where a neighboring effect was anticipated, was investigated. Ortho-nitrobenzyl ether was used as alcoholic hydroxy protector group of peptides, nucleosides and saccharides.<sup>5</sup> Following photodecomposition was anticipated.



Photodecomposition of ortho-nitrobenzyl(triphenyl)-silyl ether (ONBSi) was thus examined. Figure 6 shows the results. The photodecomposition was carried out under irradiation of 254 nm, 365 nm and > 390 nm UV-light. Table 9 shows the quantum yield of the photodecomposition. 254 nm light was most active for the photodecomposition. The quantum yield decreased with radiation time. The reason was explained by the fact that the decomposed azo compound absorbed the effective UV-light and retarded the photodecom-

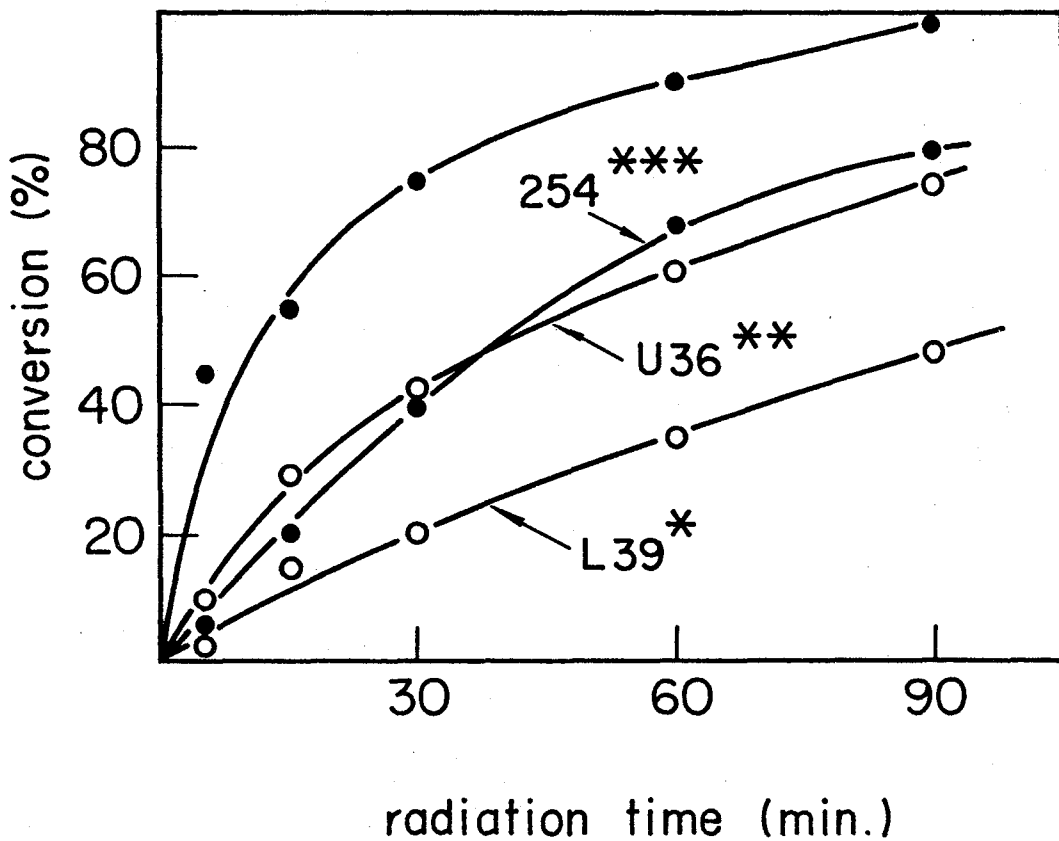


Figure 6 Photo-decomposition of ONBSi.

\* > 390 nm, \*\* 365 nm, \*\*\* low-pressure-mercury lamp ONBSi, 0.0221 M in CH<sub>3</sub>CN

Table 8 Polymerization of Cyclohexene Oxide with Al Complex/Silyl Ether/Aromatic Nitro Compound Catalyst.<sup>a)</sup>

Silyl ether	mol%	Nitro compd.	mol%	Time (h)	Yield (%)
Ph <sub>3</sub> SiOCH <sub>2</sub> Ph	0.1	C <sub>6</sub> H <sub>5</sub> NO <sub>2</sub>	0.5	8	0
"	0.3	"	2.0	8	0
Ph <sub>3</sub> SiOCH <sub>2</sub> C <sub>6</sub> H <sub>4</sub> -OCH <sub>3</sub>	0.2	"	2.0	7	9
Ph <sub>3</sub> SiOCH <sub>2</sub> C <sub>6</sub> H <sub>3</sub> (OCH <sub>3</sub> ) <sub>2</sub>	0.2	"	2.0	7	14
Ph <sub>3</sub> SiOCH <sub>2</sub> C <sub>6</sub> H <sub>2</sub> (OCH <sub>3</sub> ) <sub>3</sub>	0.1	"	0.5	7	5
"	0.1	"	1.0	7	10
"	0.1	"	2.0	7	32
"	0.1	"	4.0	7	21
"	0.15	m-C <sub>6</sub> H <sub>4</sub> (NO <sub>2</sub> ) <sub>2</sub>	1.0	10	19
"	0.15	C <sub>6</sub> H <sub>5</sub> NO <sub>2</sub>	1.0	10	14

a) 40°C, Al(Etaa)<sub>3</sub> 0.02 mol% to monomer, 400W-high pressure mercury lamp.

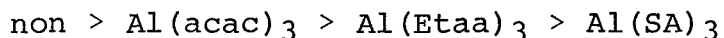
Table 9 Quantum Yield for ONBSi<sup>a)</sup>

Filter	Radiation time (min.)				
	5	15	30	60	90
L391)	0.1	0.1	0.1	0.1	0.1
U362)	0.2	0.2	0.15	0.1	0.1
2543)	0.3	0.4	0.4	0.3	0.3

a) 40°C in acetonitrile, 1) over 390 nm, 2) 365 nm (400W-high pressure mercury lamp), 3) low pressure mercury lamp, ONBSi 0.0221 M.

position, where, as the extent of decomposition was confirmed to be about 100 % by means of separation with column chromatography, triphenylsilanol forms by decomposition of the ONBSi.

In order to use the ONBSi as a photogenerated catalyst, the silyl ether must be used with an aluminum complex. Therefore decomposition of the silyl ether in the presence of an aluminum complex was examined.  $\text{Al}(\text{acac})_3$ ,  $\text{Al}(\text{Etaa})_3$  and  $\text{Al}(\text{SA})_3$  were used as aluminum complex. Table 10 shows the results. The decomposition rate decreased in the following order.



The decomposition rate of ONBSi under 365 nm light was higher than that under 254 nm light in the presence of  $\text{Al}(\text{Etaa})_3$  (Table 11). The  $\text{Al}(\text{Etaa})_3$  had UV-absorption at about 270 nm,  $\epsilon = 10^4$ , therefore the dependence of the photodecomposition rate on the structure of the aluminum complex and on wave number of UV-light was explained by the fact that the absorption of the aluminum complex overlapped with that of ONBSi (Figure 7) therefore, ONBSi could not absorb the effective UV-light.

Table 12 shows the photopolymerization results for cyclohexene oxide with  $\text{Al}(\text{Etaa})_3/\text{ONBSi}$ . The maximum catalytic activity was obtained at the concentration of 0.05 mol% in the case of ONBSi and 0.02 mol% in the case of



Table 10 Photodecomposition of ONBSi in the Presence of Aluminum Complex.a)

aluminum complex	ratio of decomposition (%)					
	time (min.)	5	15	30	60	90
non		43	71	88	97	99
Al(acac) <sub>3</sub>		25	61	83	93	96
Al(Etaa) <sub>3</sub>		23	56	79	93	96
Al(SA) <sub>3</sub>		23	53	62	80	91

a) ONBSi 0.0258 M, aluminum complex 0.012 M in acetonitrile.

400W-high pressure mercury lamp.

Table 11 Quantum Yield for Decomposition of o-nitrobenzyl(triphenyl)-silyl ether in the presence of aluminum complex

UV light	254 <sup>1)</sup>			365 <sup>2)</sup>		
Radiation time (min.)	10	20	40	10	20	40
Conversion (%)	3.7	10.5	21.3	17.5	32.0	43.0
Quantum yield	0.1 <sub>2</sub>	0.1 <sub>7</sub>	0.1 <sub>7</sub>	0.2	0.1 <sub>8</sub>	0.1 <sub>2</sub>
QE-Al(acac) <sub>3</sub> /QE-non <sup>3)</sup> (%)	34	45	47	95	90	92
Conversion (%)	7.8	17.2	28.5	16.0	28.3	39.0
Quantum yield	0.2 <sub>5</sub>	0.2 <sub>7</sub>	0.2 <sub>3</sub>	0.1 <sub>8</sub>	0.1 <sub>6</sub>	0.1 <sub>1</sub>
QE-Al(Etaa) <sub>3</sub> /QE-non <sup>3)</sup> (%)	71	71	64	85	80	84

1) Low pressure mercury lamp, 2) High pressure mercury lamp, filter U-36,

3) Ratio of quantum yield of o-nitrobenzyl(triphenyl)silyl ether in the presence and absence of aluminum compound.

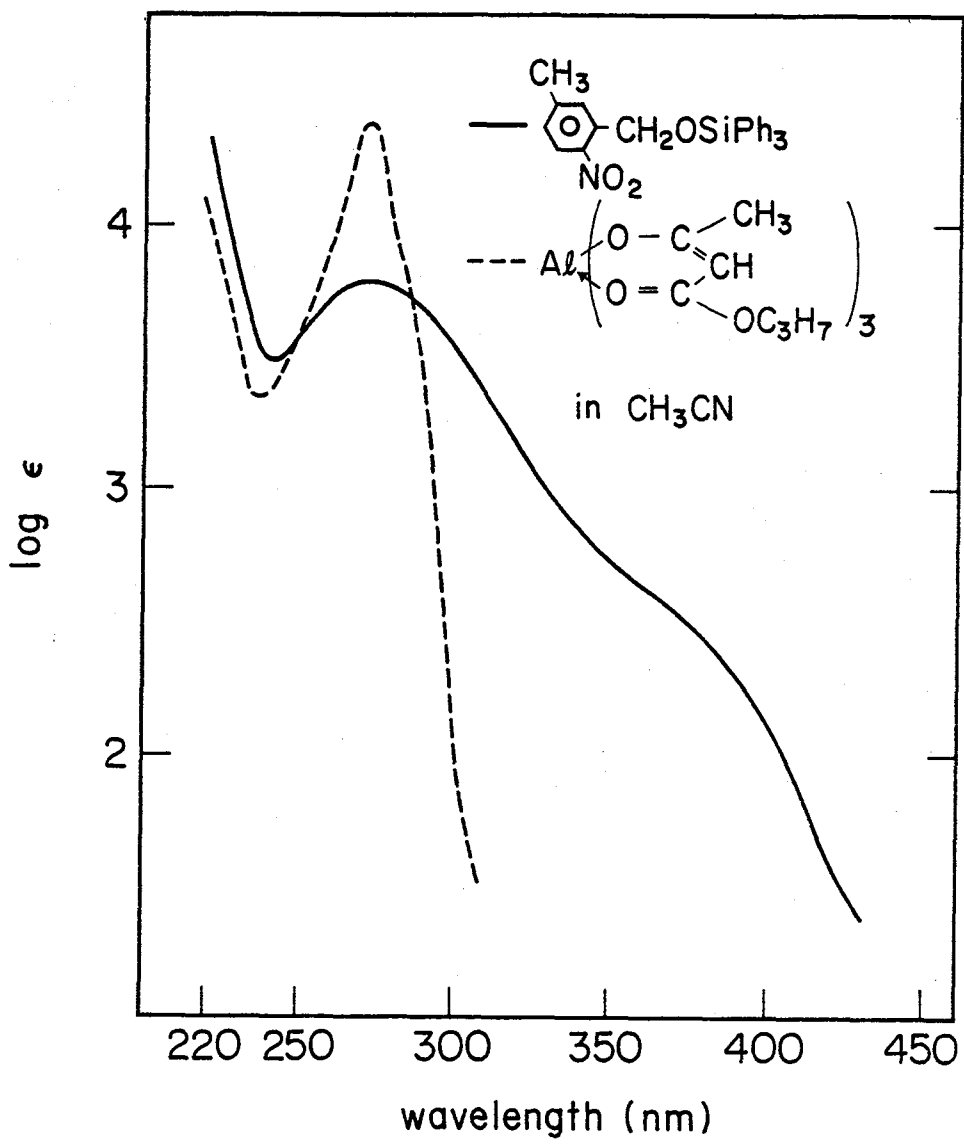


Figure 7 UV spectra of components of the catalyst.

Table 12 Photopolymerization of Cyclohexene Oxide  
with  $\text{Al}(\text{Et})_3/\text{ONBSi}$  catalyst

$\text{Al}(\text{Et})_3$ mol%	ONBSi mol%	radiation time(min.)	yield (%)
0.1	0.01	5	5
0.1	0.02	5	9
0.1	0.05	5	73
0.1	0.10	5	64
0.1	0.25	5	60
0.1	0.02	50	20
0.5	0.02	50	10
0.02	0.02	50	28
0.005	0.02	50	25

40°C, 400W-high pressure mercury lamp

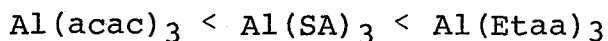
$\text{Al}(\text{Etaa})_3$ .

The dependence of the catalytic activity on the concentration of ONBSi will be explained by the fact that the decomposition rate of ONBSi have a maximum value at the concentration of ONBSi, because rise of the concentration of catalyst disturbs the transparency of UV light to inner of test tube. The dependence of the activity on the concentration of  $\text{Al}(\text{Etaa})_3$  will be explained as follows. Two factors were needed for the explanation.

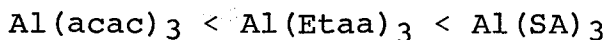
- 1) Photodecomposition rate of ONBSi in the presence of  $\text{Al}(\text{Etaa})_3$
- 2) Thermal polymerization rate with  $\text{Al}(\text{Etaa})_3$ /triphenylsilanol.

The rate decreased with increased in  $\text{Al}(\text{Etaa})_3$  concentration, and the rate increased with increase in  $\text{Al}(\text{Etaa})_3$  concentration under such a low concentration as about 0.005 mol%. 0.02 mol% of  $\text{Al}(\text{Etaa})_3$  will be most suitable point on consideration of 1) and 2).

Dependence of the catalyst activity on the structure of the aluminum complex was examined. The results are shown in Figure 8. At initial step, the activity increased in the following order,



however at the last step, the activity was as follows.



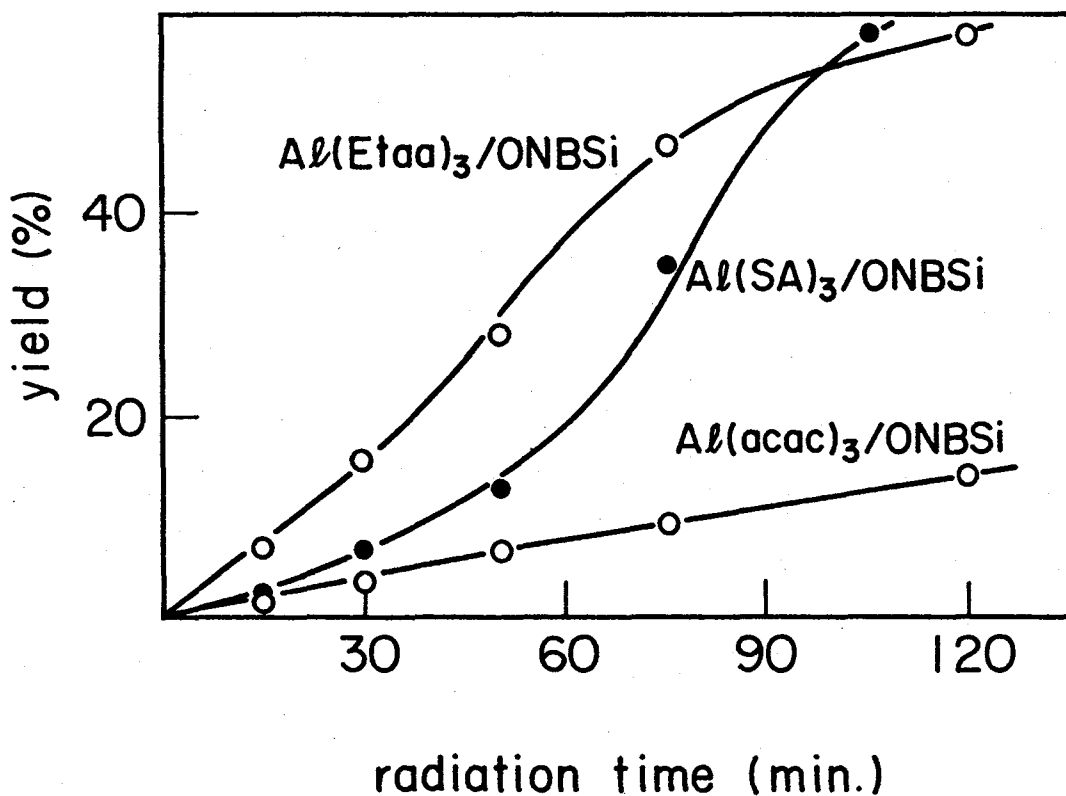
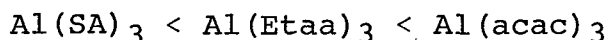
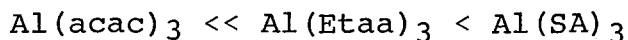


Figure 8 Photo-polymerization of cyclohexene oxide with Aluminum complex/ONBSi catalyst 40°C, Al 0.02 mol%, ONBSi 0.02 mol% 400W-high-pressure-mercury lamp.

The phenomena could be also explained by 1) photodecomposition rate and 2) thermal polymerization rate. Namely, photodecomposition rate of ONBSi in the presence of the aluminum complex increased in the following order,



however thermal polymerization rate of cyclohexene oxide was as follows.



The photopolymerization rate at initial stage will be affected by the photodecomposition rate of ONBSi mainly, and the rate at the last stage will be mainly affected by the thermal polymerization rate.

Dependence of the catalyst activity on wavelength of UV light was examined (see Table 13). 365 nm UV light was found to be most active. The reason will be explained as the same way as the explanation for the photodecomposition in the presence of aluminum complex.

Dependence of the catalyst activity and photodecomposition rate on the structure of silyl ether was investigated. The results are shown in Table 14 and 15. Introduction of a methoxy group to the benzene ring of silyl ether decreased the photodecomposition rate and the photopolymerization rate. On the other hand, introduction of a methyl or a chloro group to the benzene ring of silyl

Table 13 Photopolymerization of Cyclohexene  
Oxide with Aluminum Complex/ONBSi Catalyst.

filter	aluminum complex	radiation time(min.)	conversion (%)
U36	Al(acac) <sub>3</sub>	20	4
"	Al(Etaa) <sub>3</sub>	20	27
"	Al(SA) <sub>3</sub>	20	2
L39	Al(acac) <sub>3</sub>	45	2
"	Al(Etaa) <sub>3</sub>	45	12
"	Al(SA) <sub>3</sub>	45	1
254	Al(acac) <sub>3</sub>	35	1
"	Al(Etaa) <sub>3</sub>	35	7
"	Al(SA) <sub>3</sub>	35	5

a) 40°C, aluminum complex 0.03mol%, ONBSi 0.03mol%  
400W-high pressure mercury lamp.



Table 14 Photopolymerization of Cyclohexene Oxide

silyl ether	conversion (%)			
	radiation time	10min.	40min.	100min.
Si-I		13	51	100
Si-II		4	10	22
Si-III		6	12	26
ONBSi		9	21	55
Si-IV		16	18	19*
Si-V		32	36	18*
Si-VI		18	20	22*
Si-VII		12	43	86
Si-VIII		4	8	16
Si-IX		4	6	10

a) catalyst,  $\text{Al}(\text{Etac})_3$  0.02mol%, silyl ether 0.02mol%, \* 0.01 mol%,  
 polymerization temperature 40°C, 400W high pressure mercury lamp  
 abbreviation; see experimental

Table 15      Photodecomposition of Silyl ethers

silyl ether	decomposition (%)					
	radiation time (min.)	2	5	10	20	40
Si-I		37	55	74	88	96
Si-II		5	14	20	50	71
Si-III		51	60	71	82	90
ONBSi		5	27	52	89	92
Si-IV		20	29	55	75	86
Si-V		22	48	67	83	94
Si-VI		8	27	55	73	89
Si-VII		57	71	85	93	97
Si-VIII		0	13	20	37	40
Si-IX		11	33	67	93	94

a) silyl ether 0.0221M in CH<sub>3</sub>CN, 40°C, 400W high pressure mercury lamp  
 abbreviation; see experimental

ether increased the both rates.

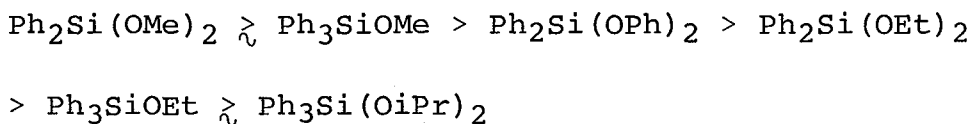
Alicyclic epoxide (II) (Figure 1) with  $\text{Al}(\text{Etac})_3/\text{ONBSi}$  catalyst could be photo-cured by high-pressure-mercury-lamp (80 W/cm). The epoxide photo-cured within 20 second.

As mentioned above, the catalyst activity of the aluminum complex/ortho-nitrobenzyl silyl ether catalyst was high and was sufficiently high for practical use.

#### 10-6 Electrical properties of epoxy resins cured by the latent catalysis

Table 16 shows electrical properties of epoxy resin cured with latent catalysts.

Dependence of the electrical properties on the structure of alkoxysilane was examined. The electrical properties deteriorated in the following order.



The order was almost coincident with that of activity of the catalyst.

Epoxy resin cured with the latent catalysts, namely, hydrolyzable catalyst, thermally generated catalyst and photogenerated catalyst had excellent electrical properties, compared with that with  $\text{BF}_3 \cdot \text{monoethylamine}$  catalyst.

Table 16 Electrical Properties of Epoxide  
Cured with the Latent Catalyst.

catalyst	phra)	tan $\delta$ at 200°C (%)
Ph <sub>2</sub> Si(OMe) <sub>2</sub>	3.0*	0.8
Ph <sub>2</sub> Si(OPh) <sub>2</sub>	4.5*	1.0
Ph <sub>3</sub> SiOMe	3.7*	1.3
Ph <sub>2</sub> Si(OEt) <sub>2</sub>	3.5*	1.5
Ph <sub>3</sub> SiOEt	4.5*	4.0
Ph <sub>2</sub> Si(OiPr) <sub>2</sub>	3.9*	8.2
FMSi	6.0*	1.2
o-nitrobenzyl (triphenyl)silyl ether	3.0**	2.0

\* Al(SA)<sub>3</sub> 2.4 phr, cured at 165°C for 15h, Epikote 828 resin.

\*\* 80A/cm, high pressure mercury lamp, distance from sample 15 cm, radiation time 60 sec., catalyst Al(Etaa)<sub>3</sub> 0.5phr, alicyclic epoxy resin (see Figure 1)

a) weight % to epoxy resin.

## References

1. U. Michel and S. Tchelitcheff, *Bull. Soc. Chim. Fr.*, 2230 (1964)
2. J. V. Crivello, J. H. W. Lam, J. E. Moore and S. H. Schroster, *J. Radia. Curing*, 5, 2 (1978); J. V. Crivell and J. H. W. Lam, *Macromolecules*, 10, 1307 (1977); J. V. Crivello and J. H. W. Lam, *J. Polymer Sci., Polym. Chem. Ed.*, 17, 2877 (1979); *ibid.*, 17, 1047 (1979); *ibid.*, 1021 (1980); *ibid.*, 17, 977 (1979); *ibid.*, 16, 2441 (1969)
3. A. G. Brook, *J. Am. Chem. Soc.*, 82, 5102 (1960); *ibid.*, 91, 355 (1969)
4. J. Libman, *J. Chem. Soc., Chem. Comm.*, 868 (1977); R. Hurley, A. C. Test, *J. Am. Chem. Soc.*, 88, 4330 (1966); J. A. Barltop and N. J. Bunce, *J. Chem. Soc., (C)*, 1467 (1968)
5. A. Patchornik, B. Amit and R. B. Woodward, *J. Am. Chem. Soc.*, 19, 6333 (1970); E. Ohtsuka, T. Wakabayashi, S. Tanaka, T. Tanaka, K. Oshie, H. Hasegawa and M. Ikehara, *Chem. Pharm. Bull.*, 29, 318 (1981); P. M. Collins and V. R. N. Munasinghe, *J. Chem. Soc., Chem. Commun.*, 1981, 362

Chapter 11 Selective Synthesis of Structurally Isometric  
Poly- $\beta$ -ester and Poly- $\delta$ -ester from  $\beta$ -(2-  
acyloxyethyl)- $\beta$ -propiolactone with Al-H<sub>2</sub>O  
and Zn-H<sub>2</sub>O Catalysts

11-1 Introduction

The polymerization of  $\beta$ -substituted- $\beta$ -propiolactones has been studied in view of stereoregular polymerization in a systematic manner.<sup>1</sup> In the course of studies it was found that organoaluminum catalyst (EtAlO)<sub>n</sub> which is obtained from Et<sub>3</sub>Al and H<sub>2</sub>O tends to give stereoregular polymers while a related organozinc catalyst (Et(ZnO)<sub>2</sub>ZnEt) which is called ZnEt<sub>2</sub>-H<sub>2</sub>O catalyst has little capability for stereoregulation.<sup>1</sup> In the preceding study<sup>1</sup> it was shown that the Al-catalyst strongly coordinates with the lactone group in the monomer while Et<sub>2</sub>Zn cannot coordinate with this group.

The new observations herewith reported by employing  $\beta$ -(2-acetoxyethyl)- $\beta$ -propiolactone (1) revealed a remarkable difference in the catalytic behaviors of the two catalysts. Namely, the Al-catalyst catalyzes normal polymerization leading to poly- $\beta$ -ester, and the Zn-catalyst forms isomerized poly- $\delta$ -ester as main product.

These observations have a dual significance that (i) a new route of isomerization polymerization is opened up, and (ii) the Al-catalyst prefers the lactonic ester group

predominantly, but the Zn-catalyst attacks on the linear ester group rather than lactonic ester group. The site-selective interactions can be used for interpretation of the difference in behaviors of the two catalysts in a more detailed manner. This seems of value in view of that these catalysts are the active entities of widely used  $\text{AlEt}_3\text{-H}_2\text{O}$  and  $\text{Et}_2\text{Zn-H}_2\text{O}$  catalytic systems.

There remained two major questions in this new polymerization behavior: (1) Whether the phenomenon is general for the cases of  $\beta$ -(2-acyloxyethyl)- $\beta$ -propiolactone series? (2) What are the effects of substituent groups at the terminal of the side-chain ester group on the polymerization behaviors, especially at the stage of cyclic intermediate? In order to answer these questions we chose two special monomers containing  $(\text{CH}_3)_2\text{CHCOO-}$  and  $(\text{CH}_3)\text{Cl-CHCOO-}$  groups and compared the results of these monomers with that obtained by  $\text{CH}_3\text{COO-}$  monomer.

I offer the experimental results of polymerization behaviors, structure of the polymers formed, and coordination behaviors of the two types of catalyst with the monomer. The structures and designations are shown in Scheme 1.

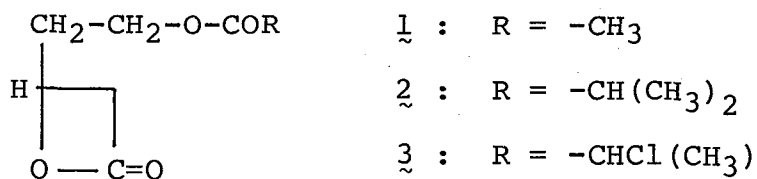
## 11-2 Polymerization of $\beta$ -(2-acetoxyethyl)- $\beta$ -propiolactone

(monomer 1)

Polymerization Behaviors:

Scheme 1

Designation of monomer:



Designation of polymer:

Monomer	Catalyst	Polymer
$\underline{1}$	$(\text{EtAlO})_n$	poly( $\underline{1}$ )-Al
$\underline{2}$	$(\text{EtAlO})_n$	poly( $\underline{2}$ )-Al
$\underline{3}$	$(\text{EtAlO})_n$	poly( $\underline{3}$ )-Al
$\underline{1}$	$\text{Et(ZnO)}_2\text{ZnEt}$	poly( $\underline{1}$ )-Zn
$\underline{2}$	$\text{Et(ZnO)}_2\text{ZnEt}$	poly( $\underline{2}$ )-Zn
$\underline{3}$	$\text{Et(ZnO)}_2\text{ZnEt}$	poly( $\underline{3}$ )-Zn



The polymerization profiles in respect to time-conversion and time-MW relations are shown in Figure 1 for the Al- and Zn-catalyses. The new polymerization behaviors with the Al catalyst were similar to the polymerization of a series of  $\beta$ -alkyl- $\beta$ -propiolactones reported previously,<sup>1</sup> i.e., gradual increase of polymer yield with almost constant MW. Polymerization behavior with the Zn catalyst, however, can be characterized by a drastic increase of polymer yield and MW after a considerably long induction period. Table 1 shows the selected polymerization results giving better yields, when a variety of polymerization factors was changed. Lower catalyst concentration, lower polymerization temperature, or solvent other than tabulated gave generally lower polymer yields.

#### 1-2. Polymer structures:

<sup>13</sup>C-NMR Spectra of Poly (1): For convenience the following designations are used hereafter for the polymers: poly(1)-Al for the polymer formed with  $(\text{EtAlO})_n$  catalyst, and poly(1)-Zn for one formed with  $\text{Et}(\text{ZnO})_2\text{ZnEt}$  catalyst. The polymers obtained by Al- and Zn-catalyses showed almost identical IR spectra (Figure 2), indicating the presence of ester structures in both polymers. No significant difference was also observed in <sup>1</sup>H-NMR spectra of both polymers (Figure 3).

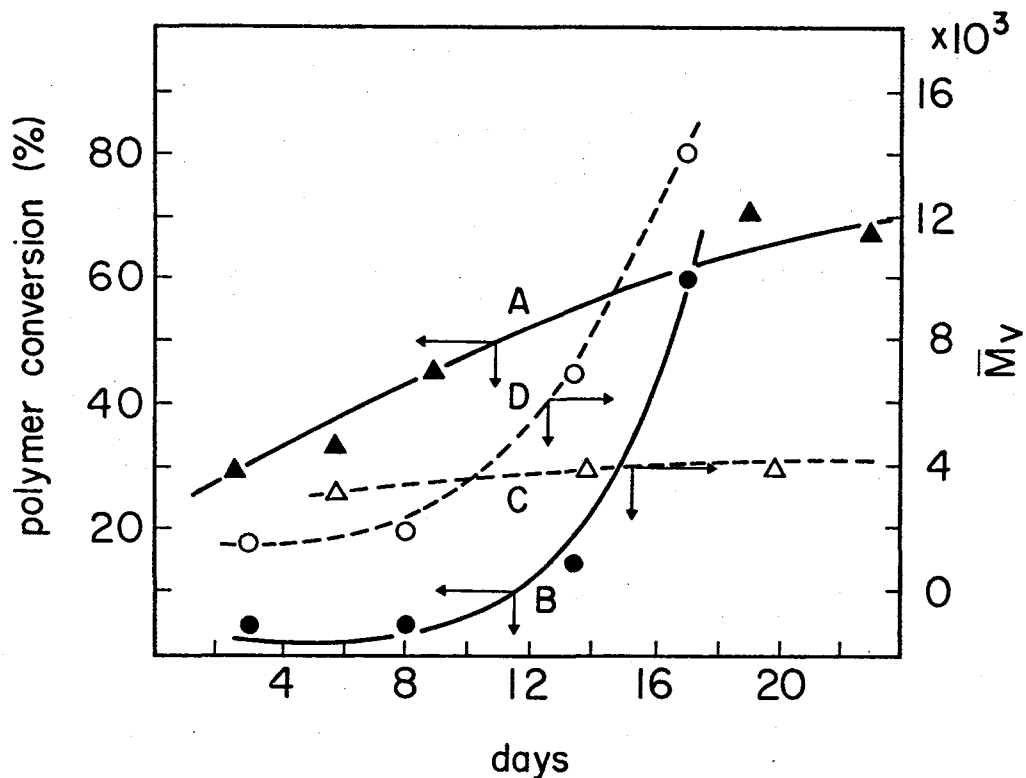


Figure 1 Time-dependent polymerization profiles of monomer (1) with  $(EtAlO)_n$  and  $Et(ZnO)_2ZnEt$  catalysts. A: Polymer conversion in Al-catalysts, B: Polymer conversion in Zn-catalysis, C:  $\bar{M}_v$  for polymer obtained with the Al catalyst, D:  $\bar{M}_v$  for polymer obtained with the Zn catalyst. Polymerization conditions: monomer, 1 ml; solvent toluene 1 ml, catalyst, 4 mol% of monomer, polymerization temperature, 60°C for Al-catalysis and 30°C for Zn-catalysis. Values of  $\bar{M}_v$  were obtained from GPC standardized with authentic polystyrene samples.

Table 1 Selected Polymerization Results of (1)a)

Catalyst	Catalyst concentration (mol% of monomer)	Polymerization			Polymer yield (%)
		Temp. (°C)	Time (days)	Solvent	
Al	2	63	30	PhCH <sub>3</sub>	61
Al	4	63	30	PhCH <sub>3</sub>	52
Al	7	63	13	PhCH <sub>3</sub>	62
Al	11	63	6	PhCH <sub>3</sub>	60
Zn	2	65	4	PhCH <sub>3</sub>	61
Zn	4	65	4	PhCH <sub>3</sub>	68
Zn	4	30	34	CH <sub>2</sub> Cl <sub>2</sub>	77
BF <sub>4</sub> OEt <sub>3</sub>	1	30	25	PhCH <sub>3</sub>	46b)
SnCl <sub>4</sub>	2.5	30	9	PhCH <sub>3</sub>	43b)

a) Monomer 2 ml, solvent 2 ml.

b) Low molecular weight polymers. An example of GPC is shown in Figure 5.

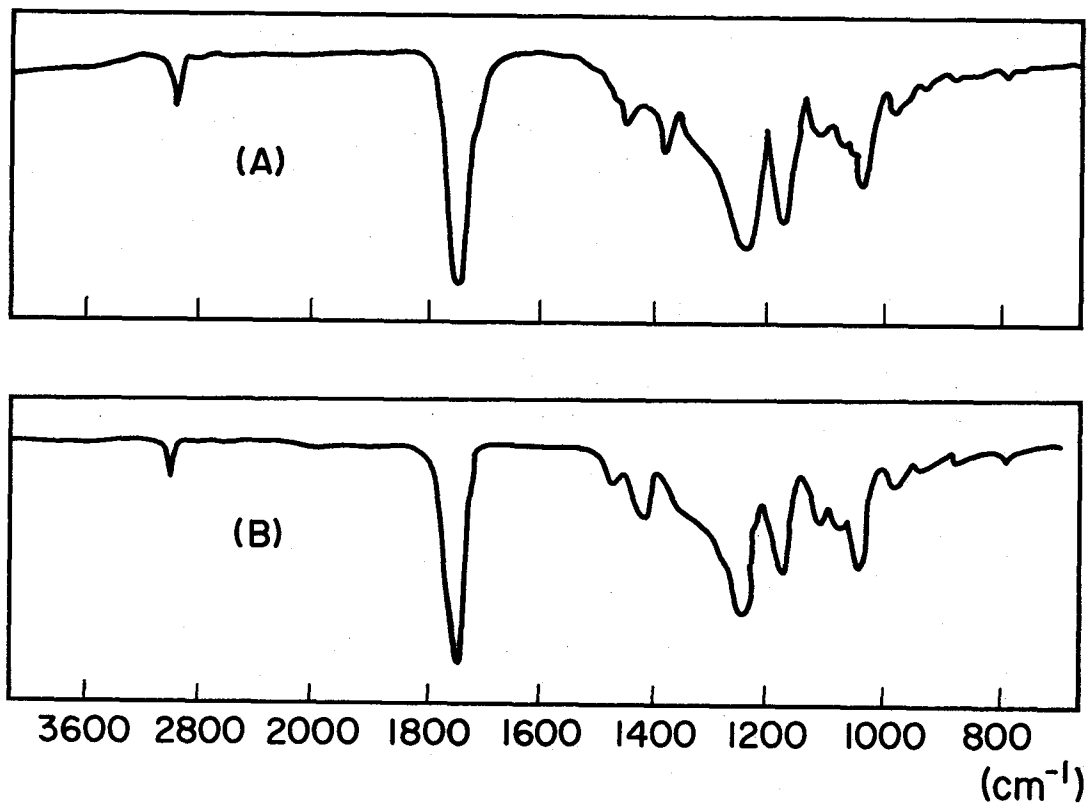


Figure 2 IR-Spectra of Poly(l)-Al and Poly(l)-Zn.

(A): Poly(l)-Al, (B): Poly(l)-Zn, (KBr disc)

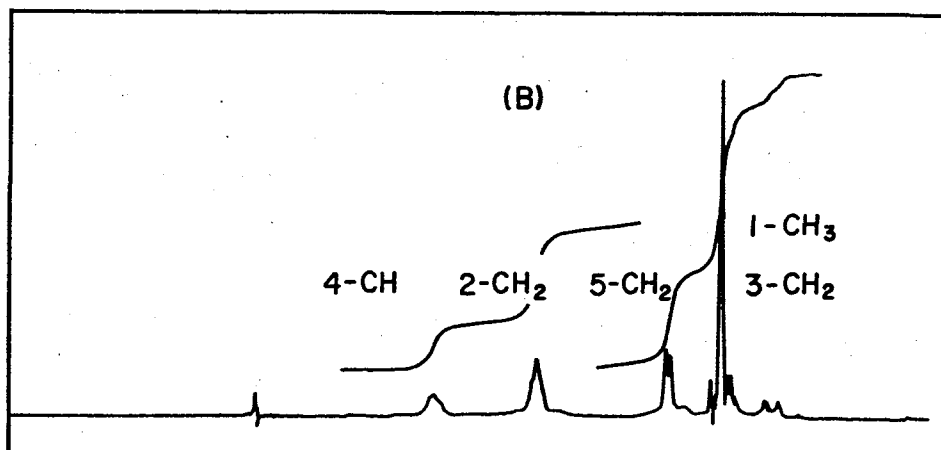
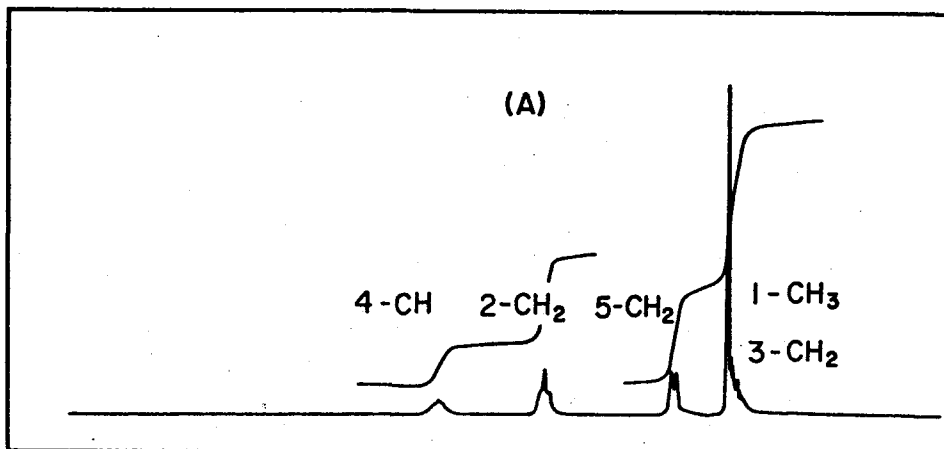
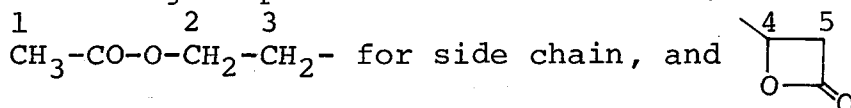


Figure 3  $^1\text{H-NMR}$  spectra of Poly(1)-Al and Poly(1)-Zn in  $\text{CDCl}_3$ . (A): Poly(1)-Al, (B): Poly(1)-Zn.

Numbering of protons is made from monomer structure



for ring-originated protons. Chemical shift values

for poly(1)-Al are 1, 1.97; 2, 4.03; 3, (1.97); 4,

5.19; 5, 2.56 ppm and for poly(1)-Zn are 1, 2.01; 2

4.11; 3, (2.01); 4, 5.25; 5, 2.60 ppm. Coupling

constants  $J_{23}$ ,  $J_{43}$ ,  $J_{54}$ , can be estimated as  $\sim 6.0$  Hz

for both polymers.

However, a characteristic difference in the polymer structure for poly(l)-Al and poly(l)-Zn was implied by  $^{13}\text{C}$ -NMR spectra (Figure 4). Assignment of the signals was performed by off-resonance technique and the numberings are noted in the Figure caption. Four sets of double-singlet resonance were observed at the carbonyl carbons (2,7) and the carbons adjacent to ether-oxygen atoms (3- $\text{CH}_2$  and 5- $\text{CH}$  carbons). Importantly, relative intensity of each set of the double-singlet signals in poly(l)-Al and poly(l)-Zn was reversed. Upon mixing the two types of polymer, a complete additiveness of the signals was confirmed, i.e., the four sets of double-singlet resonance with expected relative intensities were observed. Since the polymer samples have an identical range of MW (12,000 and 10,000) and both have monodisperse molecular weight distributions (Figure 5), these double-singlet resonances are not due to the oligomeric impurity.

The possibility of that the double-singlet signals might arise from tacticity separation is excluded on the following basis. It has been already reported that signal separation of poly( $\beta$ -alkyl- $\beta$ -propiolactones) by dyad tacticity can be observed in  $^{13}\text{C}$ -NMR with  $\sim 0.1$  ppm separation in the presence of a shift reagent,  $\text{Eu}(\text{dpm})_3$ .<sup>1</sup> This order of magnitude was held for a variety of higher series of analogous polymers,<sup>2</sup> and in the absence of the shift reagent the tacticity separation was only slight. In con-

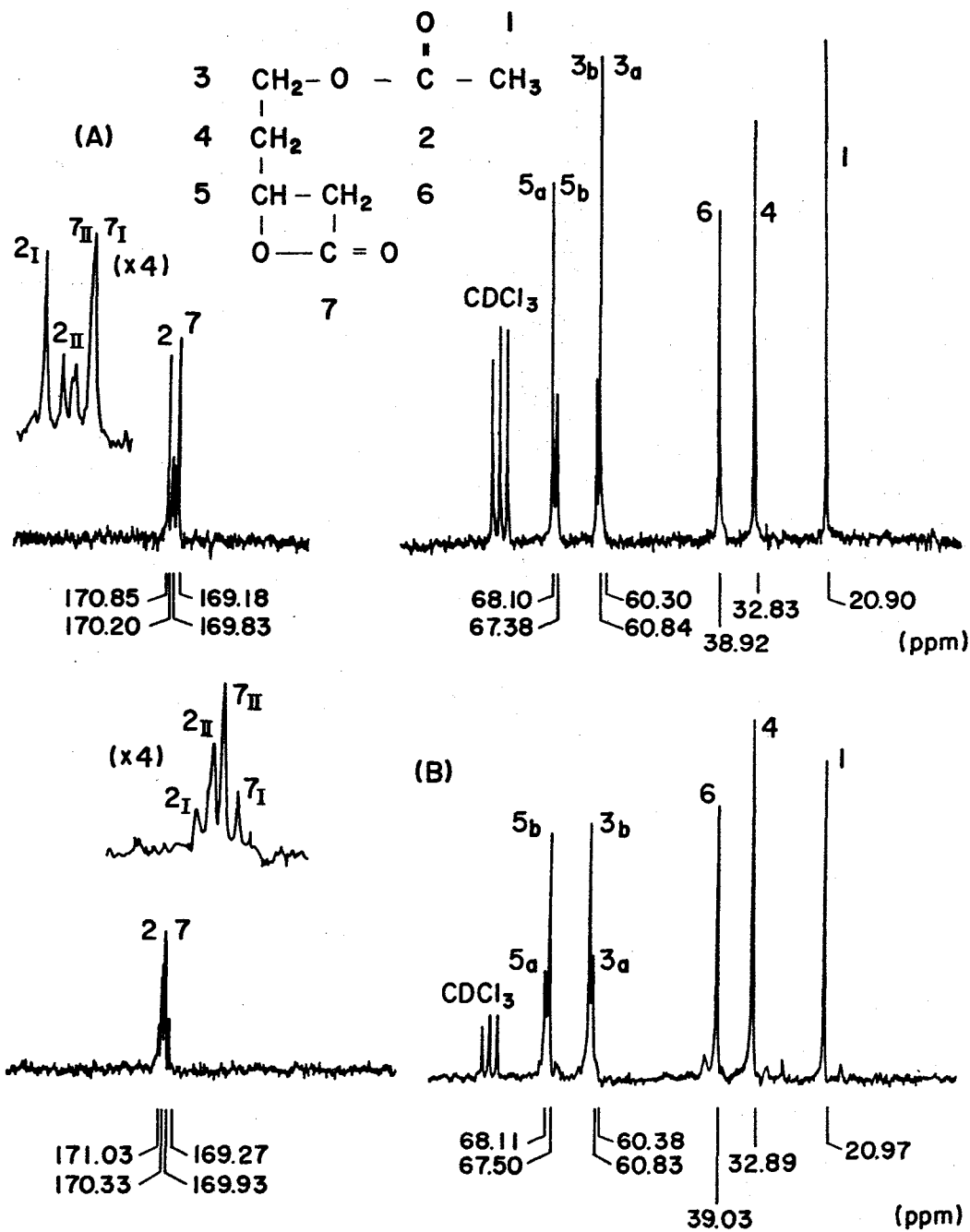


Figure 4  $^{13}\text{C}$ -NMR spectra of poly(1)-Al and poly(1)-Zn in  $\text{CDCl}_3$ . (A): Poly(1)-Al,  $M_w = 12000$ , (B): Poly(1)-Zn,  $M_w = 10000$ . Numbering of the signals should be referred to the above structure.

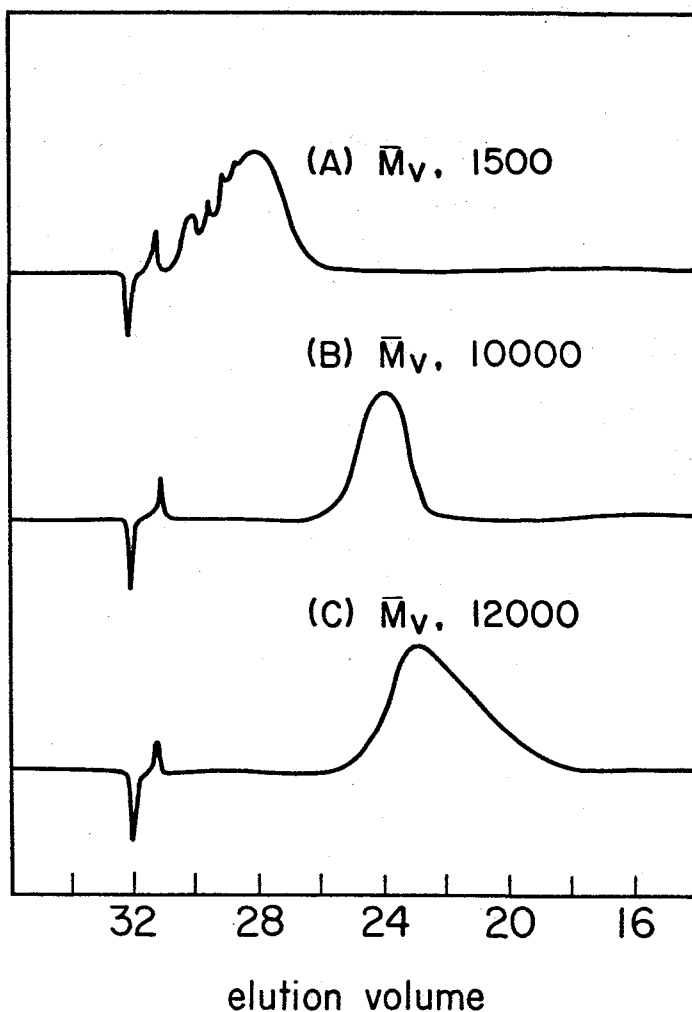


Figure 5 GPC curves of Poly(1)-Al and Poly(1)-Zn.

(A): Poly(1)-SnCl<sub>4</sub><sup>a</sup>,  $\bar{M}_v = 1500$ , (B): Poly(1)-Al<sup>b</sup>,  $\bar{M}_v = 10000$ , (C): Poly(1)-Zn<sup>c</sup>,  $\bar{M}_v = 12000$ .

Polymerization conditions: a) Monomer 1 ml; toluene 1 ml; temperature 30°C; catalyst 0.01 mol%/mol-monomer. b) Monomer 1 ml; toluene 1 ml, temperature 30°C; catalyst 0.04 mol/mol-monomer. c) Monomer 1 ml; toluene 1 ml; temperature 65°C; catalyst, 0.04 mol/mol-monomer. GPC conditions: THF at 45°C.



sistent to this fact, the signal separation of each set of double-singlet resonances of poly(1)s was an order of 0.5 - 0.6 ppm. Hence, we conclude that the Al catalyst and Zn one form polymers with different chemical structures in the monomeric units, though both of them are polyesters and their relative contents differ.

T<sub>1</sub> Measurement by <sup>13</sup>C-NMR: The relative relaxation time (T<sub>1</sub>) of poly(1)-Zn was measured in CDCl<sub>3</sub> for each carbon signal in the <sup>13</sup>C-NMR, at four limited time intervals: 0.05, 0.1, 0.5 and 3s. The value listed in Table 2 indicate the time intervals during which the signal loss occurs. The suffix a and b in carbons are used in order to distinguish the two types of structure (See Figure 4).

The structure (a) is characterized by a larger T<sub>1</sub> value at <sup>3</sup>C<sub>a</sub> and a small value at <sup>5</sup>C<sub>a</sub> carbons, while the structure (b) has an opposite property: <sup>5</sup>C<sub>b</sub> > <sup>3</sup>C<sub>b</sub>. Since T<sub>1</sub> values in <sup>13</sup>C-NMR can be related to segmental mobility of a molecule,<sup>3</sup> we can discuss the difference in structures (a) and (b) in view of the length of side chain and the number of atoms constituting the main-chain unit. The extremely large T<sub>1</sub> value of <sup>1</sup>C-carbon (CH<sub>3</sub> in acetyl) corresponds to that this carbon situates at the terminal of side chain. The structure (a), which dominates in poly(1)-Al, can reasonably be deduced as "normal" poly-β-ester when considered its shorter main-chain unit (carry-

Table 2  $T_1$  Values of Each Carbons in Poly(1)<sup>a</sup>

Carbon No.	$T_1$ (second) <sup>b)</sup>
1 <sub>C</sub>	0.72 ~ 4.32
3 <sub>C<sub>a</sub></sub>	0.14 ~ 0.72
3 <sub>C<sub>b</sub></sub>	< 0.07
4 <sub>C</sub>	0.07 ~ 0.14
5 <sub>C<sub>a</sub></sub>	0.07 ~ 0.14
5 <sub>C<sub>b</sub></sub>	0.14 ~ 0.72
6 <sub>C</sub>	0.07 ~ 0.14

a) 33 % solution of Poly(1)-Zn in  $CDCl_3$  was measured with a 25.16 MHz  $^{13}C$ -NMR apparatus, accumulated with 2000 scans.

b) Time intervals during which signal loss was observed are shown.

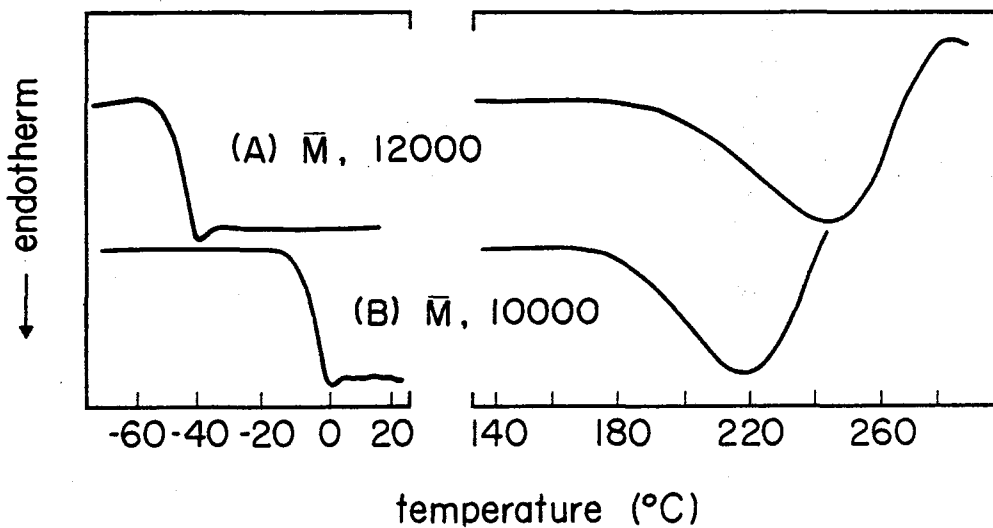
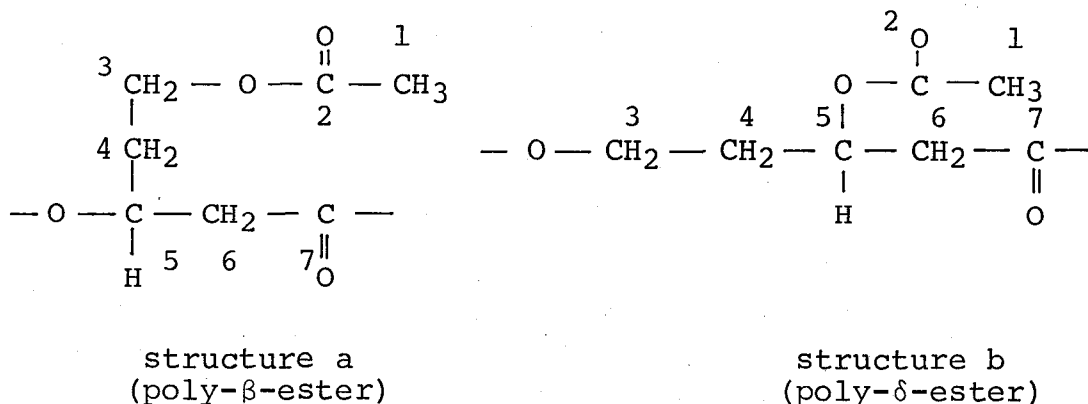


Figure 6  $T_g$  and decomposition measurement with DSC.  
 (A): Poly(1)-Al,  $\bar{M}_V = 12000$ , (B): Poly(1)-Zn,  $\bar{M}_V = 10000$ . Program rate: 10°C/min.

ing  $^5C_a$  and  $^6C$  carbons) and its larger side chain length ( $^4C$  exists at the neck of the chain, and  $^3C_b$  at the second position from the main-chain).

The structure (b), which predominates in poly(1)-Zn, becomes reasonable when considered a longer main-chain unit (carrying  $^3C_b$ ,  $^4C$ ,  $^5C_b$  and  $^6C$  carbons) and a shorter side chain containing only acetoxy group. Partial double bond character of the main-chain CO-O bond plays a stiffening role of the main-chain. The relatively high mobility of the  $^5C_b$  carbon, judged from the  $T_1$  value, seems to be reasonable in view of that there are four carbon atoms intervening the successive CO-O groups, i.e., poly- $\delta$ -ester structure.



Thermal Behaviors of Poly(1)s: The conclusion concerning the chemical structures of poly(1)-Al and poly(1)-Zn derived from the  $T_1$  measurement is supported by thermal experiments. Figure 6 shows the results of DSC measurements.  $T_g$  of the poly(1)-Al sample ( $-60^\circ\text{C} \sim -40^\circ\text{C}$ ) was lower than that of the poly(1)-Zn sample ( $-10^\circ\text{C} \sim 0^\circ\text{C}$ ).

These results indicate that the former carries longer side chains which cause a weaker interchain interaction, and the latter has shorter side chains which cause a stronger interchain interaction.  $T_{\text{decomp}}$  of the poly( $\underline{1}$ )-Al sample (ca. 240°C) was higher than that of the poly( $\underline{1}$ )-Zn sample (ca. 218°C). These facts also correspond to that the mainchain of higher mobility (poly- $\delta$ -ester) decomposes more readily than that of lower mobility (poly- $\beta$ -ester).<sup>4</sup>

Thermal decomposition of the poly( $\underline{1}$ )-Zn sample at 218°C gave 5,6-dihydro-2-pyrrone in a high yield. The product was identified by  $^1\text{H-NMR}$  and IR by comparing the authentic sample prepared separately. On the other hand, when the poly( $\underline{1}$ )-Al sample was decomposed at 240°C,  $\text{CH}_3\text{COOCH}_2\text{CH}_2\text{-CH=CHCO}_2\text{H}$  and 5,6-dihydro-2-pyrrone were confirmed to present in the decomposition product (Figure 7). These results are consistent with that the poly- $\delta$ -ester can more readily cyclize during main-chain scission, while the cyclization from the poly- $\beta$ -ester type requires a regular movement of a long side chain to attack a pre-determined position in the main chain. It is well known that poly- $\beta$ -esters decompose into acrylic acid and poly- $\delta$ -ester into  $\delta$ -valerolactone in pyrolysis.<sup>5</sup>

#### Polymerization Mechanism

Supposed Polymerization Scheme: Based on the analyses



of the polymer structures produced by the Al catalyst and the Zn catalyst, one can suppose polymerization schemes for Al-catalyzed "normal" polymerization and for Zn-catalyzed "isomerization" polymerization (Figure 8).

The "normal" polymerization involves simple ring-opening of the lactone ring without significant participation of the side chain ester group. In contrast, the "isomerization" polymerization involves a strong participation of the side chain ester group in the transition stage in a manner of forming a six-membered cyclic intermediate, followed by ring-opening through acyl migration. In order to verify the reaction mechanisms two types of experiment were carried out. First, a model polymerization using  $\beta$ -methyl- $\beta$ -propiolactone in the presence of ethylacetate as a competing ester species. Second, elucidation of coordination stages of the  $\underline{1}$  monomer with the Al- and Zn-compounds, by employing  $^{13}\text{C}$ -NMR technique.

#### Model Polymerization Systems: Ethylacetate

$(\text{CH}_3\text{COOCH}_2\text{CH}_3)$  is a model of the side chain of  $\underline{1}$  monomer  $(\text{CH}_3\text{COOCH}_2\text{CH}-)$ . Then, if the proposed mechanism shown in Figure 7 is true, the ethylacetate would interfere the polymerization catalyzed by the Zn-compound rather than that catalyzed by the Al compound. The polymerization of  $\beta$ -methyl- $\beta$ -propiolactone was carried out in ethylacetate solvent and was compared with the behaviors in toluene

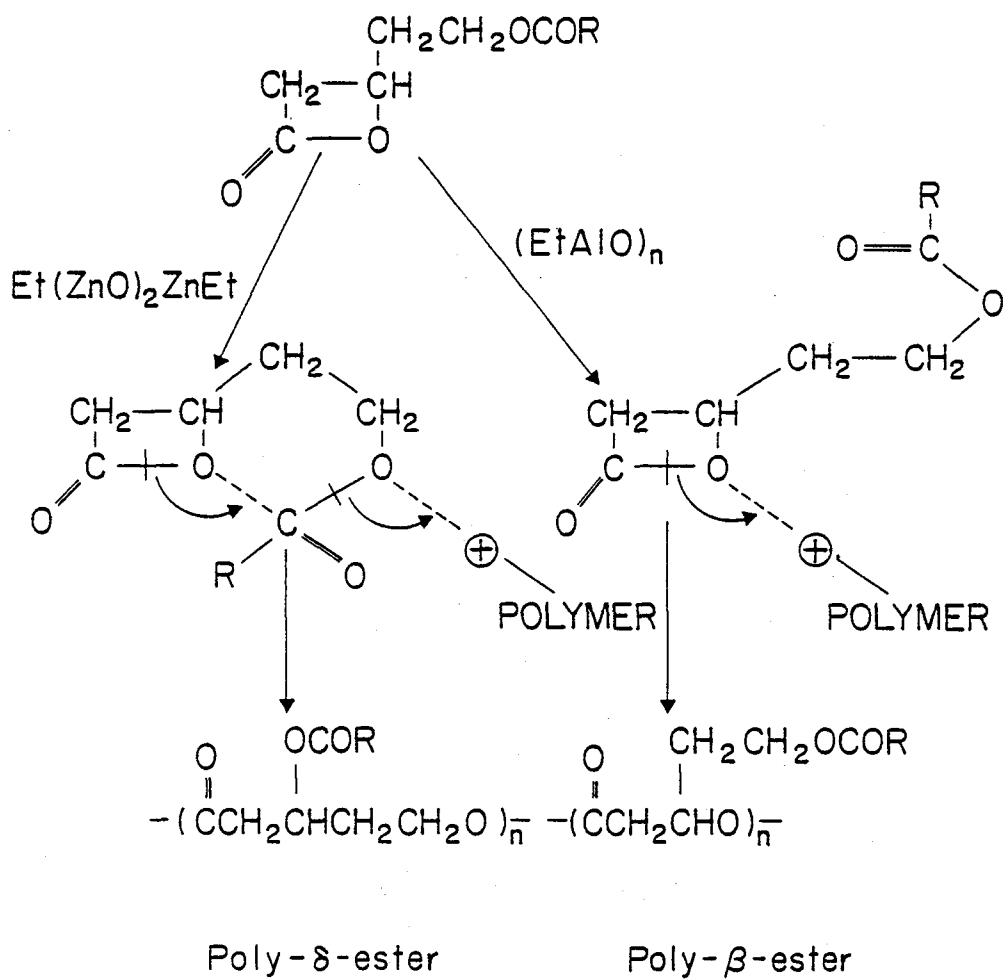


Figure 8 Reaction scheme in the polymerization.



solvent. Figure 9 shows time-dependent profiles of polymerization in ethylacetate, and Figure 10 shows the corresponding results obtained in toluene.

Clearly, the polymerization reactions in ethylacetate were considerably suppressed. In the case of Al-catalysis the rate of polymerization decreased and MW of the polymer tended to decrease after a maximum. The MW of the polymer was still high in ethylacetate keeping a range of value  $>20,000$ . In the Zn-catalysis, however, the MW of the polymer decreased to an oligomeric region as the polymerization time exceeds ca. 10 days. The polymer yield also decreases during a prolonged time, indicating decomposition of the polymer once formed. From these experiments it can be concluded that subsequent chain transfer of ethyl acetate occurs more readily in the Zn-catalysis than in the Al-catalysis.

Coordination of the Monomer 1 with Al- and Zn-compounds: The proposed intermediate stage shown in Figure 8 suggests that the structure of the monomer is different at the stages of coordination with Al-catalyst and with Zn-catalyst.  $^{13}\text{C}$ -NMR is a powerful tool for elucidating this problem. Since the rate of polymerization with the Al-catalyst is slow enough below  $20^\circ\text{C}$ , the coordination stage with the  $(\text{EtAlO})_n$  compound could directly be observed. The Zn-catalysis is much faster even

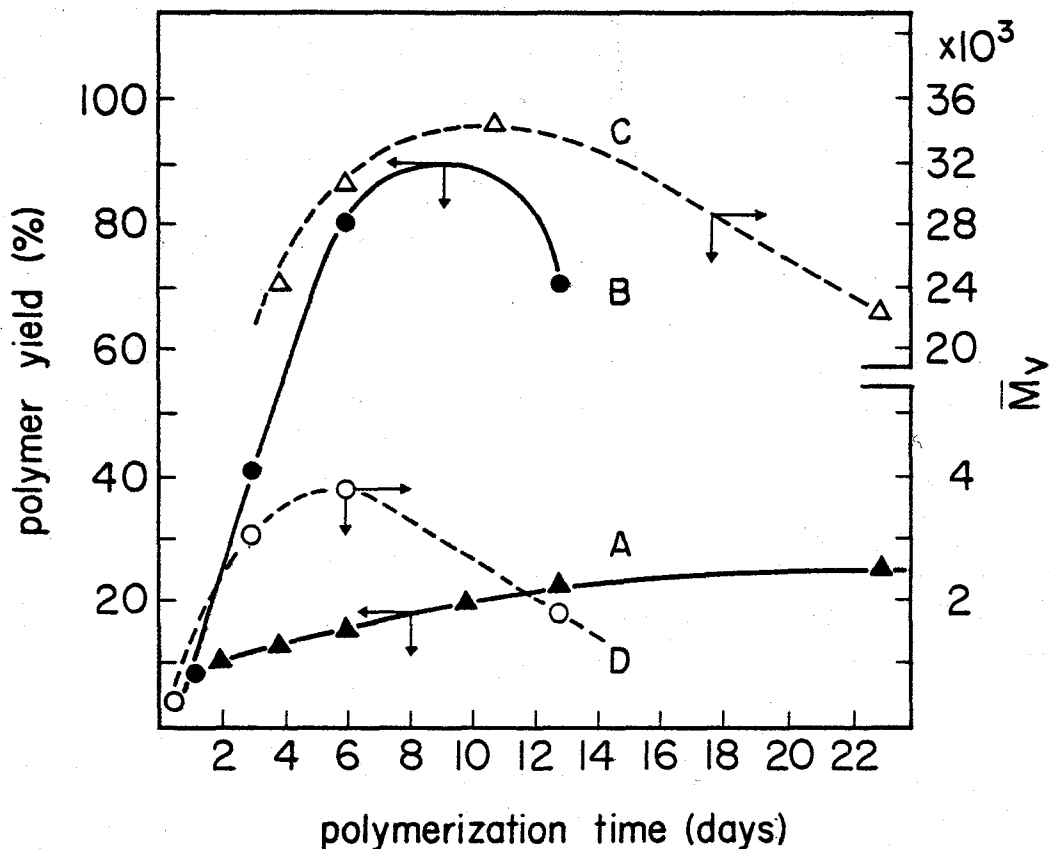


Figure 9 Time dependence of polymer yield and molecular weight for the polymerization of  $\beta$ -methyl- $\beta$ -propiolactone in ethyl acetate-toluene mixed solvent. A: Polymer yields in  $(EtAlO)_n$  catalysis, B: polymer yields in  $Et(ZnO)_2ZnEt$  catalysis, C:  $\bar{M}_v$  for polymers obtained with  $(EtAlO)_n$  catalyst, D:  $\bar{M}_v$  for polymers obtained with  $Et(ZnO)_2ZnEt$  catalyst. Polymerization conditions: Monomer, 1 ml; toluene, 0.38 ml; ethylacetate 0.62 ml; catalyst, 0.04 mol/mol-monomer; temperature  $60^\circ C$  for  $(EtAlO)_n$  catalysis and  $30^\circ C$  for  $Et(ZnO)_2ZnEt$  catalysis. Values of  $\bar{M}_v$  were obtained from GPC calibrated by standardization with polystyrene samples.

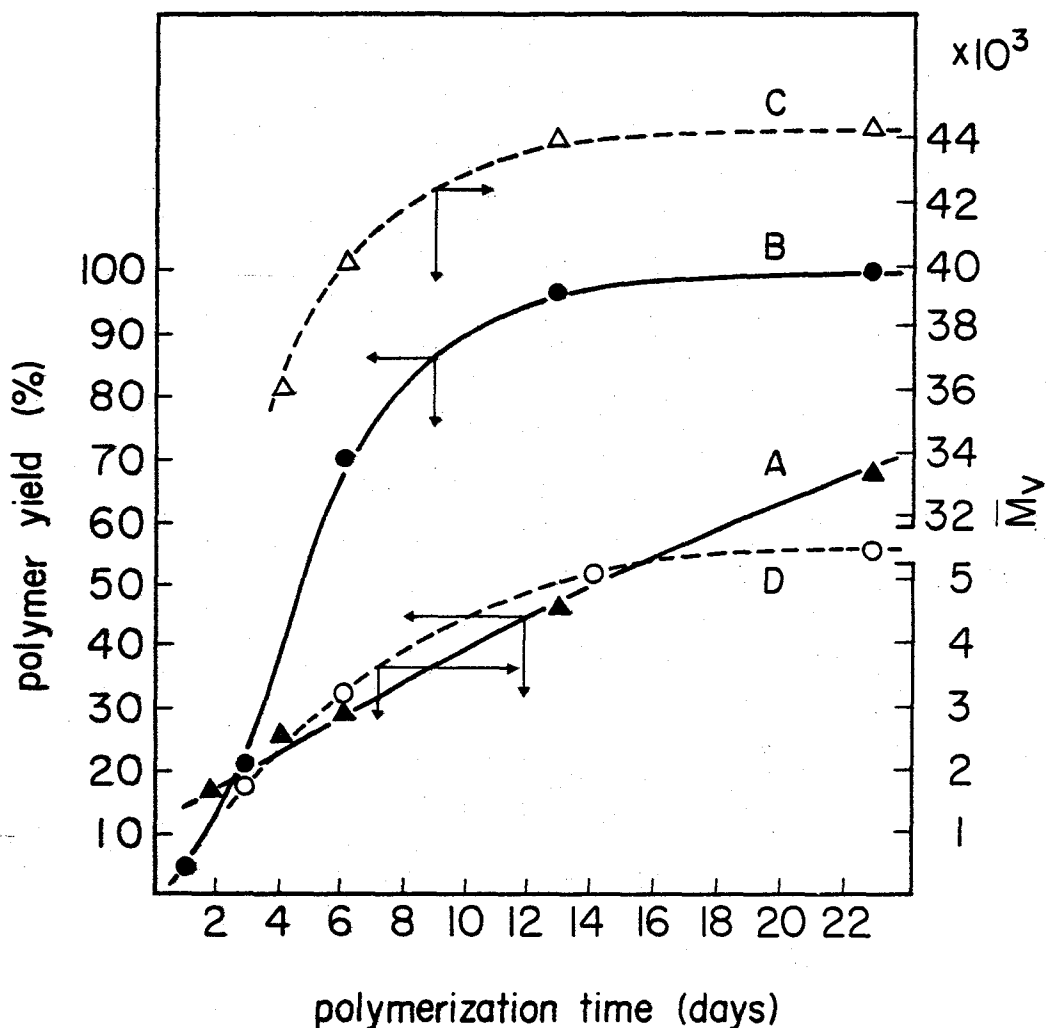


Figure 10 Time dependence of polymer yield and molecular weight for the polymerization of  $\beta$ -methyl- $\beta$ -propiolactone in toluene.

A: Polymer yields in  $(\text{EtAlO})_n$  catalysis, B: polymer yields in  $\text{Et}(\text{ZnO})_2\text{ZnEt}$  catalysis, C:  $\bar{M}_V$  for polymers obtained with  $(\text{EtAlO})_n$ , D:  $\bar{M}_V$  for polymers obtained with  $\text{Et}(\text{ZnO})_2\text{ZnEt}$ . Polymerization conditions are identical as shown in Figure 9 except for toluene (1 ml) was used.

at low temperatures, and  $\text{Et}_2\text{Zn}$  was used instead of the  $\text{Et}(\text{ZnO})_2\text{ZnEt}$  compound.

$^{13}\text{C}$ -NMR spectra of an equimolar mixture of monomer, **1** and  $(\text{EtAlO})_n$  compound were taken in toluene- $d_8$  by changing the temperature from  $-50$  to  $+20^\circ\text{C}$  and the change of the chemical shift ( $\delta$ ) of each carbon was plotted in Figure 11. The corresponding results obtained with an equimolar mixture of the monomer **1** and  $\text{Et}_2\text{Zn}$  compound are shown in Figure 12. In the Al-system a large change in the chemical shift was observed for the ring-carbonyl carbon (C7) and the ring methine carbon (C5), while the side chain carbonyl (C2) was relatively unaffected. In contrast, the chemical shift change in the Zn-system was remarkable only for the side chain carbonyl carbon (C2), while the ring carbons (C7, C5) were almost unaffected. These observations are consistent with the idea that the Al-compound interacts more strongly with the lactone ring moiety in the monomer molecule, but the Zn-compound more strongly with the side chain ester group rather than lactone ring. This idea is a key for understanding the polymerization routes whether the "normal" formation of poly- $\beta$ -ester or the "isomerized" product poly- $\delta$ -ester is predominant.

Other Factors Affecting Polymerization Courses: The discussions above are made by assuming that the nature of

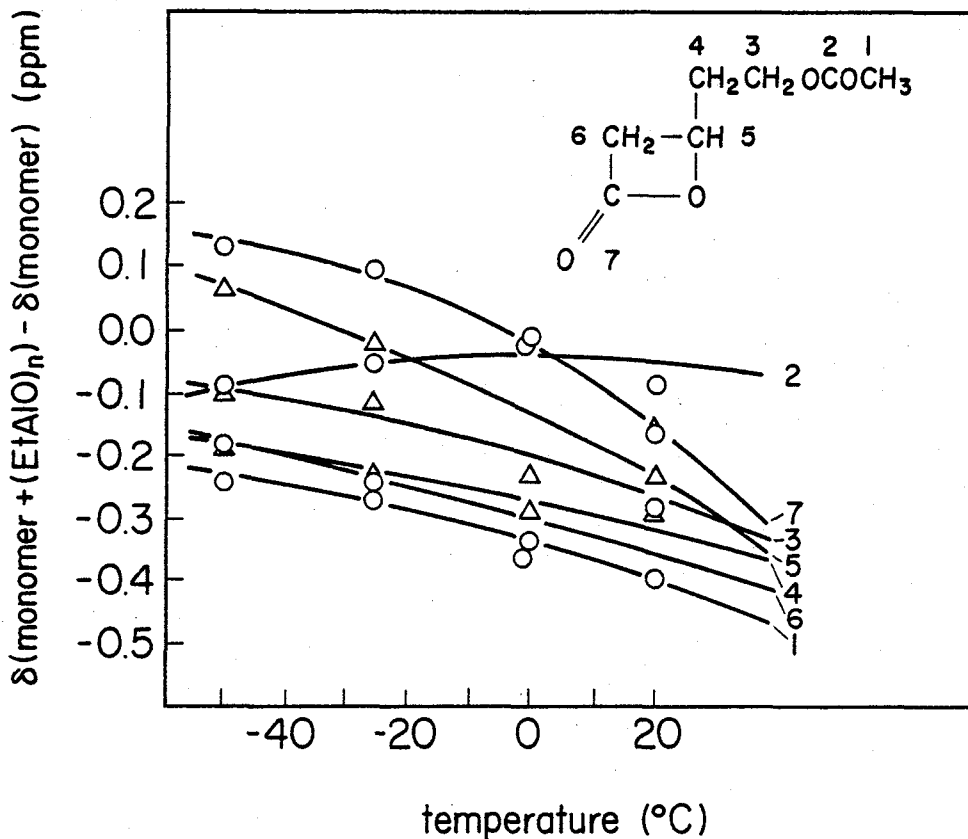


Figure 11 Temperature dependence of  $^{13}\text{C}$ -NMR chemical shift value of (1) in the presence and absence of  $(\text{EtAlO})_n$ . Accumulated with 200 scans. Chemical shift values (ppm) are internally standardized from  $d_8$ -toluene-ring carbon signal. (1) 1 ml;  $d_8$ -toluene 2 ml and equimolar amount of  $(\text{EtAlO})_n$  to (1) were used.

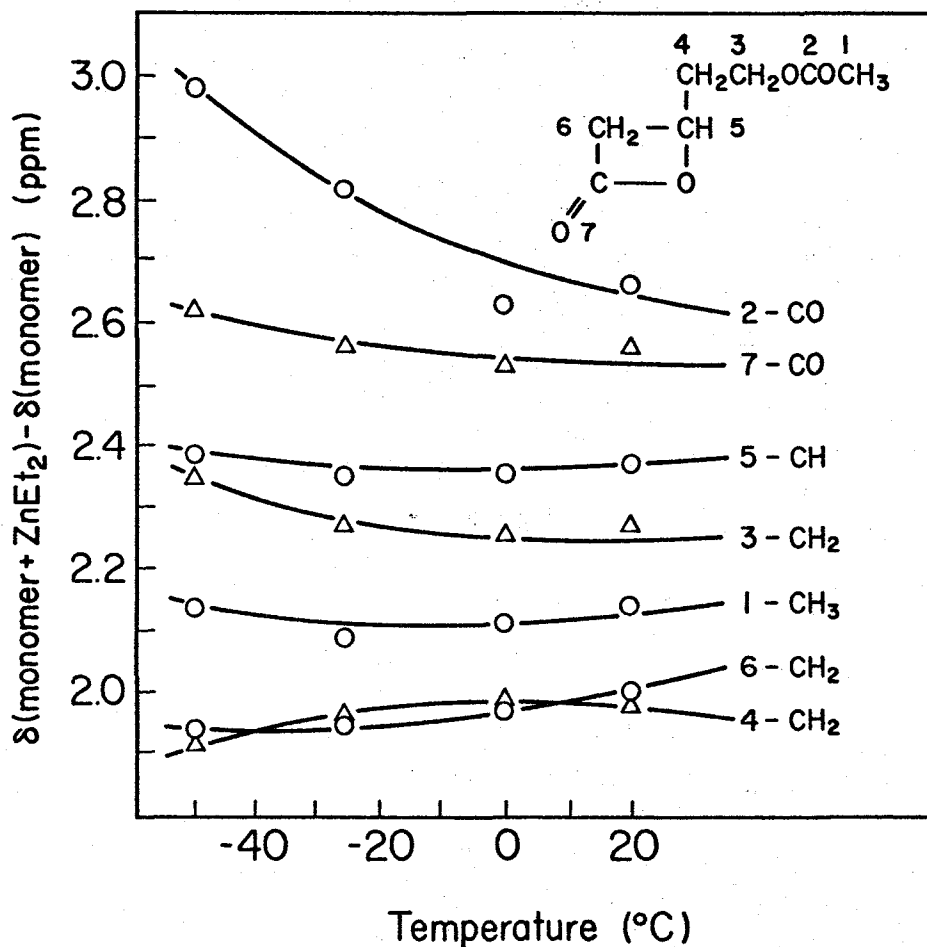


Figure 12 Temperature dependence of  $^{13}\text{C}$ -NMR chemical shift value of (1) in the presence and absence of  $\text{Et}_2\text{Zn}$ .  
 (1) 1 ml and  $d_8$ -toluene 2 ml for the measurement of  $\delta(\text{monomer})$ ; (1) 1 ml,  $\text{ZnEt}_2$  0.72 ml and  $d_8$ -toluene, 1.28 ml for  $\delta(\text{monomer} + \text{ZnEt}_2)$ .  
 Other conditions: see Figure 11.

catalyst is a major determining factor for the polymerization routes. This assumption was verified by the results shown in Table 3, where the isomer ratio obtained with a given catalyst is almost independent of polymerization temperature and catalyst concentration.

A typical cationic catalyst,  $\text{SnCl}_4$ , behaves similarly to the Zn catalyst in view of the predominant formation of the poly- $\delta$ -ester structure (cf. Table 1), although the product is a mixture of lower  $M_w$  compounds (Figure 5). In this respect, the Zn catalyst appears to act cationally. Since the Al catalyst has also been suggested as cationic in nature<sup>1</sup>, the difference in electrophilic properties of the Al and Zn atoms seems to be responsible for the site-selective interactions leading to the two types of polymer.

Stereoregularity of Poly(l)-Al: Although the Al catalyst is more stereoregulating than the Zn catalyst, the poly(l)-Al was an atactic polymer as evidenced by (i) its amorphous X-ray diffraction pattern and (ii) by  $^{13}\text{C}$ -NMR showing further  $\sim 0.1$  ppm separations at  $^7\text{C}_a$  and  $^7\text{C}_b$  carbons, respectively. As shown in the coordination study and the model polymerization system with ethylacetate, the side chain ester group cannot be completely free from coordination to the Al catalyst. This factor seems to inhibit the regular arrangement of the monomer

Table 3 Isomerization Ratio in the Polymerization of (1) a)

Catalyst	Polymerization temperature (°C)	Catalyst concentration (mol%)	Isomerization ratio (%)
Al	63	2	25
Al	63	4	33
Al	45	7	32
Al	63	7	31
Al	63	11	30
Zn	30	2	75
Zn	65	2	71
Zn	30	4	68
Zn	50	4	71

a) Monomer 2 ml, toluene 2 ml.



molecules on the catalyst during the propagation reaction, through some competition between the side-chain ester group and the lactone ring.

Relation with Stereoregulation in the "Normal" Type Polymerization: The difference of the interacting site in the monomer molecule toward the Zn and Al catalysts may be used to interpret the difference in the stereocontrolling properties of the two types of catalyst in the "normal" type polymerization of  $\beta$ -alkyl- and  $\beta$ -chloroalkyl- $\beta$ -propiolactones.<sup>1,6</sup> For example, the Al catalyst coordinates predominantly with the lactone ring of a monomer, whereas the Zn catalyst interacts with the polyester chain rather than with the attacking monomer. This leads to the former catalyst as being more stereoregulating than the latter. The Zn catalyst becomes stereoregulating only when an appropriate structure is possible between the attacking monomer and the growing chain end, as in the case of polymerization of  $\alpha$ -methyl- $\beta$ -propiolactone.<sup>7</sup>

In conclusion, the mystery of behaviors of Al-type and Zn-type catalyses for the stereoregulation in a variety of ring-opening polymerization can be solved when a simple but basic concept is applied; i.e., the strength of interaction between the catalyst and the growing chain end is of prime importance. Hence, early discussions widely made on the basis of whether a catalyst is cationic

or anionic will be only significant in considering the structure of an active end of the growing polymer chain. It should be noted, however, an effective stereoregulation in the cationic polymerization is limited where the growing chain end can effectively coordinate to the metal catalyst, and this situation is relatively restricted compared to in anionic polymerization in general.

11-3 Polymerization of  $\beta$ -(2-isopropylcarboxyethyl)- $\beta$ -propiolactone (2) and  $\beta$ -(2-(1-chloroethyl)carboxyethyl) $\beta$ -propiolactone (3)

The reason of the choice of the monomers 2 and 3 is that (1) These two are higher analogs of the monomer 1 but they are the smallest members with significant steric factor, and (2) Electronic effect of  $(\text{CH}_3)_2\text{CH-}$  and  $(\text{CH}_3)\text{ClCH-}$  groups operates in opposite ways in keeping the steric effects being almost identical.<sup>1</sup> The relative Taft's factors ( $\sigma^*$ )<sup>8</sup> for  $(\text{CH}_3)_2\text{CHCOO-}$  and  $(\text{CH}_3)\text{ClCHCOO-}$  groups can be estimated as -0.19 and +0.95 (-0.10 for addition of one  $\text{CH}_3$  and +1.05 for addition of one  $\text{Cl}$ ), respectively, when standardized by  $\text{CH}_3\text{COO-}$  as 0.00.

(3) These monomers can be prepared in similar procedures as the case of the monomer 1, and can be obtained in almost identical purities. This factor seems important for comparison of polymerization behaviors of different type of monomers in the organometallic catalyses.

2-1. Polymerization Results: Polymerization of the monomers 2 and 3 was found to proceed in a similar manner as the case of the monomer 1. The results are tabulated in Tables 4 and 5 for monomers 2 and 3, respectively, and typical results with the monomer 1 are also included. The polymer yields were determined from the amount of polymers isolated by precipitation then washing with ether. The polymerizability of the monomers evaluated from the polymer yields was found to be  $1 > 2 \gg 3$  for the Al-catalysis and  $1 \geq 2 \gg 3$  for the Zn-catalysis in toluene solvent. These results indicate that the increase of steric factors in the monomers 2 and 3 relative of 1 is more apparently reflected in the Al-catalysis rather than in the Zn-catalysis. This is in accord with the fact that the stereoregulation of the polymerization for  $\beta$ -alkyl- and  $\beta$ -chloro-alkyl- $\beta$ -propiolactone series is much effective in the Al-catalysis than in the Zn-catalysis.<sup>1</sup> Similarity in the polymer yields from 1 and 2 in the Zn-catalysis suggests that there is no significant steric factors to produce a reaction intermediate in the presence of Zn atom. Remarkable decrease of the polymerizability of monomer 3 compared with that of monomer 2 is largely due to electronic factor of the Cl group in the former since the steric factors of the monomers 2 and 3 are almost identical. Hence, decrease of the electron density in the side-chain ester group of the Cl-containing monomer causes drastic

Table 4 Polymerization Results of Monomers 1 and 2.a)

Monomer	Catalyst <sup>b)</sup>	Catalyst concn. (mol%)	Solvent <sup>c)</sup>	Temp. (°C)	Time (days)	Polymer yield (%) <sup>d)</sup>
1	Al	4	toluene	63	30	52
1	Zn	4	toluene	65	4	68
2	Al	4	toluene	80	28	43
2	Al	4	toluene	65	32	41
2	Zn	4	toluene	65	21	45
2	Zn	4	toluene	35	32	70
2	Zn	4	CH <sub>2</sub> Cl <sub>2</sub>	30	31	30
2	Zn	6	toluene	30	28	60
2	BF <sub>4</sub> OEt <sub>3</sub>	1	toluene	30	30	16

a) The results of monomer 1 are selected from Table 1.

b) Al denotes (EtAlO)<sub>n</sub> and Zn denotes Et(ZnO)<sub>2</sub>ZnEt.

c) Monomer/solvent ratio, 1/1 (v/v).

d) Determined by weight of isolated polymer.

Table 5 Polymerization Results of Monomer 3.a)

Catalyst	Catalyst concn. (mol%)	Temp. (°C)	Time (days)	Polymer yield (%)
Al	4	65	31	21
Al	6	65	21	29
Zn	4	30	9	21
Zn	4	65	23	11
Zn	6	30	40	10
BF <sub>4</sub> OEt <sub>3</sub>	1	30	31	5

a) Toluene was used as solvent, monomer/solvent ratio 1/1 (v/v). Notes described in Table 1 should be referred to.

decrease in the polymerizability. Such a effect seems to consistent with the previous observation that the side-chain ester group interacts with the catalyst, especially with Zn, in a manner of competition against "normal" ring-opening process of the lactonic ester group. For Al-catalysis decrease of the polymerizability of monomer 3 is observed, but the extent is considerably smaller than for Zn-catalysis.

2-2. Polymer Structure: The polymer structures were examined with  $^{13}\text{C}$ -NMR as was the case of poly(1)s. Figure 13 shows the spectra of poly(2)-Zn, poly(2)-Al, poly(3)-Zn, and poly(3)-Al of molecular weight 4,000. The assignment of the signals can be made straightforward by referring the results of poly(1). The signals of C-3 and C-5 carbons, which correspond to the side-chain O-CH<sub>2</sub> and the ring CH carbons, respectively, split in an essentially similar fashion as were observed in poly(1)-Zn and poly(1)-Al samples. Clearly, the intensity ratios of the C-3<sub>a</sub> (in poly-β-ester unit) to the C-3<sub>b</sub> (in poly-δ-ester unit) and C-5<sub>a</sub> (in poly-β-ester unit) to C-5<sub>b</sub> (in poly-δ-ester unit) differ with the nature of the catalyst used. These spectral evidences indicate that ring-opening isomerization polymerization occurs also in the cases of monomers 2 and 3.

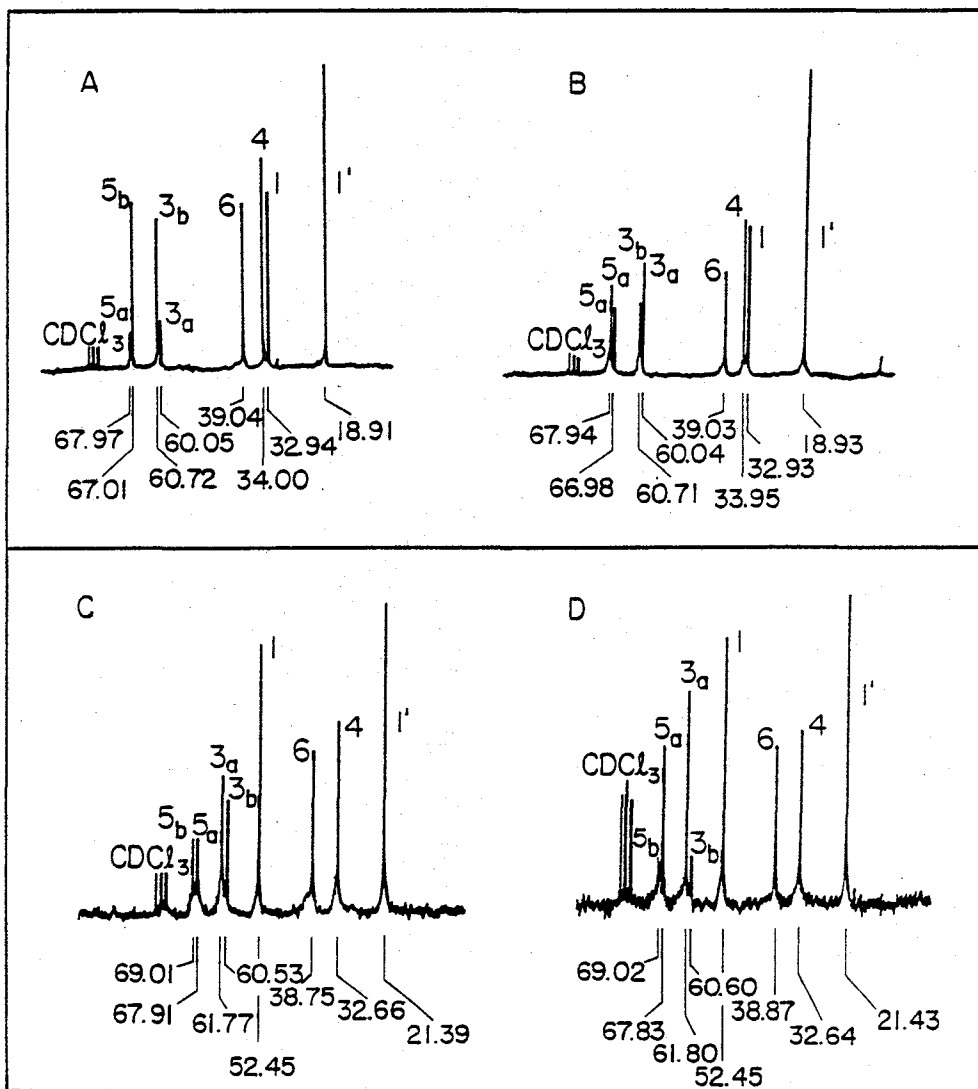


Figure 13  $^{13}\text{C}$ -NMR spectra of Poly(2) and Poly(3) samples in  $\text{CDCl}_3$ . A: Poly(2)-Zn, B: poly(2)-Al, C: poly(3)-Zn, D: poly(3)-Al. Numbering of the signals should be referred to the following monomer structure. The carbonyl signals are omitted in the Figures. Suffix a shows the signals of the poly- $\beta$ -ester unit, and suffix b that of the poly- $\delta$ -ester unit. The assignments were referred to the spectrum of poly(1).

### 2-3. Relative Amount of Isomerization Polymerization:

The intensity ratios of the C-3<sub>a</sub>/C-3<sub>b</sub> and C-5<sub>a</sub>/C-5<sub>b</sub> signals reflect the relative amounts of isomerized product to the normal polymerization product. The relative amounts of poly- $\delta$ -ester and poly- $\beta$ -ester units in the polymers thus estimated are summarized in Table 6, in comparison with the results of monomer 1.

For the cases of monomers 2 and 3 the isomerization ratios were higher for the Zn-catalysis than for the Al-catalysis. This trend is common for all of the monomers studied here. The monomer 2 showed a considerably high isomerization ratio where the Zn-catalysis afforded about 80 % of isomerized poly- $\delta$ -ester unit, and even in the Al-catalysis almost equimolar amounts of poly- $\delta$ -ester and poly- $\beta$ -ester units were formed. The Cl-containing monomer 3 converts less readily to poly- $\delta$ -ester unit compared with the monomers 1 and 2.

Thermal Behaviors of Polymers: It has been already shown that the polymer enriched with poly- $\delta$ -ester structure, which is consisted of longer main-chain units and shorter side-chains, shows higher  $T_g$  value than the polymer enriched with poly- $\beta$ -ester structure (shorter main-chain units and longer side-chains, therefore weaker interchain interaction). Further, the former has lower decomposition temperature because of its relative feasibility



Table 6 Isomerization ratio of polymers.

Monomer	Catalyst	Isomerization ratio (%)
1	Al	25-33
1	Zn	68-75
2	Al	42-54
2	Zn	76-84
3	Al	20-25
3	Zn	~50

in producing a pyrolysate as 2-dihydropyrone rather than the latter which gives substituted acrylic acid as main pyrolysate. For instance, the poly(1)-Zn and poly(1)-Al with molecular weight of ca. 10,000 showed significant differences in  $T_g$  and  $T_{decomp}$  values as cited in Table 7. Similar trends were observed for poly(2) and poly(3) samples, though the differences of the  $T_g$  values were not so remarkable. The closeness of  $T_g$  values in Zn-polymers and Al-polymers may be due to lower molecular weight and to the presence of branched side-chains which reduce the inter-chain interactions operating in both types of polymer. The difference of  $T_{decomp}$  values between poly- $\delta$ -ester rich and poly- $\beta$ -ester rich samples was significant for poly(2) and poly(3) series as shown in Table 7.

#### Transition State of Isomerization Polymerization:

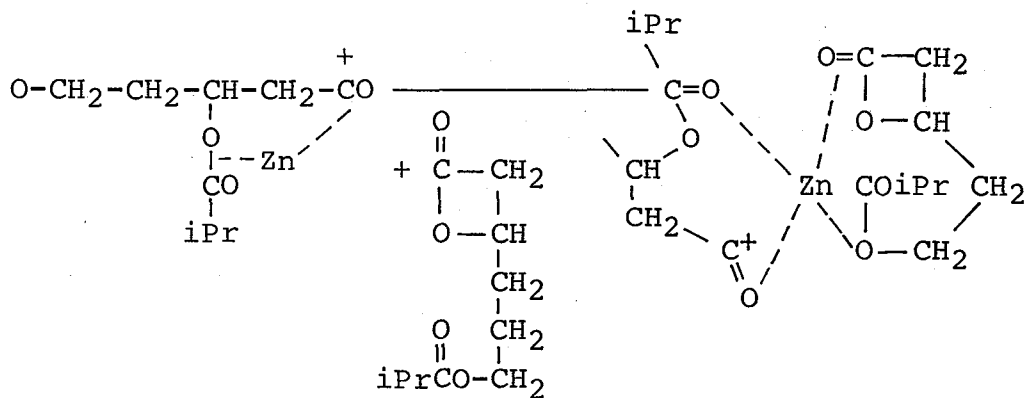
The observed trend of isomerization polymerization, i.e., monomer 2 > monomer 1 > monomer 3, can be interpreted on the basis of reaction scheme shown in Figure 8.

The isopropyl group in the monomer 2 gives rise to the highest electron density at the side-chain carboxyl moiety. Since the Zn atom can coordinate with both of carboxyl groups in the side-chain and lactone ring (in preference at the side-chain), the interaction of the Zn atom with the  $(CH_3)_2CHCOO-$  group would be strongest in due course. This effect will exert to bring the side-

Table 7 Thermal Properties of Polymers.

Polymer	M.W.	T <sub>g</sub> (°C)	T <sub>decomp.</sub> (°C)
poly( <u>1</u> )-Al	12000	-60 ~ -40	245
poly( <u>1</u> )-Zn	10000	-10 ~ 0	220
poly( <u>2</u> )-Al	4000	-30 ~ -18	260
poly( <u>2</u> )-Zn	4000	-27 ~ -12	215
poly( <u>3</u> )-Al	4000	-25 ~ -14	250 - 270
poly( <u>3</u> )-Zn	4000	-22 ~ -10	220 - 250

chain ester group near to the lactonic oxygen atom without significant resistance, giving rise to a simultaneous coordination of Zn with both of the ester group. Since the Zn atom was present at the terminal carboxyl group of the growing chain, the entity of this stage is likely to constitute a coordination state comprised of three types of ester oxygen atoms: one from growing chain, one from the side-chain, and the remainder from the lactone group. This provides a favorable condition to afford a bicyclic intermediate suitable for isomerization polymerization producing poly- $\delta$ -ester structure.



The situation of monomer 3 where  $(\text{CH}_3)\text{ClCHCOO}^-$  group is present differs considerably because of great decrease in the electron density at the side-chain ester group (cf.  $\sigma^* = +0.95$  for  $(\text{CH}_3)\text{ClCHCOO}^-$ ). Hence, the interaction of the Zn atom with the side-chain ester group becomes weakened, and the polymerization will tend to proceed by spoiling the side-chain group. This mechanism is sub-

stantially a "normal" ring-opening polymerization mechanism of  $\beta$ -substituted- $\beta$ -propiolactone.

Our results indicate that even in the Al-catalysis, an increase in the electron density at the side-chain ester group in monomer 2 causes a significant increase in contribution of bicyclic intermediate to afford poly- $\delta$ -ester structure in almost an equal probability as to form poly- $\beta$ -ester structure. This result suggests that the preference of Al-catalysis for "normal" type polymerization stands on a delicate balance of the electron density at the lactone and the side-chain groups, which participates at the coordination stage.

Kinetic Behaviors of Polymerization: The time-conversion profiles of polymerization of the monomers 2 and 3 (Figure 14), which were obtained by monitoring the monomer conversion in the NMR tube, indicate that there are general trends in the isomerization polymerization and in the normal polymerization also in view of kinetic behavior. One exception was polymerization behavior of the monomer 2 in Al-catalysis, which has the highest isomerizability.

The poly- $\delta$ -ester forming isomerization polymerization which favors the bicyclic intermediate shown in Figure 8 occurs relatively rapidly after a considerably long induction period. The long induction period may be due to

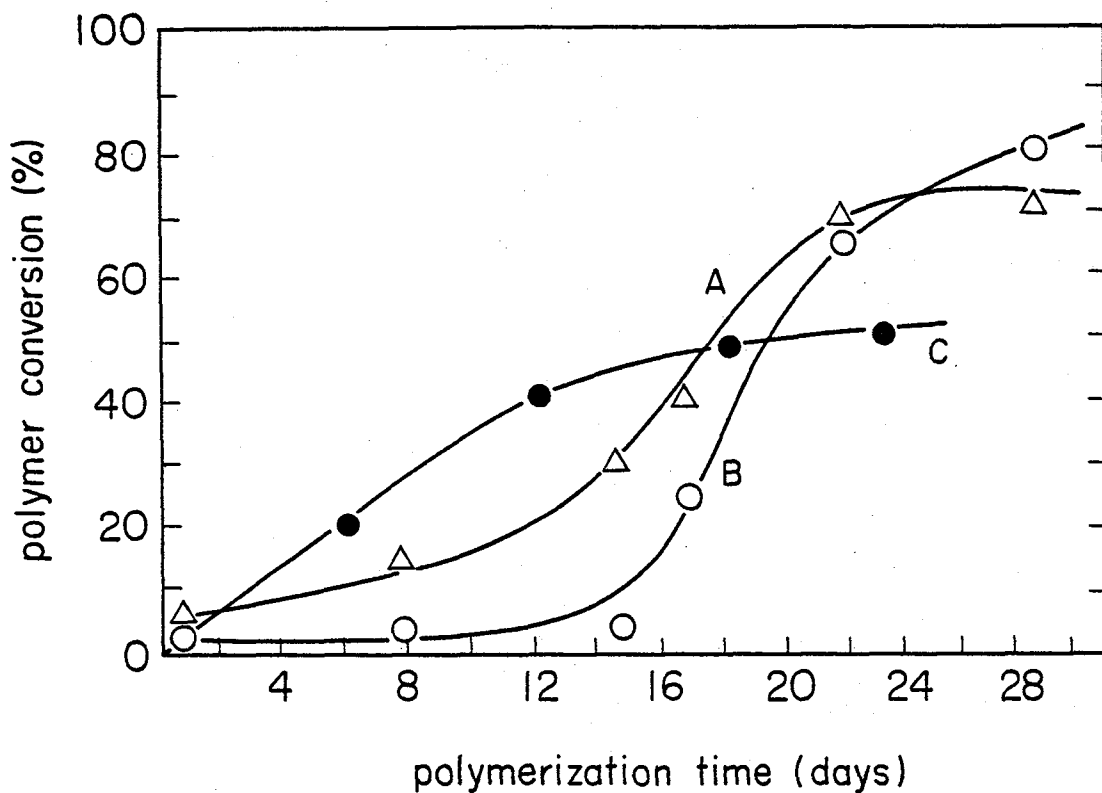


Figure 14 Kinetic profiles in polymerization of monomer (2) and (3).

A: (2) in Al-catalysis, B: (2) in Zn-catalysis, and C: (3) in Al-catalysis. Polymerization was carried out in a sealed NMR tube, and conversion was determined from relative intensity of methine signals of monomer and polymer. Polymerization conditions: monomer/toluene ratio, 1/1 (v/v); catalyst/monomer ratio, 4 mol%, temperature, 60°C for Al-catalysis and 30°C for Zn-catalysis.

requirement of movement of the long side-chains in the monomer to give a proper geometry in the bicyclic intermediate.

In contrast, the poly- $\beta$ -ester forming "normal" polymerization proceeds relatively monotonously with time as were observed in a variety of substituted  $\beta$ -propiolactones in the presence of the Al-catalyst.<sup>1</sup> The behavior of the monomer 2 in Al-catalysis resembles to the Zn-type one kinetically. This is probably associated with the fact that the polymerization proceed in an almost equal probability of poly- $\delta$ -ester and poly- $\beta$ -ester forming mechanisms. High contribution of the former mechanism seems to result in a net kinetic behavior to have an isomerization-type (Zn-type) profile.

Equibinary Copolymer: It must be noted that the poly(2)-Al and poly(3)-Zn samples contain almost equimolar amounts of poly- $\beta$ -ester and poly- $\delta$ -ester units as shown in Table 6. These polymers are statistically equibinary copolymers of two different monomeric units. Although there remains a possibility that these are alternate copolymer, I have no decisive evidence for this possibility. Rather, it is safe in this stage that the equibinary copolymers are not complete alternate copolymer, since the isomerization ratios differ within a small range by the polymerization conditions, e.g., batch con-

ditions, and in addition no remarkable characteristics in the physical properties of the equibinary copolymer when compared with other copolymers. However, it is still interesting that this type of equibinary copolymers can be synthesized by the new isomerization polymerization.



## References

1. K. Teranishi, T. Araki and H. Tani, *Macromolecules*, 5, 660 (1972); H. Tani, S. Yamashita and K. Teranishi, *Polym., J.*, 3, 417 (1972); K. Teranishi, M. Iida, T. Araki, S. Yamashita and H. Tani, *Macromolecules*, 7, 421 (1974); M. Iida, T. Araki, K. Teranishi and H. Tani, *Macromolecules*, 10, 275 (1977); M. Iida, S. Hayase and T. Araki, *Macromolecules*, 11, 490 (1978).
2. T. Araki, M. Iida and S. Hayase, *Polym. Prepr. Jpn.*, 26, 140 (1977); T. Araki, M. Iida, S. Hayase and A. Nakamura, *Preprts. 38th Annual Meeting of Chem. Soc. Jpn.*, Vol.III, p.1208, 1978, Oct. 16, Nagoya, Japan.
3. D. Shaw, "Fourier Transform N. M. R. Spectroscopy", Elsevier Scientific Publishing Company, p. 297 (1967)
4. R. D. Lunberg and E. F. Cox, "Kinetics and Mechanism of Polymerization", Vol. II, "Ring Opening Polymerization" edited by K. C. Fresch and S. L. Reegen, 1969, Marcel Dekker, New York and London, Chapter 6, p. 247
5. H. Mark and G. S. Whitby, "High Polymers", Vol. 1, "The Collected Papers of W. H. Carothers", Wiley Interscience, New York, 1940, p.81 - 140.

6. J. R. Shelton, D. E. Agostini and J. B. Lando,  
J. Polymer Sci., Part A-1, 9, 2789 (1971).
7. T. Araki, M. Iida and S. Hayase, unpublished results.
8. R. W. Taft, Jr., "Separation of Polar, Steric, and  
Resonance Effects in Reactivity" in Steric Effects  
in Organic Chemistry (M. S. Newman, ed.), John Wiley  
and Sons, Inc., New York, 1956, p.590 - 594.



Part I. A new catalyst for polymerization of epoxide

Material

Cyclohexene oxide was dried over  $\text{CaH}_2$ , distilled, and stored in a nitrogen atmosphere.

Silicon compound: Silanols were prepared by methods described in the literature.<sup>1</sup> Alkoxysilanes were synthesized from chlorosilane and alcohol, in the same manner as silanols<sup>1</sup>. Benzylsilylether and ortho-nitrobenzylsilylether were purified by means of column chromatography (ODS silica) and recrystallization from chloroform. Characterizations of new compounds are shown in Table 1. Other alkoxysilanes were purified by means of distillation. Oligomers of diphenylsilanediol were prepared by fractional recrystallization of a hydrolysis mixture of  $\text{Ph}_2\text{SiCl}_2$ <sup>2</sup>. Polymeric silanol compound, SH6018, was obtained from Toray Silicone Co., Ltd. (average OH equivalent, 400).

Syntheses of diphenyl(4-vinylphenyl)silanol: The solution of 4-bromostyrene(12.0 g) and ethyl bromide(0.4 g) in absolute tetrahydrofuran(30 ml) was added dropwise to Mg(3.2g) suspended in absolute tetrahydrofuran(10 ml). The reaction started immediately. The addition took 10 minutes, then it was stirred for 30 min. 20 ml of absolute

Table 1 Characterization of New Silyl Ethers.

	Sample	$H^1$ -NMR (ppm)	IR ( $cm^{-1}$ )	$UV\lambda_{max}^{CH_3CN}$ nm( $\epsilon$ )	Elemental analysis (%) found (calcd.)			
					C	H	N	Cl
Si-I	4-chloro-2-nitrobenzyl (triphenyl)silyl ether	5.25 7.32 - 8.08	3060 1535 1435 1120	218(34700) 252( 3600) 258( 4900) 263( 4700) 271( 3600) 306( 1500)	67.62 (67.33)	4.31 (4.52)	3.06 (3.14)	7.88 (7.95)
Si-II	4,5-dimethoxy-2-nitrobenzyl (triphenyl)silyl ether	3.84 3.93 5.34 7.36 - 7.69	3050 1510 1320 1280 1085	214(32800) 221(32400) 242(10600) 265( 2300) 271( 2400) 297( 4300) 346( 6300)	68.45 (68.77)	5.08 (5.34)		
Si-III	3-methyl-2-nitrobenzyl (triphenyl)silyl ether	2.26 4.93 7.05 - 7.68	3050 1540 1435 1120 718	219(27600) 253( 2400) 260( 2500) 265( 2500) 272( 2100)	73.46 (73.39)	5.45 (5.45)	3.05 (3.29)	
ONBSi	2-nitrobenzyl (triphenyl)silyl ether	5.30 7.36 - 8.10	3060 2920 1520 1340 1125	221(29000) 254( 5300) 257( 5700) 260( 6100) 265( 6200) 270( 5500) 306( 1700)	72.97 (72.97)	4.76 (5.14)	3.40 (3.47)	
Si-IV	di(5-chloro-2-nitrobenzyloxy) diphenyl silane	5.25 7.32 - 8.07	3060 2900 1530 1520 1340 1110	219(29800) 270(15300)	56.45 (56.22)	3.49 (3.65)	5.04 (5.04)	12.66 (12.77)

Sample	H <sup>1</sup> -NMR (ppm)	IR (cm <sup>-1</sup> )	UVλ <sub>max</sub> <sup>CH<sub>3</sub>CN</sup> nm(ε)	Elemental analysis (%)			
				found (calcd.)			
				C	H	N	Cl
Si-V	di(4-chloro-2-nitrobenzyloxy) diphenyl silane	5.21 7.34 - 8.06	3070 1530 1345 1085	217(38400) 257( 9800) 305( 3400)	55.93 (56.22)	3.59 (3.63)	
Si-VI	di(2-nitrobenzyloxy) diphenyl silane	5.27 7.31	3090 1530 1340	219(23200) 263(11900)	64.06 (64.18)	4.34 (4.56)	
Si-VII	5-methyl-2-nitrobenzyl (triphenyl)silyl ether	2.41 5.28 7.22 - 8.02	3050 2850 1540 1435 1120	218(27000) 253( 4400) 258( 5500) 264( 6500) 270( 6700) 278( 6200)			
Si-VIII	3-methoxy-2-nitrobenzyl (triphenyl)silyl ether	3.86 4.89 7.23 - 7.67	3040 1590 1530 1285 1120	217(32800) 254( 1700) 260( 2000) 265( 2100) 272( 1800)			
Si-IX	5-chloro-2-nitrobenzyl (triphenyl)silyl ether	5.27 7.29 - 8.08	3060 1518 1338				

tetrahydrofuran was added to the reaction mixture. The Grignard reagent was added dropwise to the refluxing solution of  $\text{Ph}_2\text{SiCl}_2$  (16.6 g) in absolute tetrahydrofuran (100 ml) and refluxed for 5 h. The mixture was cooled, then poured into a mixture of triethylamine (6.7 g), diethylether (250 ml) and water (250 ml) at  $0^\circ\text{C}$ . The reaction mixture was extracted with ether. The ether layer was concentrated under reduced pressure. The resultant gum-like material was dissolved in chloroform/hexane (1:2). The soluble matter was separated with Silicagel-60 (Merck). The diphenyl(vinylphenyl)silanol was obtained in the fraction eluted with chloroform. Yield 12 %, m.p.  $84 \sim 86^\circ\text{C}$ ,  $^1\text{H}$  NMR, ( $\delta$  ppm, in  $\text{CDCl}_3$ ) 2.26 (s, OH), 5.29 (dd,  $J_{13}$ , 10.7 Hz,  $J_{12}$ , 1.0 Hz,  $\text{H}_1$ ), 5.68 (dd,  $J_{23}$ , 17.6 Hz,  $J_{12}$ , 1.0 Hz,  $\text{H}_2$ ), 6.74 (dd,  $J_{23}$ , 17.6 Hz,  $J_{23}$ , 10.7 Hz,  $\text{H}_3$ ), 7.36 to 7.68 (m, aromatic proton)  $\text{H}_3$ - $\text{C}=\text{C}$ - $\text{H}_1$  IR(KBr disk),  $\text{H}_2$   
 3250, 1622, 1595,  $1590\text{ cm}^{-1}$ .

Polymerization of diphenyl(vinylphenyl)silanol: The diphenyl(vinylphenyl)silanol was polymerized in 50 volume % of  $d_8$ -tetrahydrofuran. The polymerization was carried out under UV radiation, and AIBN was used as photo-initiator. The concentration of AIBN was 10 mol% to the monomer. The polymerization was carried out in the NMR tube made of quartz. The monomer was photo-polymerized with a merry-go-round type apparatus equipped with a 400W-high-pressure-mercury lamp at  $40^\circ\text{C}$ . The monomer was placed

at 10 cm distance from the lamp. After the signal of the vinyl proton disappeared, the product was poured into methanol and the insoluble matter was dried under reduced pressure. Copolymerization of diphenyl(vinylphenyl)silanol with styrene was carried out in the same way. However, when diphenyl(vinylphenyl)silanol was soluble in the styrene monomer, the tetrahydrofuran was not used. The polymer conversion was almost 100 %, and the molecular weights of the polymer are listed in Table 6 in chapter 7.  $\text{Ph}_3\text{SiCOPh}$  was prepared by the method described in the literature.<sup>3</sup>

Other hydroxy group:  $\text{Ph}_3\text{GeOH}$  was prepared by the method described in the literature.<sup>4</sup>  $\text{Ph}_3\text{SnOH}$  was purchased commercially from Alfa Products and used without further purification. Alcohols were purified by distillation before use.  $\text{PhSH}$ ,  $\text{Ph}(\text{OH})_2$ ,  $\text{Ph}_3\text{CSH}$ ,  $\text{PhOH}$ , and  $\text{Ph}_3\text{COH}$  were commercially available and used without further purification. Formaldehyde-diethylmalonate-condensation product was synthesized by the method described in the literature.<sup>5</sup>

Aluminum complex: Aluminum complexes were prepared from aluminum isopropoxide and corresponding ligand in toluene or from aluminum sulfate and the corresponding ligand in water.<sup>6</sup> These aluminum complexes and silyl compounds were listed in Table 2.  $((\text{CH}_3)_3\text{SiO})_3\text{Al}$  was prepared by the method described in the literature.<sup>7</sup> Other complexes were purchased from Wako Pure Chemicals.  $\text{BF}_3$  complexes



Table 2 The aluminum complexes and silyl compounds used in the present study.

Aluminum complex or silyl compound	Abbreviation
tris(acetylacetonato)aluminum	Al(acac) <sub>3</sub>
tris(ethylacetoacetato)aluminum	Al(Etaa) <sub>3</sub>
tris(salicylaldehydato)aluminum	Al(SA) <sub>3</sub>
other aluminum complexes: see chapter 4	
diphenyl(4-vinylphenyl)silanol	DVPS
triphenylsilanol	
diphenylsilanediol	DP
diphenylvinylsilanol	
diphenylmethylsilanol	
phenyldimethylsilanol	
1,1,4,4-tetramethyl-1,4-dihydroxysilolethylene SH6018	HMSB
HO(Ph <sub>2</sub> SiO) <sub>n</sub> H:    n = 1	Monomer
n = 2	Dimer
n = 3	Trimer
n = 4	Tetramer
alkoxysilanes: see chapter 10-2	
ortho-nitrobenzyl ether: see chapter 10-5	
triphenylbenzoylsilane	
silyl ether: see chapter 10-5 and 12	
Ph <sub>2</sub> Si(OCH <sub>2</sub> C(COOC <sub>2</sub> H <sub>5</sub> ) <sub>2</sub> ) <sub>2</sub>   CH <sub>2</sub> OH	FMSi

were purified by distillation or crystallization before use.

Silica: Silica gel was obtained from Wako Pure Chemicals (C-200, 100-200 mesh). Zeolites were obtained from Gas-Chro Kogyo, sold as 3A, 4A, 5A, 9F (300 mesh). Porous silicas were obtained from Waters, Ltd., sold as gas chromatograph packing agent, Porasil A, B, C, D, E, F. [150 mesh; surface area ( $\text{m}^2/\text{g}$ ), mean pore size ( $\text{\AA}$ ): A, 480, 100; B, 200, 100 - 200; C, 50, 200 - 400; D, 25, 400 - 800; E, 4, 800 - 1500; F, 1.5, 1500]. Zeolites and silicas were used after heat treatment (at  $150^\circ\text{C}$  for 2 h).

### Polymer Preparation

A solution of metal compound in cyclohexene oxide was mixed with a solution of the OH compound in cyclohexene oxide in a polymerization tube at  $-78^\circ\text{C}$  in a  $\text{N}_2$  atmosphere. The polymerization tube was warmed to  $40^\circ\text{C}$  and held at that temperature. After polymerization the unreacted monomer was removed from the polymerization system under reduced pressure and the polymer was washed with acetone and dried.

### Photolysis

In order to examine the photodecomposition of silyl compound, the silyl compounds were photodecomposed in tetrahydrofuran (THF) or acetonitrile, by use of 400W-high-pressure-mercury-lamp. The lamp was surrounded by a

water-cooled Pyrex photolysis well in case of  $\text{Ph}_3\text{SiCOPh}$  photolysis experiment and by a water-cooled quartz photolysis well in case of other experiment. Samples were placed in "merry-go-round" holder that rotates about the lamp to provide even illumination during photolysis. The entire apparatus was immersed in thermostated water at  $40^\circ\text{C}$ . The decomposition of silyl compounds was followed by liquid chromatography with an octa-decyl-silane-treating silica column (Zorbax ODS, Shimadzu). The ratio of  $\text{Ph}_3\text{SiOH}$  in  $\text{Ph}_3\text{SiCOPh}$  decomposition products was determined by  $^1\text{H-NMR}$  after complete photodecomposition.

Dependence of photolysis on wavelength of UV-light was examined by use of UV-filter. The UV filter (160 x 53 mm) was placed in a stainless case at 5 positions around UV lamp. The filters used are L39 (over 390 nm) and U36 (365 nm) (Riko Kagaku). Experiment using 254 nm was carried out by use of 26W-low pressure mercury lamp (Riko Kagaku).

In order to obtain quantum yield of decomposition of silyl ether, potassium ferrioxalate as a standard chemical actinometer was used.<sup>8</sup>

### Photopolymerization

Normal photopolymerization was carried out by the following method: Catalysts were dissolved in cyclohexene oxide in a  $\text{N}_2$  atmosphere in a pyrex tube ( $\text{Ph}_3\text{SiCOPh}$ ) or in a quartz tube (other silyl compounds) with a glass stopper.

The UV irradiation was carried out in a similar manner to photolysis. After polymerization the unreacted monomer was removed from the polymerization system under reduced pressure and the polymer was washed with acetone and dried.

### Properties of silanol

Stability of silanol against self-condensation was estimated with 0.01 mol of  $\text{Al}(\text{acac})_3$  and 0.01 OH equiv of silanol dissolved in 5 mL of THF. The mixture was held at 40°C and the course of silanol condensation was followed by GPC.

Relative acidity of silanol was examined by NMR spectra at 35°C with  $1.5 \times 10^{-4}$  OH equiv of silanol in 1 mL of  $\text{CDCl}_3$  or  $d_6$ -DMSO.

The decrease in the amount of silanol in the polymerization procedure was investigated:  $1 \times 10^{-3}$  mol of silanol and  $1 \times 10^{-3}$  mol of  $\text{Al}(\text{acac})_3$  were dissolved in 1 mL of cyclohexene oxide and 1 mL of  $d_8$ -THF. The decrease in the amount of SiOH was measured by  $^1\text{H}$ -NMR.

### Interaction between aluminum complex and triphenyl silanol

A half value width of NMR peak, assigned to the SiOH group of the  $\text{Ph}_3\text{SiOH}$ , was measured in the mixture solution of 0.21M aluminum complex and 0.21M triphenylsilanol in  $\text{CDCl}_3$ . The data were corrected by the subtraction of the half value width of a peak due to tetramethylsilane from

the measured half value width of the signal.  $T_1$  value (spin-lattice relaxation time) was calculated from a slope in  $\log(M_0 - M(t)) - t$  plot ( $M_0$ : longitudinal component at infinite time;  $M(t)$ : longitudinal component at time  $t$ ) or null point in a solution having the same concentration.

### Properties of cured epoxy resin

Bisphenol A type epoxide (Epikote 828 (Fig. 1), Shell Chemical Co.,) was used as epoxy resin monomer.

Curing: The epoxy resin monomer containing the catalyst was poured into 1 mm width-opening between two glass plates. The epoxy resin monomer was cured at 150°C for 15 hours.

The measurement of thermal depolarization current was performed in the following manner. A sample was polarized under an electric field ( $E_p$ ) at 150°C for 30 min. and subsequently cooled rapidly to room temperature without removing the field. After short circuiting the electrodes the sample was heated at constant rate 3°C/min. and the current was measured, using an Electret Thermal Analyzer No. 650 (Toyo Seiki Seisakusho, LTD.)

Volume resistivity was measured as follows. Au electrode was evaporated on the cured epoxy resin plate, as shown in Figure 2. The sample was heated at 0.75°C/min. The impressed voltage was 500 V. (Model 4329, Yokokawa-Hewlett Packard)

Dielectric properties were measured by use of Schering Bridge Type 2759 (Yokokawa Electric Works LTD.) at

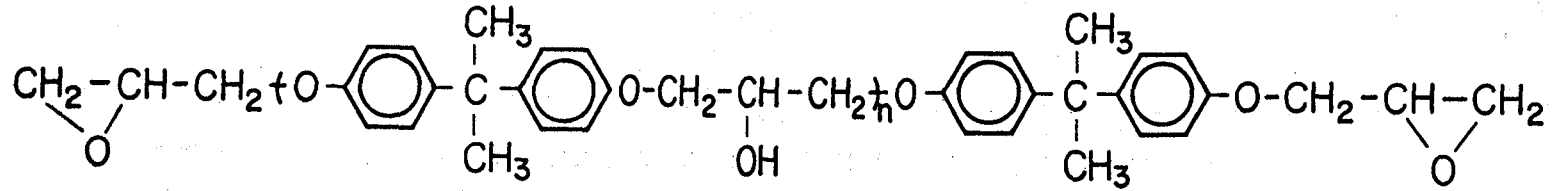


Figure 1 Bisphenol A type epoxy resin.

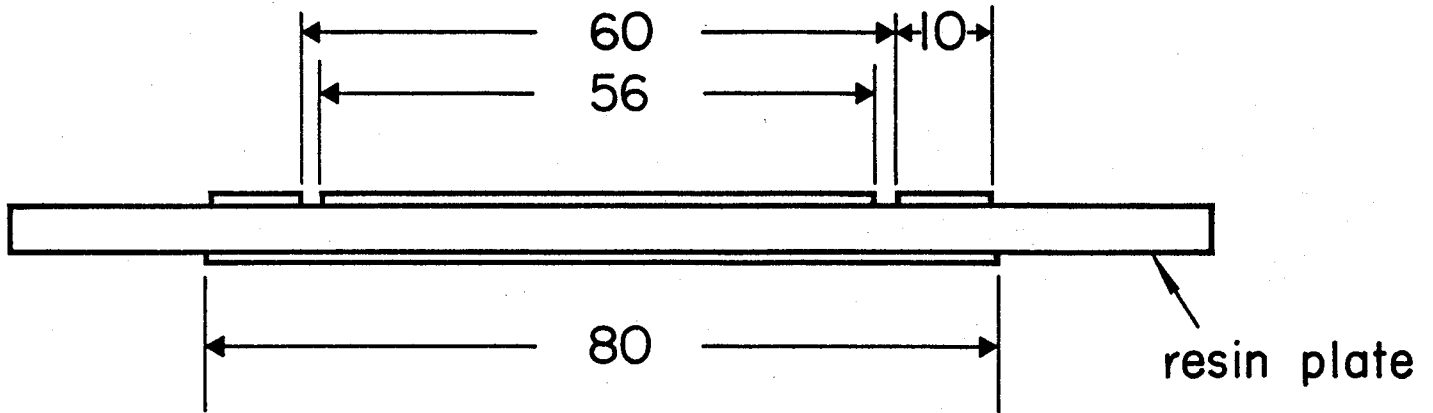


Figure 2 Electrode structure.

50 Hz, 500 V. The dependence of dielectric loss ( $\epsilon''$ ) on frequency was examined by use of LCR meter Model 4274 A (Yokokawa-Hewlett-Packard) in the frequency range from 50 Hz to  $10^5$  Hz.

Measurement of breakdown voltage was performed as follows. The sample was placed between stick electrode ( $6\phi$ ) and plate electrode in silicone oil. Applied voltage was increased at 1 kV/sec. at A.C. 50 Hz.

Shear modulus was measured by means of torsional braid analysis (RD 10 type, Resca).

Gelation time was measured by use of curast meter method or test tube method. The curast meter method<sup>9</sup> uses curast meter. Time at which stress on curing was recorded was obtained as the gelation time. The test tube method is as follows. 30 g of epoxy resin monomer was poured into 15 mm $\phi$  test tube. 2 mm $\phi$  glass rod was stood in the epoxy resin and was made up and down. When the glass rod raised with the test tube, gelation was recorded.

Reaction starting temperature was measured by use of heat of reaction. The measurement was carried out by use of the apparatus shown in Figure 3.

### Apparatus

The molecular weight distribution of the polymer was determined with a Toyo Soda model 801 gel permeation chromatograph operated at 40°C. The four columns were connected in series, each packed with G2000H<sub>8</sub>, G2000H<sub>8</sub>,



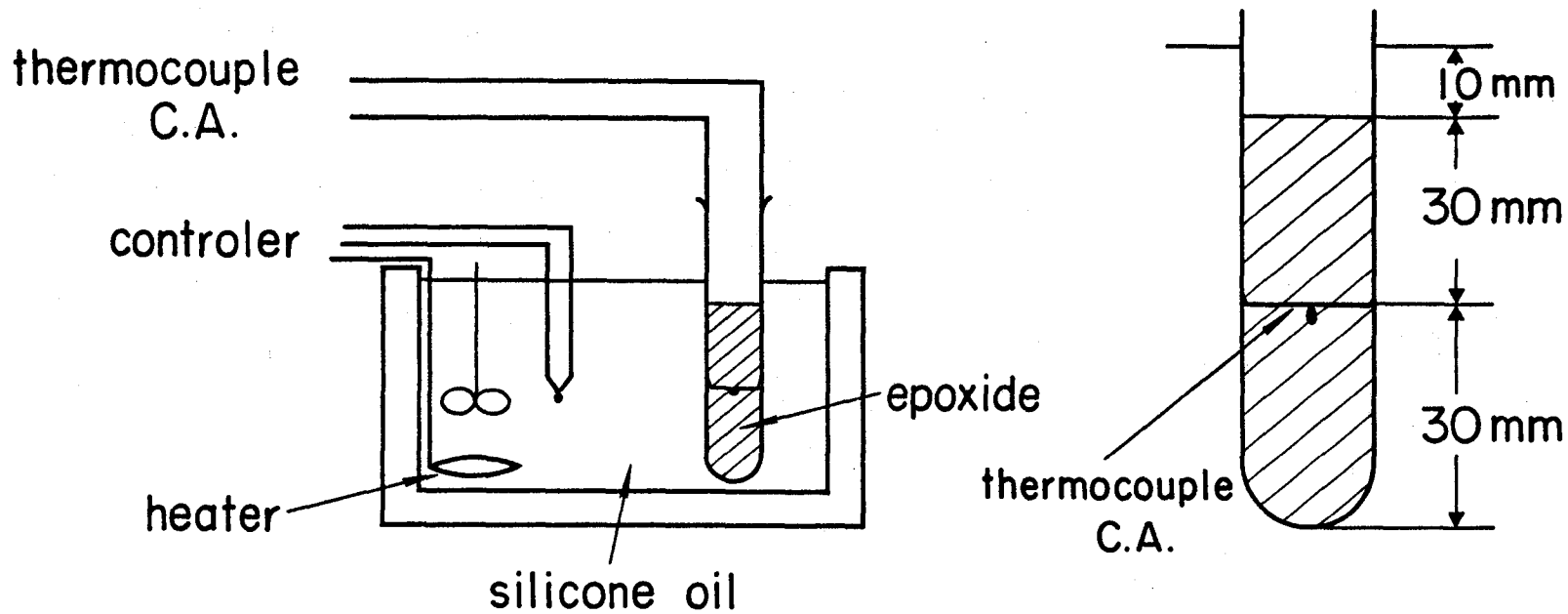


Figure 3 Apparatus for measurement of reaction heat.

G3000H<sub>8</sub>, and G4000H<sub>8</sub> (Toyo Soda polystyrene gel), respectively. THF was used as solvent and the instrument was calibrated to a first approximation with polystyrene of known molecular weights. Nuclear magnetic resonance spectra were determined with FX-100 and FX-90Q (JEOL LTD) instruments. The chemical shifts were referred to TMS. Infrared (IR) spectra were determined with IRA-2 (Japan Spectroscopic Co., Ltd.) equipment. X-ray diffraction of polymers was determined with RU-33L, SG-8R (Rigaku) equipment. Separation of reaction products was carried out with a Toyo Soda model HLC-807 gel permeation chromatograph packed with G-2000H<sub>8</sub> (polystyrene gel); chloroform was used as the solvent. A Shimadzu-5A model gas chromatograph with a Apiezon grease L (celite) was used for GC analysis.

Liquid chromatography was performed on a Shimadzu apparatus, model LC-3A, with ODS silica column (Zorbax ODS, Shimadzu), and methanol was used as solvent.

Part II Selective Synthesis of Structurally Isometric Poly- $\beta$ -ester and Poly- $\delta$ -ester from  $\beta$ -(2-Acyloxy-ethyl)- $\beta$ -propiolactone with Al-H<sub>2</sub>O and Zn-H<sub>2</sub>O catalysts

Syntheses of 2-acetoxyethyl-propionaldehyde, 2-isopropyl-carboxyethyl-propionaldehyde and 2-(1-chloroethyl)-carboxy

### ethyl-propionaldehyde:

These aldehydes were synthesized by the addition of the corresponding carboxylic acid to acrolein in a column containing Amberlite IRA-400 (acetate type, ion-exchange resin).<sup>10</sup> (b.p., yield) 2-acetoxyethyl-propionaldehyde, 55°C/0.9 mmHg, 26.6 %, 2-isopropyl-carboxyethyl-propionaldehyde, 53°C/1 mmHg, 18 %, 2-(1-chloroethyl)carboxyethyl-propionaldehyde, 75°C/0.7 mmHg, 30.5 %.

Syntheses of  $\beta$ -(2-acetoxyethyl)- $\beta$ -propiolactone (1),  $\beta$ -(isopropylcarboxyethyl)- $\beta$ -propiolactone (2) and  $\beta$ -(2-(1-chloroethyl)carboxyethyl)- $\beta$ -propiolactone (3).

$\beta$ -propiolactones were synthesized by reacting aldehyde with ketene, referring the literature.<sup>11</sup> (b.p., yield,  $d^{20}$ , elemental analysis, (calculated)), monomer (1), 104 - 107°C/0.7 mmHg, 18 %, 1.10, C, 53.15 (53.16), H, 6.42 (6.37), monomer (2), 110 - 114°C/0.3 mmHg, 33 %, 1.04, C, 57.87 (58.05), H, 7.64 (7.58), monomer (3), 150 - 155°C/0.3 mmHg, 40 %, 1.19, C, 46.22 (46.50), H, 5.43 (5.37), Cl, 16.92 (17.16).

### Polymerization of $\beta$ -substituted- $\beta$ -propiolactones.

Distillation of solvents, preparation of catalysts and polymerization were carried out under argon atmosphere. Preparation of catalyst:  $(EtAlO)_n$  and  $Et(ZnO)_2ZnEt$  catalyst were prepared, referring the literature.<sup>11</sup>  $SnCl_4$  was used without further purification.  $BF_4OEt_3$  was synthesized, referring the literature.<sup>12</sup>

Polymerization was carried out as follows. Monomer was added to toluene containing a given amount of a catalyst at  $-70^{\circ}\text{C}$  under argon atmosphere. After a homogeneous solution was formed by stirring, the polymerization tube was sealed and allowed to stand at a given temperature. Polymerization was terminated by pouring the polymerization mixture into a large excess of diethyl ether or diethyl ether-petroleum ether. Then the polymer precipitated was purified by extraction with diethyl ether. The polymers were tacky except for rubberlike (poly(3)-(Al)). Tg of the polymers are summarized in Table 7. (chapter 11)

#### Thermal decomposition of polymers:

Thermal decomposition of the polymers was carried out in an all glass apparatus consisting of two cylindrical tubes with a bridging arm (Figure 4). One gram of a polymer sample was heated in vacuo in one of the tubes at a given temperature while the other tube was cooled to  $-78^{\circ}\text{C}$  to collect the decomposed products.

#### Preparation of 5,6-dihydro-2-pyrrone:

5,6-Dihydro-2-pyrrone for identification of the thermal decomposition product of poly- $\beta$ -ester was synthesized from vinyl acetate and paraformaldehyde by the method described in the literature.<sup>13</sup>

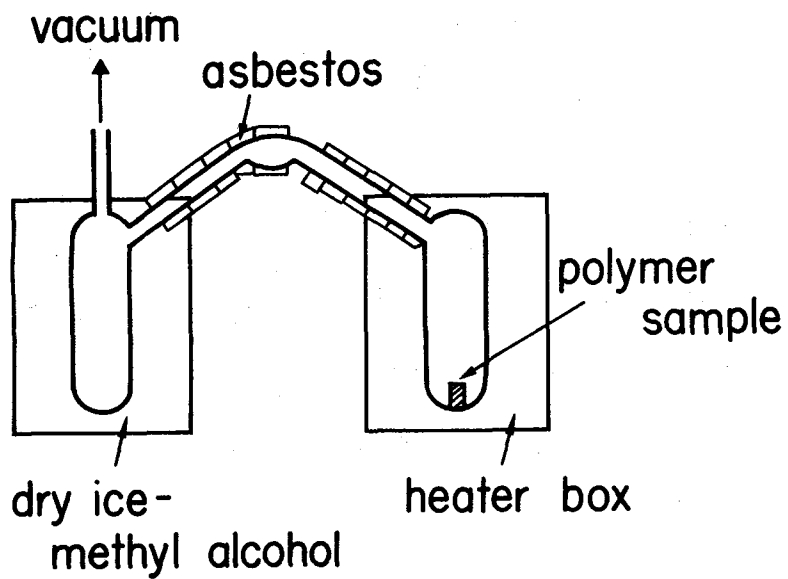


Figure 4 Apparatus for thermal decomposition of polymer.

## Apparatus:

IR spectra of the polymers were measured with a Hitachi model EPI2 spectrometer with a KBr disc method. NMR spectra were taken at room temperature with Varian T-60, Varian A-60 and Varian XL-100 spectrometers.  $^{13}\text{C}$ -NMR spectra were recorded at  $38^\circ\text{C}$  with a Varian Model XL-100 spectrometer at 25.16 MHz with a FT accumulator. Number of the data point in the FT accumulation was 8192 data length value. The molecular weight and the molecular weight distribution of the polymers were measured by gel permeation chromatography with a Shimadzu-Du Pont 830 type apparatus (column constitution, HSG-60 (50cm)-HSG-40 (50cm)-HSG-20 (50cm)) by eluting with THF at  $45^\circ\text{C}$ . Calibration was carried out with standard polystyrene mixtures. Thermal behavior of polymers was measured by a differential scanning calorimeter (Rigaku Denki). X-ray diffraction experiments were carried out with  $\text{Cu}/\text{K}\alpha$  source.

## Words

OH equivalent: molecular weight/the number of OH in a molecule.

OH equivalent %: (the number of OH equivalent/mole of monomer)  $\times$  100.

## References

1. T. Takiguchi, J. Am. Chem. Soc. (B), 81, 2359 (1959)
2. G. I. Harris, J. Chem. Soc. (B), 1963, 5973 (1964)
3. A. G. Brook, J. Am. Chem. Soc., 82, 5102 (1960);  
ibid., 91, 355 (1969)
4. A. G. Brook and H. Gilman, J. Am. Chem. Soc., 76,  
77 (1954)
5. U. Michel and S. Tchelitcheff, Bull. Soc. Chim. Fr.,  
2230 (1964)
6. E. W. Berg and N. M. Herrera, Anal. Chim. Acta.,  
60, 117 (1972)
7. H. Schmidbaur, Chem. Ber., 96, 2696 (1963)
8. C. G. Hatchard, C. A. Parker, Proc. R. Soc. London,  
A235, 518 (1956)
9. JSR type curast meter, technical paper (Nichigo Shoji)
10. Reynir Eyjolfsson, Acta. Chem. Scand., 24, 3076  
(1970)
11. K. Teranishi, T. Araki and H. Tani, Macromolecules,  
5, 660 (1972); H. Tani, S. Yamashita and K. Teranishi,  
Polym. J., 3, 417 (1972); K. Teranishi, M. Iida,  
T. Araki, S. Yamashita and H. Tani, Macromolecules,  
7, 421 (1974); M. Iida, T. Araki, K. Teranishi and  
H. Tani, Macromolecules, 10, 275 (1977); M. Iida,  
S. Hayase and T. Araki, Macromolecules, 11, 490  
(1978)

12. Organic Synthesis, 46, 113
13. L. J. Polby, C. N. Lieske, D. R. Rosencrantz and  
M. J. Schwarz, J. Am. Chem. Soc., 85, 47 (1963)





## Acknowledgments

The author wishes to express his sincerest thanks to Prof. A. Nakamura, Prof. T. Araki and Prof. T. Kodaka for their continuing guidance and encouragement throughout the course of this work. Particular thanks are due to Dr. T. Takamura, Mr. M. Wada and Mr. S. Suzuki for encouragement and useful discussions.

The author's grateful thanks are expressed to professors and other members of Department of Science in Osaka University, and members of Toshiba Corporation.

Finally, the author's grateful thanks are expressed to Toshiba Corporation.



## List of publication

1. "Polymerization of cyclohexene oxide with  $\text{Al}(\text{acac})_3$ -silanol catalyst" S. Hayase, T. Ito, S. Suzuki and M. Wada, J. Polymer Sci., Polym. Chem. Ed., 19 (9), 2185 (1981)
2. "Polymerization of cyclohexene oxide with  $\text{Al}(\text{acac})_3$ -silanol catalyst supported by zeolite and porous silica" S. Hayase, T. Ito, S. Suzuki and M. Wada, J. Polymer Sci., Polym. Chem. Ed., 19 (10), 2541 (1981)
3. "Polymerization of cyclohexene oxide with aluminum complex/silanol catalysts. Part III. Dependence of catalytic activity on bulkiness of silanol and its intramolecular hydrogen bond" S. Hayase, T. Ito, S. Suzuki and M. Wada, J. Polymer Sci., Polym. Chem. Ed., 19 (11), 2977 (1981)
4. "Polymerization of cyclohexene oxide with aluminum complex/silanol catalyst. IV. Photopolymerization with  $\text{Ph}_3\text{SiCOPh/Al}$  complex/alcohol catalyst system" S. Hayase, T. Ito, S. Suzuki and M. Wada, J. Polymer Sci., Polym. Chem. Ed., 20 (6), 1433 (1982)
5. "Polymerization of cyclohexene oxide with aluminum complex/silanol system. V. Dependence of catalytic activity on the structure of aluminum complex" S. Hayase, T. Ito, S. Suzuki and M. Wada, J. Polymer Sci., Polym. Chem. Ed., in press.

6. "Polymerization of cyclohexene oxide with aluminum complex/silanol catalyst. (VI) Oligomer and polymer effect. S. Hayase, Y. Onishi, S. Suzuki and M. Wada, J. Polymer Chem., Polym. Chem. Ed., in press.
7. "Selective synthesis of structurally isomeric poly  $\beta$ -ester and poly  $\delta$ -ester from  $\beta$ -(2-acetoxyethyl)- $\beta$ -propiolactone. A new difference between  $(EtAlO)_n$  and  $Et(ZnO)_2ZnEt$  catalysts". T. Araki, S. Hayase and M. Iida, J. Polymer Sci., Polymer Letters Edition, 16 (10), 519 (1978)
8. "Selective synthesis of structurally isomeric poly  $\beta$ -ester and poly  $\delta$ -ester from  $\beta$ -(2-acetoxy-ethyl)- $\beta$ -propiolactone with Al and Zn catalysts". T. Araki, S. Hayase and A. Nakamura, J. Polymer Sci., Polym. Chem. Ed., in press.
9. "Isomerization polymerization of  $\beta$ -propiolactones carrying side-chain ester groups". T. Araki, S. Hayase and A. Nakamura, Submitted in J. Polymer Sci., Polym. Chem. Ed.,
10. "Polymerization of epoxide with aluminum complex/silanol catalyst. Part VII. Thermal and electrical properties of epoxy resin cured with the new catalyst. S. Hayase, S. Suzuki, M. Wada, Y. Inoue and H. Mitsui, Submitted in J. Appl. Polym. Sci.